IDENTIFICATION AND CHARACTERIZATION OF NOVEL FACTORS NEEDED FOR TWO ASPECTS OF *MYXOCOCCUS XANTHUS* PHYSIOLOGY: SOCIAL MOTILITY AND OSMOREGULATION

by
Sapeckshita Agrawal

A dissertation submitted to Johns Hopkins University in conformity with the requirements for the degree of Philosophy

Baltimore, Maryland
November, 2013

ABSTRACT

Myxococcus xanthus is a non-pathogenic Gram-negative, delta proteobacterium. This bacterium has become an important model system for the study of complex bacterial phenomena such as cell-to-cell communication, motility, predation, developmental differentiation, and the production of pharmacologically interesting secondary metabolites. This thesis identifies and characterizes important structures that are involved in: I. motility and II. osmoregulation.

I: Motility: *M. xanthus* cells use two different types of motility: Adventurous (A-) motility and social (S-) motility. A-motility is predominantly used on dry surfaces such as hard agar, while S-motility is the preferred mode of motility on moist surfaces like soft agar. So far the molecular motor of A-motility has not been identified with certainty, whereas the molecular motor for S-motility has been known for quite some time. For this motility, *M. xanthus* uses the power generated by the extension and retraction of type IV pili, proteinaceous filaments that propel the cells forward. Although several details of the molecular mechanisms of S-motility have been resolved, some outstanding questions still remain. First, it is proposed that type IV pili bind to the secreted carbohydrate-comprised extracellular matrix (ECM), which causes the retraction of the pilus, and thus, initiates the power stroke that propels the cell forward. However, the major pilin protein, PilA, does not have a predicted lectin domain and thus, it is difficult to imagine how exactly the pilus binds to the carbohydrate. Second, S-motility is a complex behavior, requiring both cell-to-cell contacts and cell-to-ECM contacts. How does PilA accomplish both of

these tasks simultaneously since the two interactions certainly require very disparate interactions? Lastly, type IV pili from other bacterial species, such as *Pseudomonas aeruginosa* and *Neisseria gonorrhoeae* possess tip proteins, PilY1 and PilC1, respectively, which mediate binding to host cells or ECM components, as well as bacterial aggregation and piliation. No such tip protein has been identified for *M. xanthus* so far leaving the question unsolved whether a protein other than PilA mediates the interaction of the pilus with the environment.

In my lab, a novel type IV pili isolation protocol for *M. xanthus* has been developed which allows purification of large quantities of pili. In these isolations, a minor, high molecular-weight (HMW) protein consistently co-purifies with the pili. Using mass spectrometry, this HMW protein was identified as MXAN_1365 (hereby referred to as PilY1), a homolog of the type IV pilus tip protein PilY1. Analysis of the *M. xanthus* genome shows that there exist two other paralogs, which I termed PilY2 and PilY3. Using gene deletions and motility assays, I show that *M. xanthus* uses not just one but two of these PilY proteins, PilY1 and PilY2, to achieve piliation, aggregation, and normal S-motility, while PilY2 is dominant for S-motility and aggregation. In contrast, the function of the third paralog, PilY3 in these processes is less clear and not thoroughly evident using conventional assays. Sequence analyses show that PilY1 has an N-terminal integrin-like domain, while PilY2 possesses an N-terminal lectin-like domain. Thus, I propose that the type IV pilus uses PilY1 to mediate cell-to-cell interactions while PilY2 is used for cell-to-ECM contacts. These important findings augment the field's understanding of type IV pilus-mediated social motility in *M. xanthus* and highlight the

diversity of molecular mechanisms used by these structures to facilitate interactions with a wide variety of surfaces.

II: Osmoregulation: Osmoregulated periplasmic glucans (OPGs) are found in many Gram-negative bacteria. These glucans can exist as either linear oligomers of 6-8 glucose residues, as seen in *E.coli*, or as cyclic structures, as seen in *Rhizobium*. The main functional role described so far for periplasmic glucans is osmoprotection under low osmolarity of the external milieu. This protection is achieved through the attachment of various anionic groups to the oligomers that attract and bind water molecules keeping the periplasmic space and the cytoplasm hydrated. I describe here the discovery and characterization of a novel polysaccharide polymer in *M. xanthus* that is located in the periplasm and surprisingly appears to replace the oligomeric carbohydrates found in most bacteria. Chemical analyses show that the polysaccharide is composed of equal parts N-acetyl-glucosamine and glucose, as well as mannose and rhamnose, as opposed to OPGs, which are only made of glucose. Through linkage analysis and NMR, I have also determined the molecular structure of this polysaccharide. Electron microscopy of the isolated polymer reveals that it is composed of fibers forming a loose meshwork. Interestingly, this meshwork becomes highly hygroscopic when the cells are grown under high osmolarity conditions indicating that this polymer indeed acts as an OPG which under these conditions appears to change its composition to keep the periplasmic space and the cytoplasm well hydrated.

ACKNOWLEDGEMENTS

First and foremost, I would like to acknowledge Dr. Egbert Hoiczyk, under whose mentorship, I have completed this thesis. Dr. Hoiczyk sets high standards for his students, by himself demonstrating unrivaled enthusiasm, motivation, and commitment for science. He has taught me to never give up on something that is worth pursuing in the first place, and that it is only with perseverance and steadiness that we can get to the finish line. His remarkable ability to connect all the dots using his observations, experience, and knowledge of the literature helped tremendously in the advancement of my work. I appreciate Dr. Hoiczyk's patience with me at the beginning of my thesis work, when I had to overcome a steep learning curve, while facing other personal issues. On a personal level, Dr. Hoiczyk has always been a friend and a well-wisher for me and my family, and I thank him for that.

I am grateful to the Sommer Scholar Program for funding my research. The Sommer Scholar program gave me the flexibility of joining a lab of my choice.

I am also thankful to my thesis committee members Dr. Richard Markham, Dr. Nicole Parrish, Dr. Thomas Hartung, and Dr. P. C. Huang. Their inputs have been instrumental in augmenting my work, and their encouragement has sustained my morale all these years. I am also thankful to Dr. Gary Ketner and Dr. Kellogg Schwab for serving as alternates for my final oral exam.

I would also like to acknowledge the scholastic support of the Hoiczyk lab current and past members. Dr. Matthias Koch performed the MALDI MS on PilY1. He also helped train me when I first joined the lab. Dr. David Zuckerman often came up with

objective ideas for my work, and provided much-needed technical insights. Dr. Colleen McHugh was always on top of the literature, and was very helpful with discussions, and taught me several techniques in the lab. Dr. Kefang Xie was always a great listener and a wonderful friend. I want to also thank the Masters students Amy, Leda, Liz, and Radhika for their friendship.

I am also grateful to the members of the Coppens lab, Yu lab, and Markham lab, Zhang lab and Levitskaya lab. Dr. Julia Romano helped me several times with the upright Microscope training. Dr. Karen Ehrenman taught me protein expression; Dr. Jane Voss is a wonderful friend. Sean Evans often provided excellent scientific discussion and advice. All labs graciously shared reagents and instruments. I also want to thank Djeneba Dabitao of the Bream lab for teaching me qRTPCR and sharing reagents.

I am thankful to Carol Cooke for performing the immuno-gold labeling experiments, the researchers in the group of Dr. Parastoo Azadi, Radnaa Naran and Ian Black, at University of Georgia Center for Complex Carbohydrate Research for performing the chemical analysis on my samples and Kip Chirchir at the Johns Hopkins School of Medicine for teaching me TLC and sharing reagents.

I also want to thank my parents for their moral support throughout my life, and particularly during my PhD. My father is a role model for life-long scholastic pursuit and I plan to always follow in his footsteps. I am thankful to my siblings and their families for their constant love and encouragement. I want to also highlight the support of my mother and mother-in-law in helping me take care of my newborn son for the past 5 months, while I was finishing up this work.

Last but not least, I would like to acknowledge the love and support of my husband throughout my PhD. He took care of the mundane formalities of life, so that I could pay undivided attention to my work. Through his social efforts, he kept my life fun and lively, and through his positivity, he helped me remain on track. Our baby is the most beautiful fruit of our marriage, and I want to thank him for being a wonderful father and husband.

TABLE OF CONTENTS

LIST OF FIGURES

LIST OF TABLES

ABBREVIATIONS AND ACRONYMS

°C- Celcius

µg- microgram

µl- microliter

µm- micrometer

µM- micromolar

ATP- adenosine triphosphate

BLAST- basic local alignment search tool

bp-base pair

c-di-GMP- cyclic diguanylate monophosphate

CTT-casitone tris media

CYE- casitone yeast extract

EPS- exopolysaccharide

glc-glucose

glcN- glucosamine

HPLC- high performance liquid chromatography

kDa- kilo Dalton

KEGG- Kyoto encyclopedia of Genes and Genomes

LB- Luria-Bertani media

LPS- lipopolysaccharide

Mb-megabase

ml-milliliter

mm-millimeter

mM-millimolar

M-molar

OD-optical density

OPG-osmoregulated periplasmic glucans

PEG-polyethylene glycol

pN- piconewton

PTA-phosphotungstic acid

RPM-rounds per minute

S-motility- social motility

T4P- type IV pili

TEM- transmission electron microscopy

TFA-trifluoroacetic acid

TLC-thin layer chromatography

TPM- tris phosphate magnesium

UV-ultraviolet

w/v- weight over volume

wt-wild-type

CHAPTER I

Myxococcus xanthus uses three PilY1 homologs to accomplish swarming motility, type IV pilus biogenesis, aggregation, EPS localization, and fruiting body formation.

I.1 INTRODUCTION

Motility in bacteria

To survive, bacteria use a plethora of mechanisms of which motility is unique because it allows the cells to actively explore their environment. Although seemingly simple, prokaryotes use a wide variety of different types of motility that have often been phenotypically characterized such as swimming or gliding. Here I will review what is known about bacterial motility in general, as well as discuss some of the phenomena that are less well understood.

In 1972, Jorgen Henrichsen described six different forms of motility in his review about bacterial locomotion (see TABLE I.1.1): swimming, swarming, gliding, twitching, sliding and darting (1). Subsequent studies further characterized these forms as swarming and swimming being flagella-based, while twitching (sometimes wrongly termed gliding) relies on type IV pili as motors. True gliding as shown by *M. xanthus* is powered by a currently unknown mechanism, while sliding and darting appear to be passive movements (2).

Motility	Organelle	Some Genera
Swimming/"swarming"	Flagella	*Escherichia, Proteus, Pseudomonas, Salmonella, Serratia, Vibrio, Yersinia*
Twitching/Social motility	Type IV pili	*Bacteroides, Moraxella, Myxococcus, Pseudomonas, Streptococcus, Vibrio*
Gliding/Adventurous motility	Unknown	*Anabaena, Cytophaga, Flavobacterium, Flexibacter, Mycoplasma, Myxococcus,*
Sliding/Spreading	None	*Bacillus, Escherichia, Flavobacterium, Mycobacterium*

TABLE I.1.1: Various forms of motility in bacteria (Adapted from 2)

The bacterial flagellum, a universal motor for swimming

Robert Koch was the first person to successfully stain and visualize bacterial flagella in 1877, although their presence was known even earlier than that (reported in 3). Flagella are large protein structures made of at least 30 different components (4). The main part of the flagellum is a helical filament protruding from the cell surface, which rotates using the energy generated by the basal body motor located at the base of the filament, and thus, generates torque like a propeller (FIGURE I.1.1).

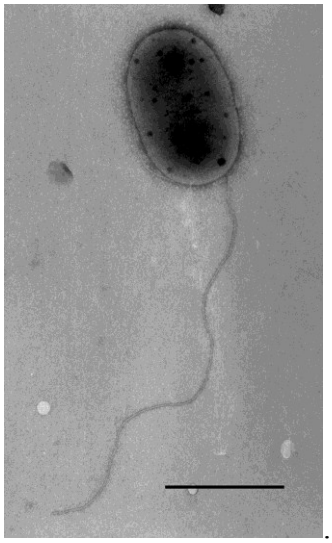

FIGURE I.1.1: Electron micrograph of *Methylobacterium jeotgali* possessing a single polar flagellum (5).

The filament of the flagellum is made of thousands of copies of a single protein, flagellin, and anchored to the basal body, which works as a reversible rotary device generateing energy from the cell's proton motive force. Flagella can be located at just one pole of the cell, or both, or distributed evenly over the entire cell surface (2, 102).

Flagella are responsible for both swimming of individual cells as well as for a form of surface-associated swimming that in the past has often been erroneously termed "swarming" (6). Interestingly, the rate of surface-associated swimming by so-called swarmer cells is often equal to or more than the rate of swimming through liquids by cells of the same species. Most of the surface-associated swimming occurs at the edge of the swarm where the cells have the longest and highest number of flagella, whereas the cells at the center of the swarm are usually less motile (2).

Flagellar-based swimming is present in many pathogenic bacteria. These include *E. coli*: causing infections of the intestines, kidneys, bladders etc., *Pseudomonas*

aeruginosa: responsible for infections of lungs in patients with cystic fibrosis, *Vibrio cholera*: the agent of cholera, and *Yersinia pestis*: the etiological agent of bubonic plague. Bacterial mutant strains with disrupted flagellar-based motility are often impaired in infection of host cells, thus, demonstrating the importance of flagella and flagella-mediated motility for bacterial pathogenesis (7).

Type IV pili-independent gliding motility

Henrichsen described true gliding as an energy-dependent smooth translocation of cells along their long axis, seen in three main bacterial groups: *Cytophaga-Flavobacterium,* cyanobacteria, and myxobacteria (2, 8). One proposed mechanism for gliding of filamentous cyanobacteria as well as myxobacteria is the secretion of slime, which is suggested to lubricate the surface or even generate thrust propelling the cells forward. Nozzles for secretion of the slime have been observed in the outer membrane fractions of *P. uncinatum* and *M. xanthus* (FIGURE I.1.2) (9,10).

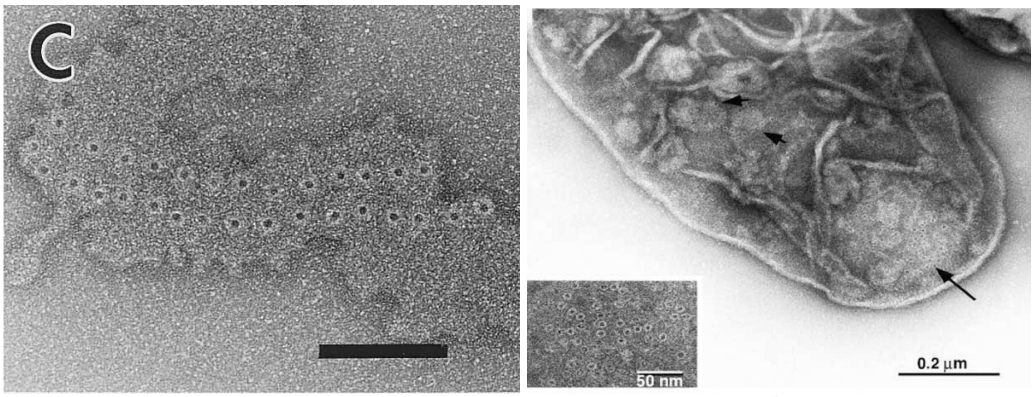

FIGURE I.1.2: Outer membrane fractions of *P. uncinatum* (left) and *M. xanthus* (right) showing the nozzles as dark spots surrounded by a lighter stained circle (10).

Several other mechanisms have been proposed to explain type IV pili-independent gliding motility (8). However, no one clear mechanism explaining gliding motility has so far been found and there may, in fact, exist more than one mechanism for this type of motility. The mechanism of gliding motility in *M. xanthus* will be discussed in more detail in subsequent chapters.

Type IV-dependent motility

Type IV pili are thin proteinaceous filaments on the surface of bacterial cells, capable of extending and retracting from the cell body using energy generated by ATPases located in the cytoplasm. I will first discuss pili in general, and then discuss type IV pili-dependent motility in various bacteria, including *M. xanthus* in more detail later.

Pili

Bacterial cell surface filamentous structures other than flagella were first described in the 1950s using electron microscopic pictures of metal-shadowed whole bacteria, which revealed "thin and fragile" filaments on the bacterial surface, thinner than flagella, and more irregular in structure (FIGURE I.1.3) (11). These filaments were named pili based on their resemblance to hair (pilus is Latin for hair). The study proposed them as organs for attachment, since they were found on bacteria colonizing solid surfaces.

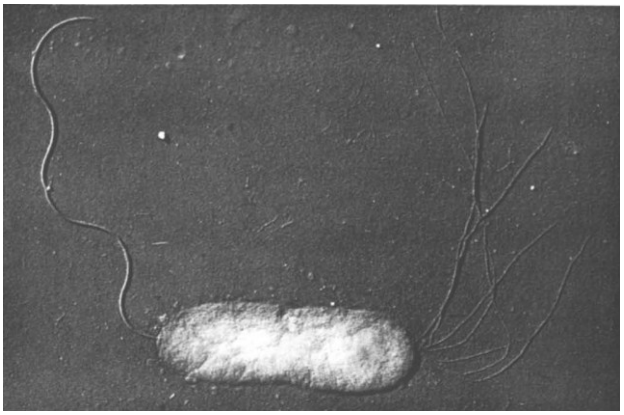

FIGURE I.1.3: *P. pyocyanca* with a single polar flagellum on the left pole and several pili on the opposite, right pole (11).

Another group identified these appendages around the same time, and named them independently "fimbriae" based on the Latin word for threads (FIGURE I.1.4). This group showed that cells possessing fimbriae could agglutinate red blood cells, while cells without fimbriae could not (11). This critical observation revealed an important function

of type IV pili in bacterial attachment, a function particularly critical for the pathogenicity of bacteria.

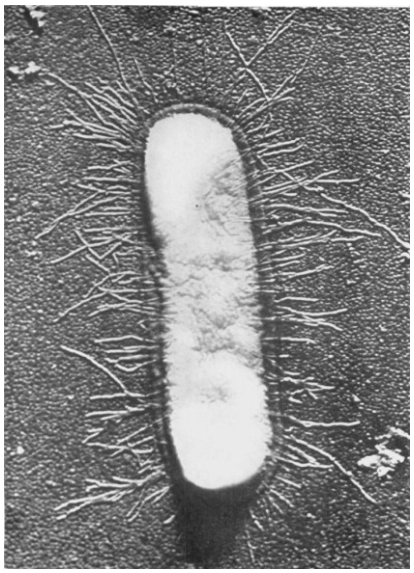

FIGURE I.1.4: Electron micrograph of bacterium *coli* (*E. coli*) showing many peritrichously arranged pili on the cell surface (12).

Many bacterial species, both Gram-negative and Gram-positive, possess pili, which are involved in a number of critical functions. These include attachment to host cells, formation of biofilms, evasion of host immune response, and DNA uptake (13). Pili are classified based on their assembly mechanisms. These, summarized in FIGURE I.1.5, include the chaperone-usher pathway of the type I pilus, the extracellular nucleation-precipitation pathway of curli, the type IV pili, the pili of the type III secretion systems (sometimes called needle because of their short length), and the type IV secretion pili of bacterial conjugation systems (13,14).

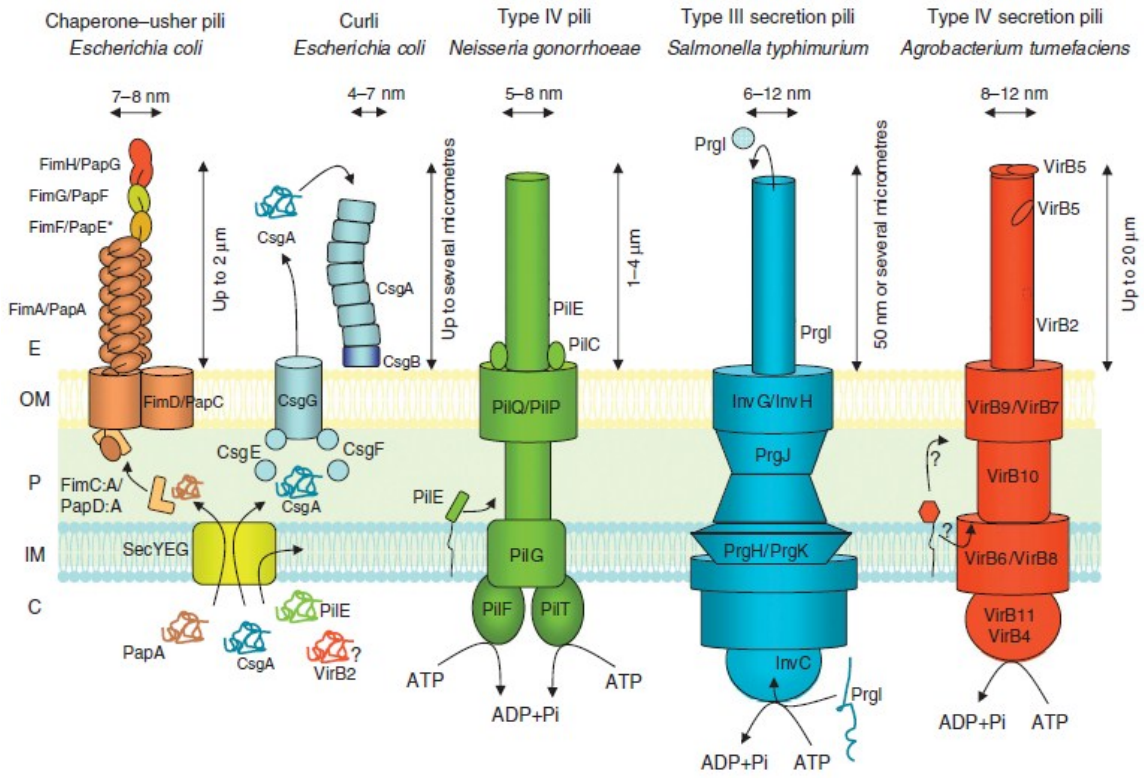

FIGURE I.1.5: The five main classes of pili. From left to right: Chaperone usher pathway of type I pili of i.e. enteropathogenic bacteria, including *E. coli;* curli pili assembled outside the cell; extendable and retractable type IV pili, type III secretion pili (needles) of *Salmonella* and *Yersinia spec.*, and type IV secretion pili of the *Agrobacterium tumefaciens* conjugation system (13, 15).

Chaperone-usher pathway

The chaperone-usher pathway has three key proteins. An immunoglobulin-like chaperone located in the periplasm, a pore-forming usher protein in the outer membrane, and the major pilin protein (16). The major pilin protein has an incomplete immunoglobulin fold with a groove in place of a missing beta strand in its C-terminal domain. Four residues of the chaperone protein complement this groove. This process, the donor-strand complementation results in the formation of a stable chaperone-pilin complex (16). The chaperone-pilin subunits also have an N-terminal disordered peptide

region (16). During pilus formation the beta strand donated by the chaperone is replaced by this disordered N-terminal region of the incoming chaperone-subunit complex. The last complex in the polymer is sent to the usher dimer on the outer membrane, which puts the pilus out to the cell surface (16). Examples of pili assembled via this pathway include the Pap and the Fim pili of pathogenic *E.coli* (FIGURE I.1.6)

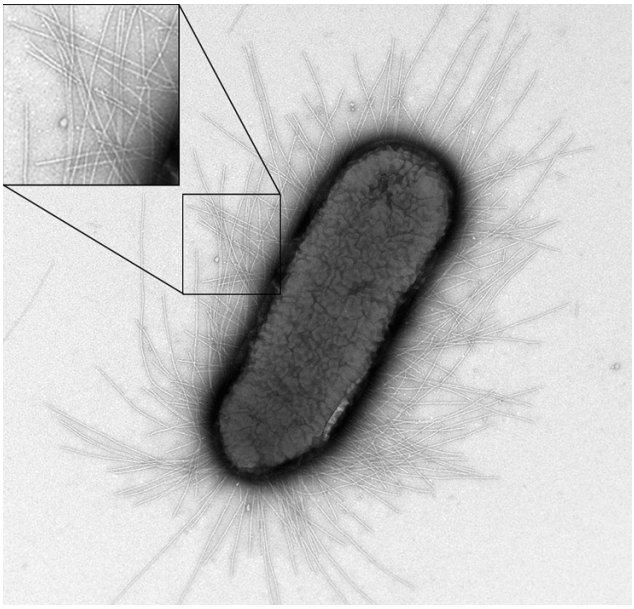

FIGURE I.1.6: Electron micrograph of type I pili from uropathogenic *E.coli* strains (17).

Extracellular nucleation-precipitation pathway

Curli pili of *E.coli* are assembled via the extracellular nucleation-precipitation pathway. Unlike pili assembled from the base as in the chaperone-usher pathway or the general secretion pathway, curli pili are assembled outside the cell, from secreted soluble subunits of the protein CsgA that polymerizes on the membrane-associated minor protein CsgB. CsgA subunits are secreted from a pore-forming lipoprotein (13,14). Curli pili

form highly aggregative amyloid-like fibers that promote host cell adhesion and invasion (13) (FIGURE I.1.7).

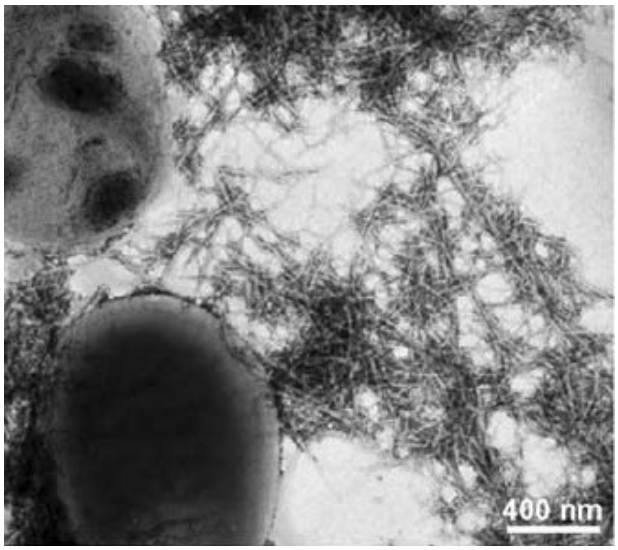

FIGURE I.1.7: Electron micrograph of curli pili of *E.coli*. (18)

Type III secretion pili ("needles")

Type III secretion pili ("needles") are found on many bacterial pathogens such as *Salmonella* and *Yersinia*, which secrete effector proteins into host cells *via* the type II secretion system. This system uses a thin hollow needle that connects the bacterial outer membrane with the host cell membrane during protein translocation (FIGURE I.1.8). The type II secretion machinery is also used for the assembly of the flagellum (13).

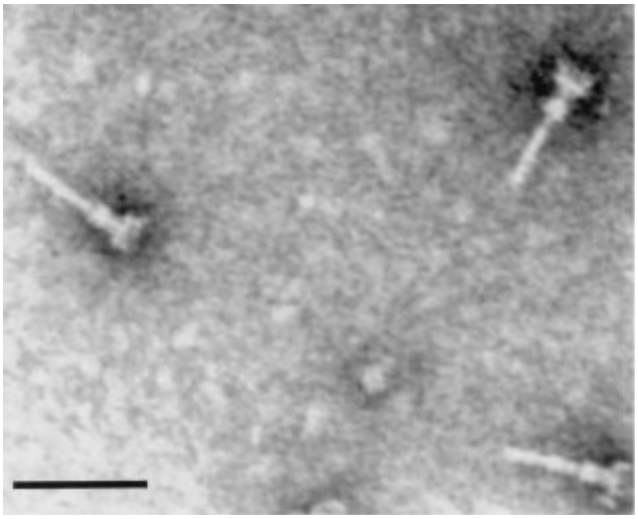

FIGURE I.1.8: Electron micrograph of isolated type III secretion systems showing the needles and the basal body-like part of the machinery (19).

Type IV secretion pilus

Type IV secretion pili are related to proteins involved in mating pair formation during conjugation (FIGURE I.1.19). Similar to type III secretion needles, type IV secretion pili are used by plant and human pathogens to directly deliver effectors into host cells (13). However, they differ from the type III secretion systems by simultaneously delivering DNA.

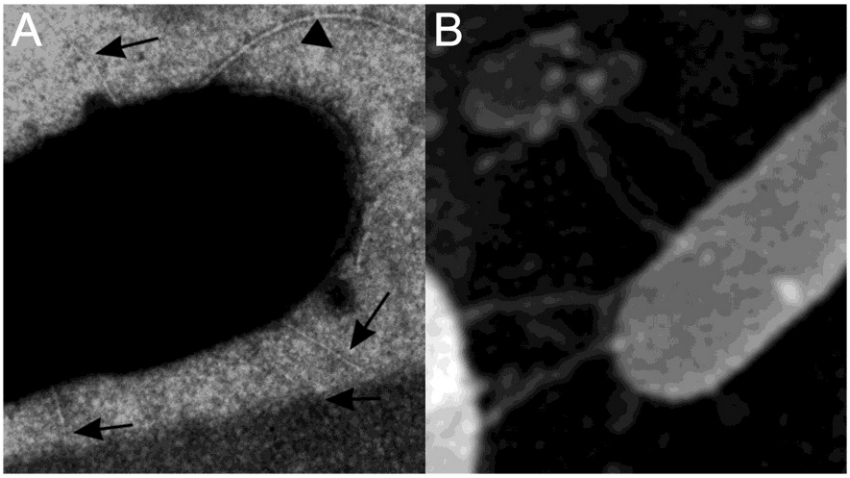

FIGURE I.1.9: Type IV secretion pili of *Agrobacterium tumefaciens*. (20).

The general secretory pathway

Type IV pili are assembled via the general secretory pathway, a complex protein machinery that is dedicated to the translocation of proteins into the extracellular milieu (21). Type IV pili are proteinaceous polymers protruding from the bacterial cell surface that are several micrometers long and about 5.5 nm wide. Electron microscopy has been traditionally used for identifying these pili as distinct structures (FIGURE I.1.10) (22).

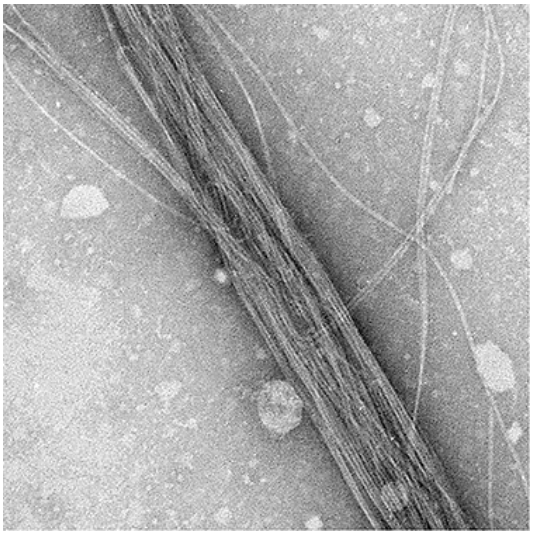

FIGURE I.1.10 Transmission electron micrograph of T4P from *Neisseria meningitidis* (22)

Along with *N. gonorrhoeae, N. meningitidis, P. aeruginosa*, and *M. xanthus*, T4P are found on *Aeromonas hydrophila, Azoarcus spp., Bacteroides ureolyticus, Branhamella catarrhalis, Comomonas testosteroni, Dichelobacter nodosus, Eikenella corrodens, Kingella denitrificans, K. kingae, Legionella pneumophila, Moraxella bovis, M. lacunata, M. nonliquefaciens, M. kingii, N. meningitidis, Pasteurella multocida, P. stutzeri, P. putida, P. syringae, Ralstonia solanacearum, Shewanella putrefaciens, Suttonella indologenes, Synechocystis* sp. PCC 6803, *Vibrio cholerae*, and *Wolinella* spp. (23). FIGURE I.1.11 shows a phylogenetic tree of species possessing type IV pili.

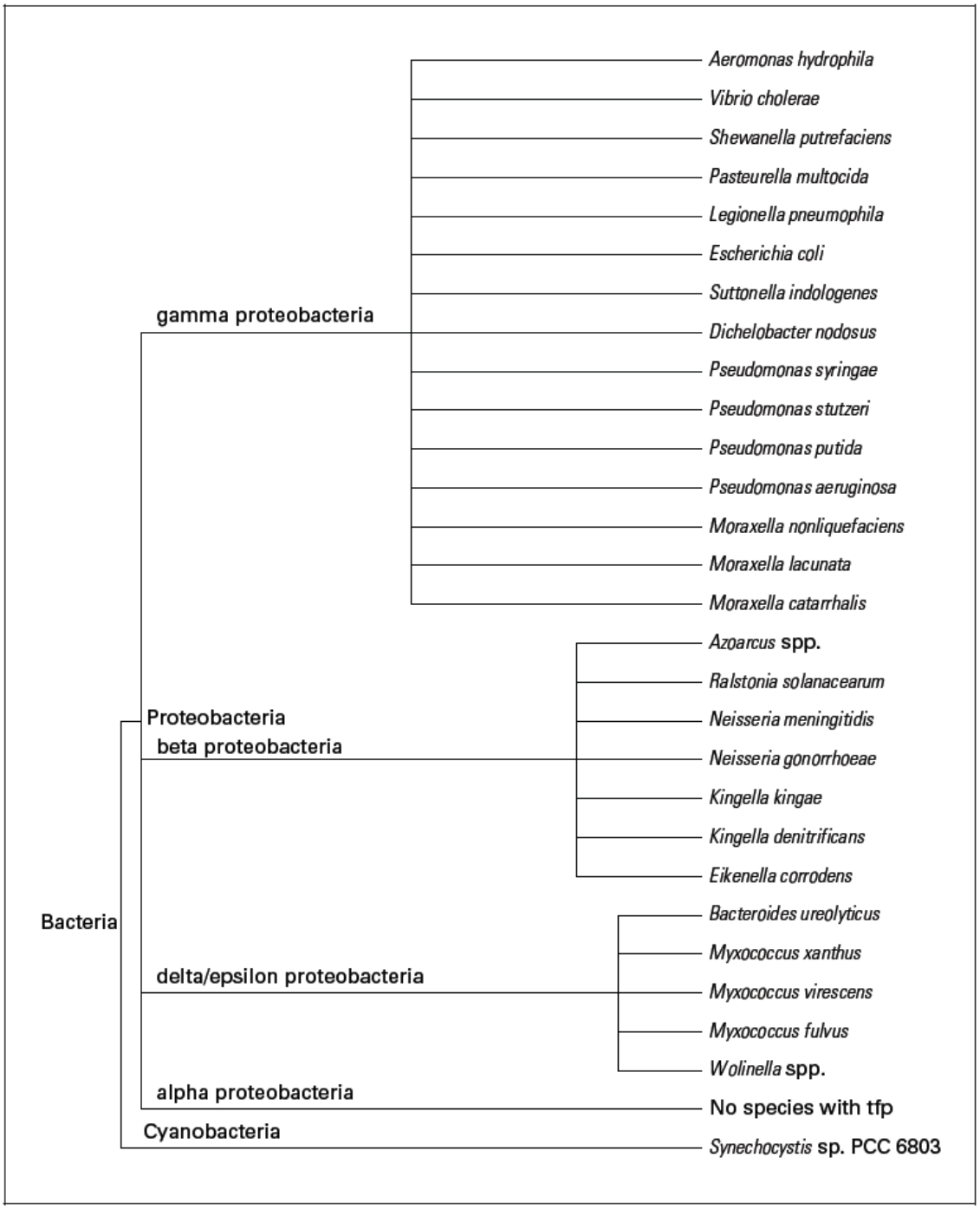

FIGURE I.1.11 Bacterial families and species possessing T4P (24).

Type IV pili are classified further as either type IVA or type IVB. Type IVA pili are found on *Pseudomonas, Neisseria and Myxococcus* species, while type IVB pili are

found on pathogenic *E. coli* and *V. cholera* (25). The major pilus subunit, PilA, of type IVA pili is typically shorter in length and possesses a shorter leader peptide, in comparison to the major pilin of type IVB pili (25). Other differences between type IVA type IVB pili are summarized in TABLE I.1.2

Comparison between type IVA and IVB pilus		
Feature	Type IVA pilin	Type IVB pilins
Organism	*Neisseria gonorrhea* PilE *Neisseria meningitides* PilE *Pseudomonas aeruginosa* PilA *Mycobacterium bovis* pilin *Eikenella corrodens* EcpA *Dichelobacter nodosus* FimA *Moraxella nonliquifaciens* TfpA *Moraxella lacunata* fibril protein Q *Myxococcus xanthus* PilA *Azoarcus* sp.	*Vibrio cholerae* TcpA *Enteropathogenic E.coli* BfpA *Enterotoxigenic E.coli* LngA, CFA/III *Salmonella enterica serovar* Typhi PilS *Citrobacter rodentium* CfcA
Length of leader peptide	5-6 amino acids	15-30 amino acids
Average length of mature protein	150 amino acids	190 amino acids
N-methylated N-terminal residue	Phenylalanine	Methionine, Leucine or Valine
Average length of D region	22 amino acids	55 amino acids

TABLE I.1.2: Difference between type IVA and type IVB major pilins (25).

Structural components of the type IV pilus

Type IV pili are complex macromolecular structures that are composed of a small number of different proteins. While some of these proteins may be unique to certain type of IV pili, others are indispensable core proteins that are conserved in all type IV pili. The presence of these core proteins is usually used to classify a pilus as a canonical type IV pilus. The core proteins include the major pilin subunit, PilA, a leader peptidase, traffic ATPases, an inner membrane complex of proteins, and a secretin protein in the outer membrane (TABLE I.1.3) (25).

TABLE: Core proteins involved in the biogenesis of type IVA and type IVB pili							
	P. aeruginosa	***Neisseria spp.***	***M. xanthus***	***E.coli (EPEC)***	***E. coli (ETEC)***	***E. coli (ETEC)***	***Vibrio cholerae***
Pilus Name				Bundle forming pilus	Longus pilus	Pilus colonization factor antigen III	Toxin co-regulated pilus
Protein Function							
Major subunit	PilA	PilE	PilA	BfpA	LngA	CofA	TcpA
Traffic ATPase	PilB PilT PilU	PilF PilT PilU	PilB PilT	BfpD BfpF	LngH LngJ	CofH	TcpT
Platform	PilC	PilG	PilC	BfpE	LngI	CofI	TcpE
Peptidase	PilD	PilD	PilD	BfpP	LngP	CofP	TcpJ
Secretin	PilQ	PilQ	PilQ	BfpB	LngD	CofD	TcpC
Pilotin	PilF	PilW	Tgl	BfpG	LngC	CofC	TcpQ
SDA protein	PilP	PilP	PilP	BfpU	LngG		TcpS
Assembly proteins	PilM PilN PilO	PilM PilN PilO	PilM PilN PilO	BfpC	LngE LngF	CofE CofF	TcpR TcpD

TABLE I.1.3: Core components involved in assembly of type IV pili (Adapted from 72).

The need for multiple proteins for the assembly of T4P was first appreciated with the observation that expression of the *P. aeruginosa* pilin in *E. coli* did not result in assembled pili, however when expressed in the original bacterium proper pilus assembly occurred. This suggested the involvement of additional proteins necessary for T4P assembly that differed from the ones used by the Chaperone-usher pathway pilus (26). Sequencing studies later revealed that the genes encoding these additionally necessary core proteins usually cluster together in an operon (FIGURE I.1.12) (27).

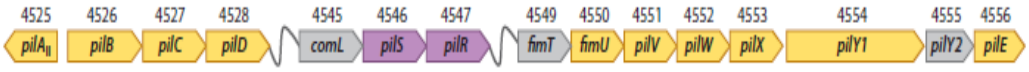

FIGURE I.1.12: Gene cluster of T4P components of *P. aeruginosa*. The names of the genes are written in the arrows and the corresponding gene numbers are shown above. Yellow represents genes encoding structural components, genes encoding regulatory components are in purple, gray represents genes associated with T4P, but lacking a pilus-related phenotype (27).

The major pilin

X-ray crystallography has been used to solve the structure of several type IVA and type IVB pilins. The major pilin subunit has a hydrophobic N-terminus (residues 2-24), which forms the helical stem of the ladle-shaped PilA molecule. The extended N-terminal α helix of the pilin has two parts: α1-N and α1-C. α1-N anchors the pilin to the inner membrane until the assembly of the pilus occurs and then forms the core of the hollow tube. The second part of the helix, α1-C, is wrapped by an antiparallel four-

stranded β-sheet that forms the globular head domain. (FIGURE I.1.13) (28). This β sheet is flanked by two regions that show sequence variation and are responsible for the observed heterogeneity of the PilA molecule. The first of these variable regions is the αβ-loop that connects the N-terminal helix to the beta sheet. The second one is formed by a disulfide bridge, which creates a β-hairpin that protrudes from the C-terminal globular domain. (14). The proposed model for the polymerization of the pilins is a helical assembly process during which the N-termini build the core of the pilus, while the variable globular domains make longitudinal and lateral contacts with each other (29).

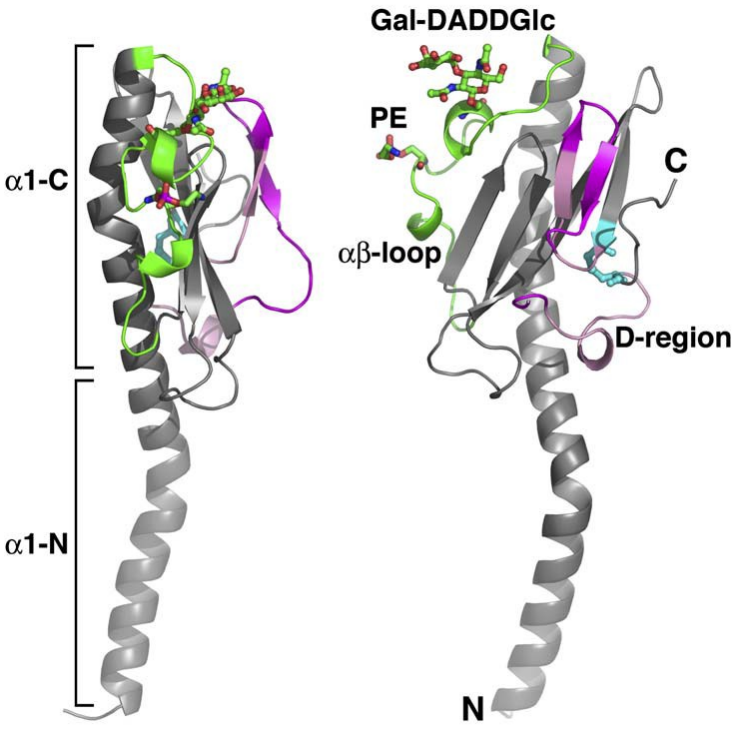

FIGURE I.1.13: Ribbon diagram of the PilA pilin from *Neisseria gonorrhoeae*. Left: side view of the molecule. Right: front view of the molecule. Shown are the N-terminal α-helix, β-sheets, disulfide bridge (cyan), the α-β-loop (green), and the variable D-region (purple) (28).

Leader peptidase

Early analysis of the pilin PilA showed that during pilus formation the protein molecule is posttranslationally processed losing a few amino acid residues. The enzyme needed for this cleavage and processing of the prepilin to the pilin was first identified in *P. aeruginosa* (30). The enzyme named PilD is located in the inner membrane and contains a highly conserved domain with two cysteine residues, which are responsible for its peptidase activity (31). The signal sequence of PilA proteins is a canonical type III sequence, different from the type I signal sequence recognized by signal peptidase I and the type II signal sequence characteristic for lipoproteins (32). PilD, after cleaving the signal peptide, also methylates the first amino acid of the newly formed N-terminus characterizing it as a bifunctional enzyme (31).

ATPases

Both the retraction (PilT) and the extension (PilB) ATPases belong to the Type II/IV secretion NTPases. Forest and coworkers crystallized the first type IV pilus retraction ATPase, PilT, from the archaebacterium *Aquifex aeolicus*. PilT has a hexameric bilobed structure, which binds and hydrolyzes ATP generating the mechanical force for pilus retraction through conformational inward-tilted movements of the lobe structures (33). Mutations in the retraction ATPase normally yield non-motile, non-retractile, hyperpiliated phenotypes (24), while mutations in the extension ATPase PilB result in a non-piliated phenotype. Retraction occurs at a rate of about 1000 PilA subunits

per second (24) at a force greater than 100 pN making the type IV pilus one of the strongest known biological motors (34).

Platform protein

The platform protein PilC is a member of the GspF family of integral inner membrane proteins (TABLE I.1.3; 35). PilC is responsible for recruiting the assembly and disassembly ATPases to the cytosolic side of the inner membrane (36). The X-ray diffraction data of PilC from *Thermus thermophiles* (37) reveals that the protein forms a tetrameric structure (35).

The assembly proteins

The inner membrane subcomplex of the type IVA pilus assembly machinery comprises of two bitopic membrane proteins and a cytoplasmic protein. Conserved assembly proteins in *Pseudomonas, Neisseria* and *Myxococcus* include PilM, PilN, and PilO (TABLE I.1.3), which are encoded all in a single gene cluster in synteny (38). Disruption of genes encoding any of these assembly proteins leads to loss of surface-exposed pili. PilN and PilO have both a transmembrane domain and a periplasmic domain, while PilM is an actin-like cytoplasmic protein for which the exact function is currently unknown (38).

Secretin and secretin-associated proteins

PilQ was identified as the T4P secretin in *P. aeruginosa* through the analysis of non-piliated mutants obtained from transposon mutagenesis screens (39). The mutation was mapped to a locus that contained the gene *pilQ*, encoding a 77 kDa large protein. PilQ mutants were non-piliated and incapable of twitching motility. Based on homology to PilQ, a homolog protein was also identified for the T4P machinery of *Neisseria gonorrhoeae* (40).

Single particle analysis of purified negatively stained PilQ complexes revealed a 12-fold rotational symmetry of the complex (41). In its center the complex has a channel that is formed at one side by a 10 nm deep cavity that is funnel-shaped on the top of the molecule. This cavity becomes narrow towards the center of the complex to close the pore formed by the secretin. Based on these data it is clear that a conformational change is required to open up the pore to allow the passage of a ca. 6 nm wide pilus. This idea is further supported by observations that indicate that interactions between the pilus and the secretin cause conformational changes in PilQ (42).

PilQ interacts with two other classes of proteins that play roles in stabilizing the secretin pore. These are the secretin-dynamic associated (SDA) protein and the pilotin proteins (72)

Model for pilus assembly

A lot of progress has been made in understanding the events leading to T4P assembly (FIGURE I.1.14), although not all details are completely understood such as the exact mechanism of polymerization which remain unresolved. Immature PilA subunits with N-terminal leader peptides are inserted into the inner membrane via the general secretory pathway. Next, the leader peptidase, PilD, processes these pilins by cleaving the signal peptide and adding a methyl group to the N-terminal phenylalanine (43). Force generated by the PilB extension ATPase and the PilT retraction ATPase allows the assembly and disassembly of the pilus (33).

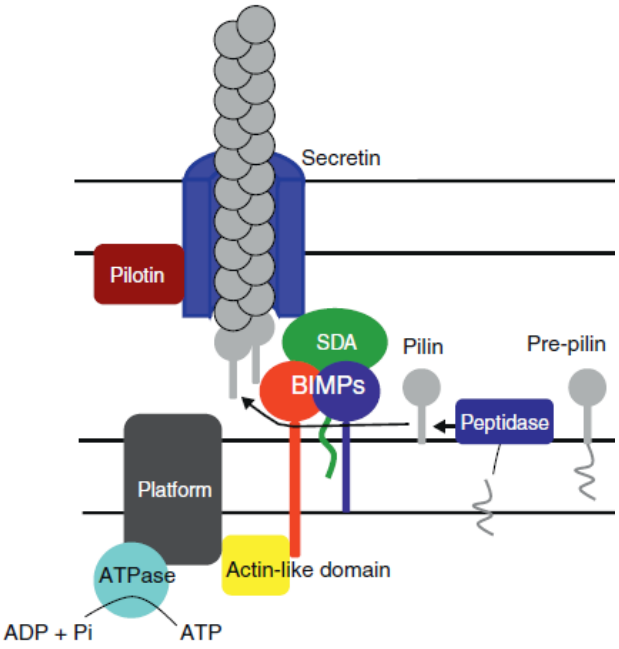

FIGURE I.1.14: The core components of the T4P machinery. The cytoplasmic ATPases interact with the inner membrane platform protein PilC (Platform), as well as the inner membrane subcomplex comprising the bitopic inner membrane proteins, and the cytoplasmic actin-like PilM (BIMPs). The peptidase PilD (Peptidase) processes the prepilins that get polymerized and put out onto the cell surface, via the outermembrane-located secretin (stabilized by the pilotin and SDA proteins) (44).

Minor pilins

Several minor proteins accessorize the type IV pilus, and play various other roles in pilus biogenesis and function. These proteins are expressed in small amounts, compared to the major pilins, and are therefore called minor pilins (45). The minor pilins include FimU, PilV, PilW, PilX, PilE PilY1 and PilY2 in *P. aeruginosa*. The gene cluster for *fimUpilVWXY12E* is expressed as a polycistronic operon. Overexpression or loss of any of these minor pilins impairs type IV pilus-mediated twitching motility suggesting that a finely balance stoichiometry of these proteins is essential for functionality of the pilus (45). FimU and PilX are key promoters of pilus assembly on the cell surface. Antibody labeling has shown that the minor pilins, FimU, PilV, PilW, PilX, and PilE are all processed by the pilus-specific leader peptidase PilD, and incorporated into the growing pilus during assembly (FIGURE I.1.15). Thus, the minor pilins are implicated in the initiation of pilus assembly rather than termination (45). It is important to note that in the case of *P. aeruginosa*, these minor pilins are located in the neighborhood of the T4P core proteins, i.e., PilA, PilD, PilQ etc. (FIGURE I.1.12), and that the minor pilins have about the size of PilA.

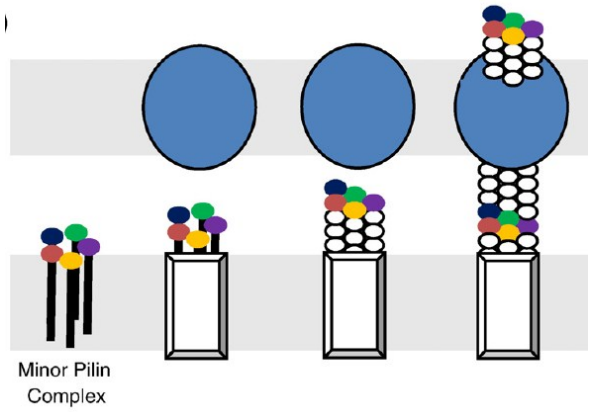

FIGURE I. 1.15: Model for T4P assembly. The minor pilin complex comes together at the inner membrane subcomplex (white rectangle), and initiates assembly of pilin subunits underneath. Thus, the minor pilins end up outside the cell using, like the pilin, the secretin (blue) as translocation pore (45).

High molecular-weight minor pilins

Compared to the other minor pilins of *P. aeruginosa*, PilY1 is a large protein of about 127 kDa (54). Initially, PilY1 was identified via homology to the previously identified minor pilin, PilC of *N. gonorrhea* (54) that was found as a low-abundance protein in pili preparations of this species (FIGURE I.1.16) (49). PilC was identified as a high molecular weight "outer membrane" protein of 110 kDa that was expressed in small amounts in the cells (46, 49). Genetic analysis eventually revealed that *N. gonorrhoeae* has not only one but two genes encoding for homologue proteins that were subsequently termed PilC1 and PilC2. Transposon mutagenesis of *pilC1* had no effect on piliation, while mutagenesis of *pilC2* abolished type IV pilus biogenesis (46-49). Interestingly, expression of PilC in *Neisseria* is phase variable during invasive infection, and can be turned on and off through frame shift mutations in a stretch of guanines located in the part of the gene encoding the signal peptide (49,50).

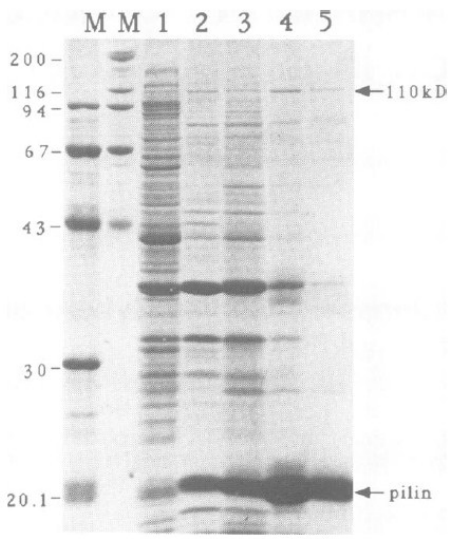

FIGURE I. 1.16: SDS-PAGE of various fractions of purified pili from *Neisseria gonorrhoeae*, with the high molecular weight band corresponding to PilC marked on the right (49).

Neisseria pili have hemagglutination ability which is independent of PilC (51). However, in *Neisseria gonorrhoeae*, PilC expression also causes bacterial adherence to host cells (51), and is tropic to attachment to primary epithelial cells from human cornea, but not to that of sheep, bovine, or porcine cornea explants. This ability to attach to host cells is attributed to the N-terminus of PilC, while its function in pilus biogenesis appears to be located in the C-terminus (52).

Initial transmission electron microscopy revealed that PilC is located at the tip of the pilus (FIGURE I.1.17) (46). However, in a follow up study of another group, it was found that PilC may in fact be localized to the outer membrane in both piliated and non-piliated strains questioning its original positioning (46, 53).

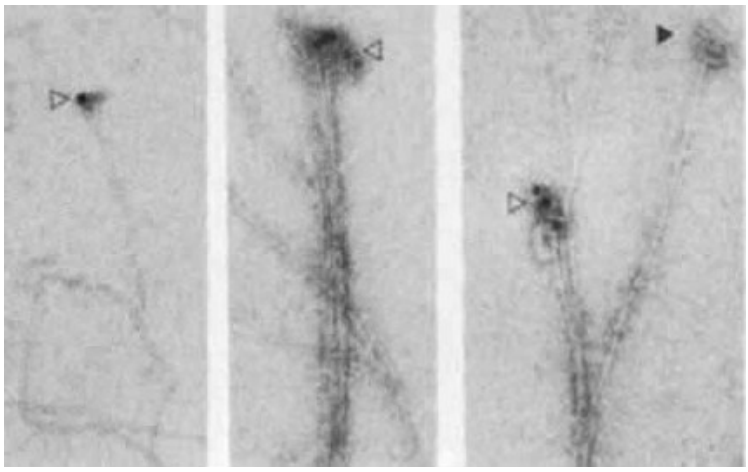

FIGURE I.1.17: Purified gold-labeled type IV pili showing PilC located at one end of the fiber structure (46).

Transposon mutagenesis screens identified in *P. aeruginosa* a gene that encodes a 127 kDa large protein (54). Based on a 43% homology to the C-terminus of PilC this protein was named PilY1 (since the name PilC was already given to the membrane platform protein in this species). PilY1 is found in both membrane fractions, as well as pilus fraction, which can be recovered from the cell-surface. Inactivation of *pilY1* by transposon insertion in a non-piliated *P. aeruginosa* strain increased the resistance of the mutant bacteria to killing by host cell neutrophils. Moreover, in a wild-type background PilY1 influences twitching motility, T4P biogenesis, and production of pigments called pyocyanin and quinolones. Due to these disparate roles, the function of PilY1 as a specialized T4P tip-located adhesin, like its homolog PilC, has been called into question and remains controversial (55). Some studies, however, have supported the idea that PilY1 is important to adherence to human host cells. Using a mucosal epithelial model system, it was shown that *P. aeruginosa* preferentially binds exposed basolateral host cell surfaces, while a pilY1 mutant strain of the same species is unable to invade this tissue firmly supporting the role of PilY1 as adhesin (FIGURE I.1.18; 56).

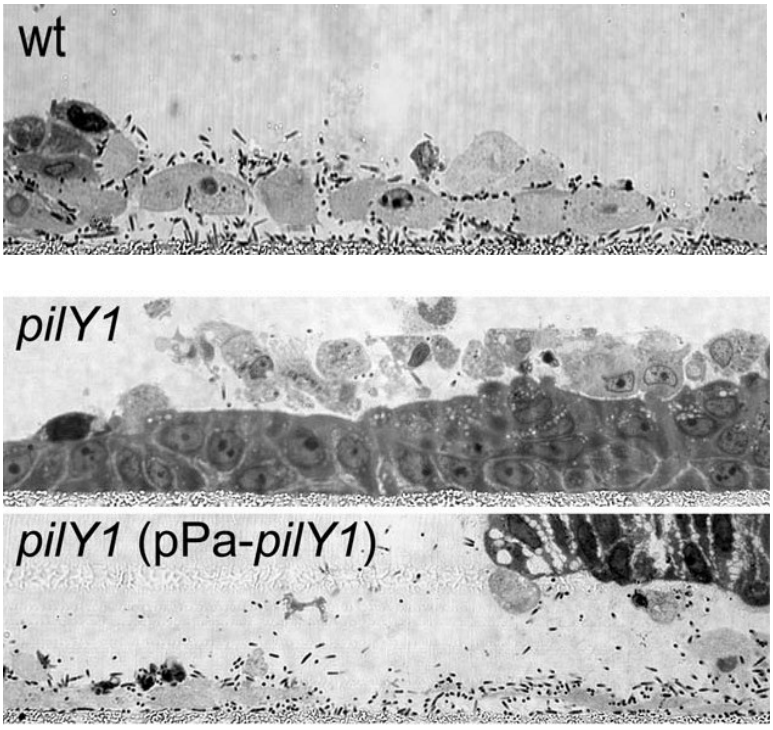

FIGURE I.1.18: PilY1 facilitates *P. aeruginosa* invasion of host epithelial cells. From top to bottom: Exposed basolateral epithelial cells (large round structures) are invaded by wild-type *P. aeruginosa* (small dark rods and dots), whereas, *pilY1* mutant cells are not able to attach and invade the epithelial cells, while a *pilY1* complemented mutant restores the invasive phenotype of the bacterium (56).

Although the entire structure of PilC or PilY1 is currently unknown, the structure of the C-terminus of PilY1 has recently been solved using X-ray crystallography (FIGURE I.1.19) (57).

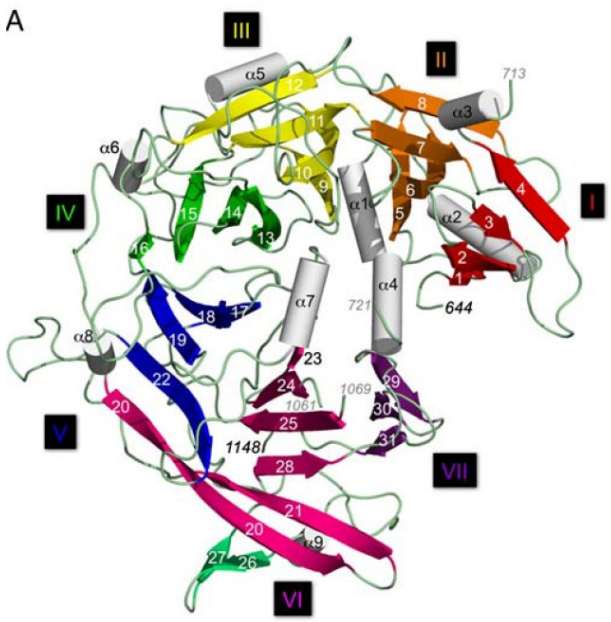

FIGURE I.1.19: Crystal structure of a *P. aeruginosa* PilY1 C –terminal fragment comprising 614-1163 amino acids. The protein is made of seven blade-shaped β-sheets that are shown in different colors (57).

One of the surprise findings of this structural analysis was that PilY1 appears to influence pilus production and twitching motility *via* a nine amino acid calcium-binding loop in the C-terminus (57). Disruption of the calcium binding by a chelator eliminated surface pili strongly suggesting that this step is essential for proper T4P assembly (57). PilY1 also has an integrin-binding arginine-glycine-aspartic acid (RGD) domain in the C-terminus (58). This is significant because anti-integrin antibodies reduce *P. aeruginosa* attachment to host cells suggesting that this domain may engage in binding to host cell surface receptors (58, 59). PilY1 also appears to influence swarming motility through a regulation of c-di-GMP, an intracellular signaling molecule promoting the transition in many bacteria from a motile to a sessile state. A phosphodiesterase mutant, Δ*bifA* that cannot longer degrade c-di-GMP is defective in swarming and a Δ*pilY1* deletion restores

the swarming phenotype (60). Thus, PilY1 seems to affect swarming via multiple pathways that respond to various parameters of the cellular environment.

Functions of the type IV pili

Motility

Henrichsen was the first to recognize the relationship between surface motility and type IV pili presence by identifying bacteria that were able to move over moist surface without flagella (1). T4P-based motility often called twitching motility describes a jerky movement of individual cells or the quick spreading of cell colonies on moist agar surfaces (61). Thereby, cells are able to move through the before described extension and retraction of their pili. Initial proof for the retraction of the T4P came from the observation that upon attachment to bacteriophages, pili became shorter, bringing the bacteriophages closer to the cell surface (62). Although indicative of a shortening of the pili, more direct evidence for the retraction came from studies using optical tweezers on *Neisseria* pili. These studies showed that the distance between pili and attached beads would reduce while generating forces of ~100 pN (27, 33). Moreover, biochemical evidence showed that the cells consume ATP to power these extensions and retractions. Finally, observation of fluorescently labeled pili allowed the direct visualization of the pili retraction and extensions (63). These experiments also showed that pili attach to surfaces via their tip, subsequently shorten in length, and that this retraction causes movement of the cell (27). Intriguingly, pili are motors that can pull but not push.

Moreover, individual pili appear to work cooperative, because cells with the highest number of pili traveled furthest (64).

Biofilm development

Biofilm formation of *P. aeruginosa* on surfaces requires functional type IV pili (65). Non-piliated cells, while capable of forming a monolayer of cells, are unable to form microcolonies that eventually convert into full-fledged biofilms (65). This requirement for type IV pilus for biofilm formation has also been demonstrated in a number of other bacteria, including *Neisseria* and *Myxococcus* (65, 66).

Pathogenesis

Type IV pili are critical for the pathogenesis of many bacterial species, including *Pseudomonas* and *Neisseria.* Interestingly, studies with human volunteers that were inoculated with various clones of *N. gonorrhoeae* showed that some of these clones were proficient in causing venereal disease in volunteers, while others were not (67, 68). Careful analysis of the clones revealed that the pathogenic capacity correlated with the presence of pili (69). This association between T4P and pathogenesis was also demonstrated for *P. aeruginosa.* If the bacteria were pretreated with various protein-inhibiting compounds that blocked adherence to mammalian buccal epithelial cells no infection was observed (70).

Similarities between type IV pili and type II secretion systems

The type II secretion machinery is composed of about 12-15 proteins that are dedicated to the translocation of folded proteins from the periplasmic space into the extracellular milieu (71). Bacterial species that possess T2SSs include *P. aeruginosa,* enterotoxic and enterohemmorrhagic *E.coli* strains*, L. pneumophilia, Y. enterocolitica, V. cholera,* etc. Biochemical and genetic analyses have shown that T2SS and T4P are functional and structural similar. Thus, both of these systems have been suggested to share a common evolutionary ancestor (71).

Unsurprisingly, key components of the T2SS are analogous to that of T4P, and include, SDA proteins, pilotins, outer-membrane secretins, peptidases/N-methylases, platform proteins, traffic ATPases, and a major "pilus" subunit (71). TABLE I.1.4 compares key components of the T2SS and T4P in various Gram-negative bacteria (TABLE I.1.4).

Instead of forming a true surface-exposed pilus, T2SS assemble a periplasmic pseudopilus that is composed of the major pseudopilin and 4 other minor pseudopilins. It has been suggested that the pseudopilus works like a piston pushing cargo proteins, mostly enzymes, into the extracellular milieu (71). The N-terminus of the pseudopilins and the major T4P pilin subunit share a short positively charged sequence followed by a hydrophobic stretch of amino acids. Similar to the T4P, the pseudopilin is also N-terminally processed by a specific peptidase, which cleaves the signal sequence and methylates the first amino acid of the nascent N-terminus. Interestingly, in some species, the same peptidase is responsible for processing both pseudopilins and pilins and

although the pseudopilin does normally not form a surface-exposed pilus it can do so if overexpressed (71).

Protein Function	*M. xanthus*		*P. aeruginosa*		*V. cholerae*	
	T4P	**T2SS**	**T4P**	**T2SS**	**T4P**	**T2SS**
Major Subunit	PilA	GspG	PilA	XcpT	TcpA	EpsG
Traffic ATPases	PilB PilT	GspE	PilB PilT PilU	XcpR	TcpT	EpsE
Platform	PilC	GspF	PilC	XcpS	TcpE	EpsF
Peptidase/N-methylase	PilD	GspO	PilD	XcpA	TcpJ	VcpD
Secretin	PilQ	GspD	PilQ	XcpQ	TcpC	EpsD
Pilotin	PilF	GspS	Tgl		TcpQ	
SDA protein	PilP	GspC	PilP	XcpP	TcpS	EpsC
Assembly proteins	PilM PilN PilO	GspL GspM	PilM PilN PilO	XcpY XcpZ	TcpR TcpD	EpsL EpsM EpsN

TABLE I.1.4: Functional homologs between T4P and T2SS (71 and 72).

Role of pili as lectins

Many pili of pathogenic bacteria have lectin- like properties and bind specific sugar residues on the host cell surface (73). For example, type I fimbriae bind to mannose residues *via* their minor tip protein FimH. Although this protein is found at low frequency throughout the pilus filament, only the subunit present on the tip of the pilus is able to actually bind mannose (73). Likewise, the pap pilus of *E. coli* binds glycosphingolipids using its distally located tip protein PapG. Finally type F17 fimbriae of enterotoxic *E. coli* strains mediate attachment to host cells by binding N-acetylglucosamine moieties with their pilus tip protein (73).

Myxobacteria

Myxobacteria were first described in 1892 by Ronald Thaxter, a botanist (74), who characterized their multicellular behavior such as swarming, aggregation, and fruiting body formation. Next, the microbiologist Hans Reichenbach built on this knowledge and systematically collected species from various locations around the globe. Based on their 16S ribosomal RNA, myxobacteria belong to the delta proteobacteria (74). They are the only group among the proteobacteria that undergo developmental differentiation forming elaborate spore-containing fruiting bodies. Most myxobacteria are predatory and able to lyse other bacterial cells for nutrients. Although hundreds of these species have been described, research focuses on three model species: *M. xanthus, Stigmatella aurantiaca, and Sorangium cellulosum* (74).

Myxococcus xanthus

M. xanthus has a 9.14 Mb large genome; 15% of which is derived from more than 1500 selective gene duplications (74, 75). The Gram-negative cells are rod shaped about 7 microns in length and 0.5 microns wide. Because of easy growth in culture and the completion of its genome sequence, *M. xanthus* has become the model system to study many bacterial processes, including cellular differentiation, production of secondary metabolites and antibiotics, non-flagellar dependent surface motility, biofilm formation, type IV pilus biogenesis, spore formation, predation, and phase variation to name a few.

Under vegetative conditions, *M. xanthus* spreads as a swarm on moist surfaces using T4P-derived S-motility, while on dryer surfaces the cells preferentially use A-motility to translocate individually. Six to eight hours after depletion of nutrients, cells start to aggregate and about $1x10^5$ cells form a multilayered mound that eventually will maturate over time into a spore-containing fruiting body (FIGURE I.1.20). During this developmental differentiation a majority of cells die, while only about 10% of the cells will eventually convert into spores, that are resistant to desiccation, heat, and sonication. When nutrients become available again, spores germinate and transform into rod-shaped vegetative cells completing the cycle. Interestingly, a small percentage of the start population differentiates into another subpopulation of cells termed peripheral rods that are non-aggregating cells that survive despite the lack of nutrients (76).

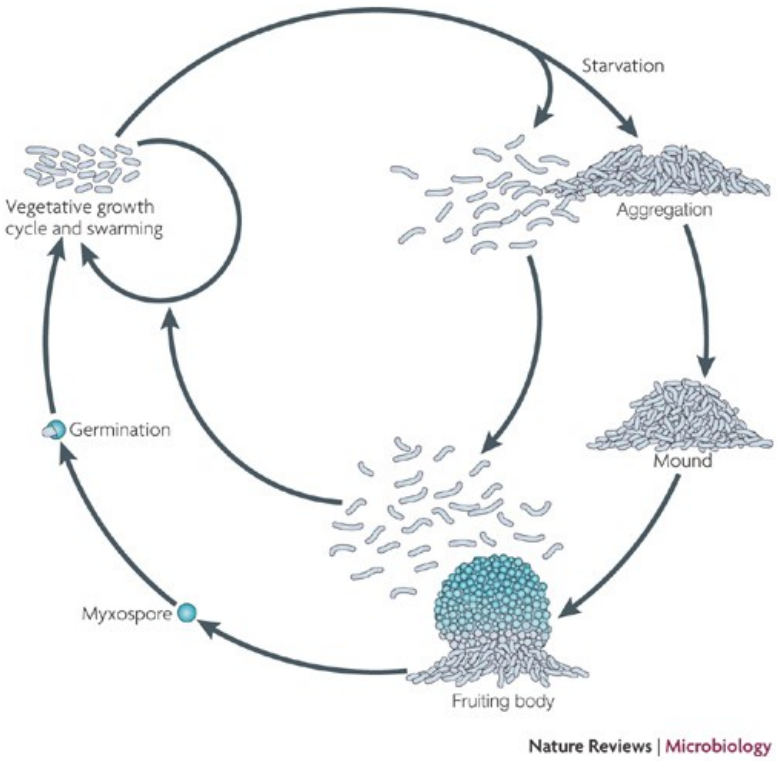

FIGURE I.1.20: The life cycle of *M. xanthus*, a model myxobacterium: Vegetative cells move as a swarm to search for nutrients and prey cells. Once nutrients are depleted, the cells start to aggregate to form mounds, in which most cells die, while only a few convert into spores. Peripheral rod cells never aggregate. When nutrients become available, the spores germinate and form rod-sheaped vegetative cells (76).

Gliding in M. xanthus

For all aspects of the *M. xanthus* life cycle motility is paramount. Chemical and UV-induced mutagenesis experiments revealed that the cells use two independent systems termed adventurous (A-) and social (S-) motility to glide (77). A-motility describes the gliding of isolated individual cells, while S-motility refers to group movements of cells, which is only possible if cells are no further apart than a two cell length to allow type IV pilus interactions. Although genetically distinct, both of these systems work synchronously and coordinated to enable motility (78).

Mechanism of adventurous motility

About 40 different genes have been reported to play a role in A-motility (79). Despite this impressive number, however, the exact mechanism by which A-motility is accomplished is currently not well understood. Several models have been proposed that could account for these movements. Among them are slime secretion from polarly arranged nozzles (80) and the continuous movement of focal adhesion complexes that attach to the substrate pushing the cells into the opposite direction (81).

Mechanism of social motility

Type IV pili

While A-motility is not well understood, the motor of S-motility has long been identified as type IV pili that pull the cells through their extension and retraction. The correlation between S-motility and pilus presence in *M. xanthus* was first observed in 1977 (82) and shortly afterwards firmly established through careful correlation of motility and ultrastructural studies (FIGURE I.1.21) (83).

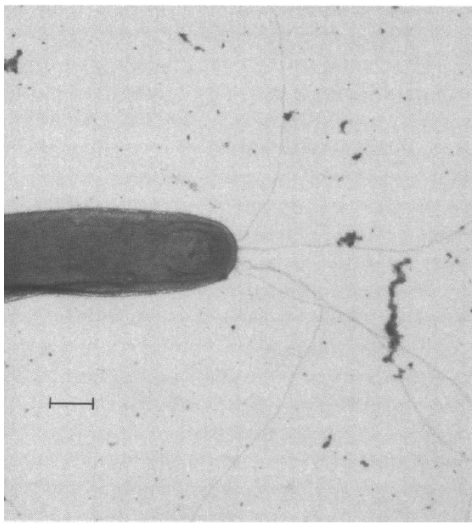

FIGURE I.1.21: Electron micrograph of a *M. xanthus* cell pole showing surface T4P (83).

Social gliding in *M. xanthus* requires three components: cell-to-cell contacts, cell-to-EPS contacts, as well as LPS (84). Evidence for the requirement of cell-to-cell contacts was derived from the observation that swarm expansion rates on soft agar increases with increasing density of cells (85-88). Type IV pili are also stimulated to retract via binding to EPS (88). Direct visualization of the binding of pili to EPS fibrils was achieved using fluorescently labeled EPS and PilA. Therefore, a C-terminal GFP-fusion of PilA was generated and incubated with Texas red-labeled wheat germ agglutinin-labeled EPS fibrils showing that both fluorescence signals overlapped (89). Furthermore, mutants defective in EPS fibril production are not only defective in social motility but also are hyperpiliated, thus suggesting that EPS controls the level of piliation in cells (88, 90). Finally, experiments have demonstrated that hypo-piliated strains also produce less EPS (87) again suggesting that the cells sense and respond to the presence of EPS with the assembly of pili. Like in other bacteria, T4P of *M. xanthus* are complex and

most of their structural components are located on a large multi-gene cluster (FIGURE I.1.22).

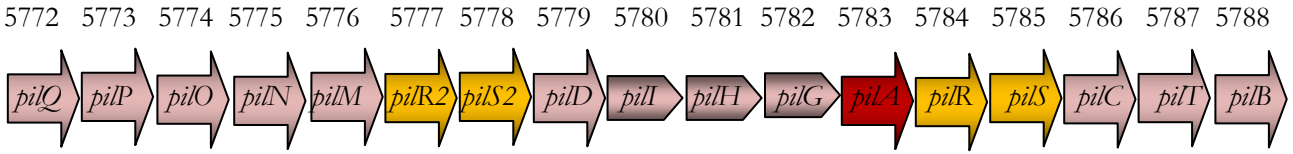

FIGURE I.1.22: Schematic representation of the operon encoding type IV pilus components (MXAN_5772-MXAN_5778). Purple indicates genes encoding pilus biogenesis proteins, yellow indicates genes important for transcription control of pilus components, red is the gene *pilA*, for the major pilin subunit, and narrow arrows are ABC transporter (91)

M. xanthus EPS

The second component that is necessary for S-motility is EPS. EPS was first described in *M. xanthus* as long extracellular fibrils of unknown composition (92). These fibrils form a network surrounding cells capable of S-motility while missing from *dsp* non-cohesive mutant cells unable to move using S-motility (FIGURE I.1.23) (93). This correlation was further supported by the observation that Congo red, a dye that binds to EPS, rendered wild-type cells non-cohesive and interfered with their ability to move (94). Ultrastructurally, EPS fibrils are about 50 nm long slightly fuzzy structures that are clearly distinguishable from the thinner T4P (94).

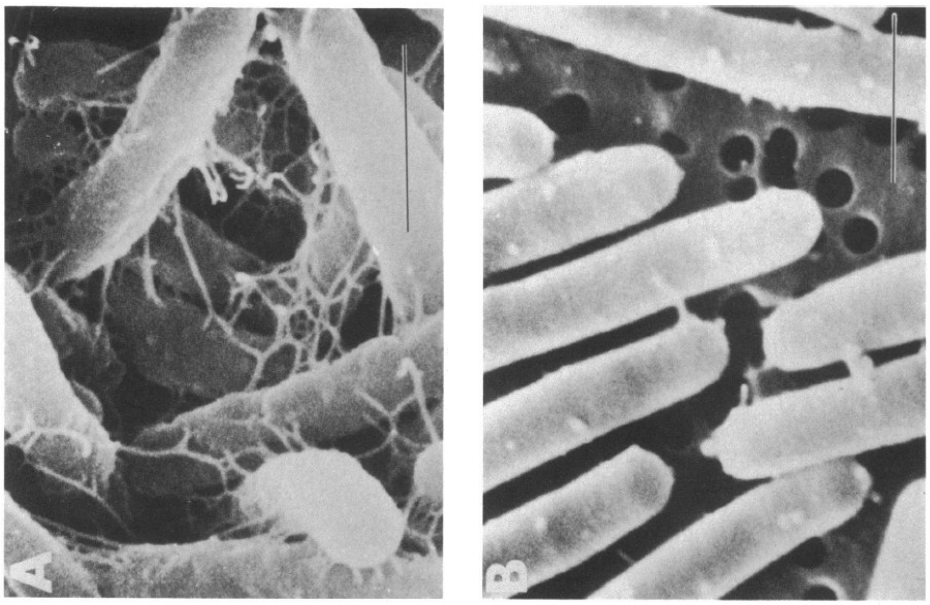

FIGURE I.1.23: Scanning electron micrograph of *M. xanthus* EPS. Left: cohesive wild-type cells covered with EPS fibrils. Right: non-cohesive *dsp* mutant lacking extracellular fibrils (93).

Chemical analysis showed that the extracellular matrix is composed of equal amounts of protein and polysaccharides at a ratio of about 1:1.2. HPLC analysis of isolated material identified galactose, glucosamine, rhamnose, glucose and xylose as main monosaccharide components of the polysaccharide of the matrix (94). *M. xanthus* mutants that are deficient in EPS synthesis are also deficient in social motility showing that this component is absolutely necessary for S-motility. Accordingly, *dsp* or the *dif* mutants that lack EPS are also defective in S-motility (95). The *dif locus is* an operon that encodes homologues to chemotaxis proteins that appear to be involved in the regulation of EPS production[1]. It has been hypothesized that type IV pili act as sensors for the presence of EPS thereby activating the *dif* pathway (FIGURE I.1.24). Moreover, mutants that are deficient in the production of pili are usually also defective in EPS production. How the T4P thereby transmit a signal to the genes encoding the EPS synthesis machinery is currently not well understood (97).

[1] The chemotaxis system is the way of transmitting chemical signals from outside of the bacterial cell to the periplasm where these chemicals interact with transmembrane chemoreceptors called methyl-accepting chemotaxis proteins and cause conformational changes in them. This leads to activation of downstream kinase and in turn phosphorylation of the response regulator, which causes changes in bacterial motility to allow chemotaxis (97).

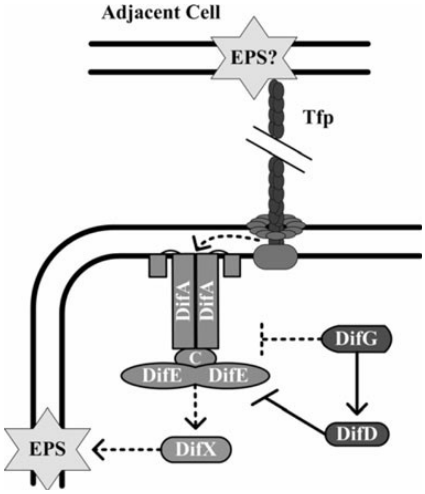

FIGURE I.1.24: Interaction between T4P components and the *dif* pathway. T4P act as sensors for signals that are transmitted to the *dif* pathway, which in turn regulates the production of EPS (97).

This link between EPS and S-motility has been further established through transposon insertion mutagenesis screens that identified besides of known genes further genes involved in EPS production and S-motility; among them many genes encoding proteins involved in carbohydrate synthesis. Intriguingly, these screens also identified additional genes that are somehow linked to this process. For an overview of these 31 newly identified genes see TABLE I.1.5 (79).

Gene	Name	Putative function
Central Metabolic Functions		
MXAN_0358	*sgmA; ileS*	Isoleucyl t-RNA synthetase; downstream of *pilW, fimT*
MXAN_3759	*sgmM; pccB2*	Propionyl –CoA carboxylase
MXAN_3797	*sgmN*	Short-chain acyl-CoA dehydrogenase
Cytoplasmic and membrane proteins of unknown function		

MXAN_0440	*sgmB*	Inner membrane protein; RND exporter
MXAN_1106	*sgmC*	DnaJ/TPR repeat domain protein
MXAN_1641	*sgmD*	Hypothetical protein
MXAN_1795	*sgmE*	Lipoprotein
MXAN_2526	*sgmH*	Hypothetical protein
MXAN_4150	*sgmO*	Conserved hypothetical protein; downstream of *frzS*
MXAN_4620	*sgmR*	Hypothetical protein; downstream of *rfbC*
MXAN_4639	*sgmS*	TPR repeat protein; PilF domain
MXAN_5766	*sgmX*	TPR repeat protein; PilF domain
MXAN_5770	*sgmY*	Conserved hypothetical protein
MXAN_6125	*sgnA*	Hypothetical protein
MXAN_6518	*sgnB*	Conserved hypothetical protein; ABC transporter
MXAN_7360	*sgnE*	Lipoprotein
MXAN_7442	*sgnF*	Membrane protein
Regulators of Transcription		
MXAN_2128	*sgmF*	LysR family activator
MXAN_4640	*sgmT*	Histidine kinase/response regulator
MXAN_5592	*sgmW*	Response regulator
MXAN_6627	*sgnC*	Response regulator
Polysaccharide metabolism		
MXAN_2203	*sgmG*	Asp box motif protein
MXAN_2561	*sgmI*	Fibronectin type III domain protein
MXAN_2921	*sgmJ; wbaZ*	Glycosyl transferase group I domain

MXAN_2922	*sgmK*	LPS biosynthesis; WcaJ C-terminal domain
MXAN_3506	*sgmL*	Polysaccharide biosynthesis
MXAN_4613	*SgmP; rfbB2*	dTDP-glucose 4,6-dehydrogenase
MXAN_4616	*sgmQ*	Glycosyl transferase group I and II domains
MXAN_4707	*sgmU; rfaF*	Heptosyl transferase 9 domain
MXAN_5333	*sgmV; rfaG*	Glycosyl transferase group I domains
MXAN_5831	*sgmZ; glgP*	Glycogen phosphorylase
MXAN_6908	*sgnD; pgi*	Glucose-6-phosphate isomerase

TABLE I.1.5 : Gene numbers with putative functions that were identified in a mutagenesis screen of clones with impaired social motility (79).

OPEN QUESTIONS REGARDING M. XANTHUS *SOCIAL MOTILITY*

As has been described earlier, type IV pili are predicted to bind the carbohydrate component of the EPS. However, PilA the major pilin does not contain a predicted lectin domain to explain this effect. Moreover, social motility in *M. xanthus* requires cell-to-cell and cell-to-EPS interaction. However, there is no explanation for how PilA accomplishes these two disparate tasks. One possibility would be that PilA possesses two different domains, which would allow specific interactions with the EPS carbohydrate as well as the cell surface. Yet another possibility would be that the T4P of *M. xanthus* is accessorized with minor proteins such as the HMW tip proteins described for *N. gonorrhoeae* and *P. aeruginosa* pili that could execute these different ligand interactions. However, no such minor pilin has so far been described in *M. xanthus*.

I.2 METHODS AND MATERIALS

Bioinformatics tools and analysis

The Kyoto Encyclopedia for Gene and Genomes (KEGG) bioinformatics resource was used to obtain protein and DNA sequences. SignalP 4.1 was applied to predict signal peptides for various proteins, using the default setting for Gram-negative bacteria (102). The Basic Local Alignment Search Tool (BLAST) of the National Center for Biotechnology Information (NBCI) was utilized for determining % identities and homologies of various proteins. HHPRED was used to identify structural motifs in the N-termini of the various proteins using default settings and only about the first 500 amino acids of large proteins. Protein sequence alignments and phylogenetic trees were built using STRAP default settings (99).

Growth of M. xanthus strains

M. xanthus cells were grown in liquid CTT medium composed of 1% casitone, 1 mM K_2PO_4, 8 mM $MgSO_4$, 10 mM Tris/HCl (pH 7.6) (106). For general maintenance of the strains, CTT plates with 1.5% agar were used. For preparation of electrocompetent cells, CTTYE was used, which is composed of CTT with 0.5% yeast extract. Top agar used for clone isolation was prepared with CTTYE plus 0.5% agar. *E. coli* cells were

grown on Lennox lysogeny broth (LB) plates composed of 10 g/L tryptone, 5 g/L yeast extract, 5 g/L NaCl with 1% agar.

Construction of deletion plasmids

All primers used in the study are listed in TABLE I.2.1. In-frame, marker-less deletion plasmids were constructed by splicing of PCR products by overlap PCR (107). Specifically, the deletion plasmids were constructed by obtaining the DNA sequence ~500 base pairs above and ~500 base pairs below the gene to be deleted. Four primers, A, B, C, D, were designed. Primer A was the forward primer ~500 base pairs upstream of the gene that contained a restriction site to be used to insert the digested PCR product into the pBJ113 vector. Primer B was the reverse primer that annealed at the beginning of the gene of interest, and contained an overlap sequence complementary to an overhang sequence on primer C, which ran in the forward direction, at the end of the gene of interest. Primer D was a reverse primer designed at ~500 base pairs downstream of the gene of interest also containing a relevant restriction site. Two PCR reactions were performed; one with primers AB, and another one with primers CD using isolated genomic DNA from *M. xanthus* as template, and expand high fidelity polymerase (Roche). The PCR reaction was carried out at annealing temperatures 5-10°C less than the melting temperature of the primer, and an extension time that added ~30 seconds/500 bp. Electrophoresis of the PCR products was done using 1% agarose gels containing 10 µg/ml ethidium bromide. PCR products AB and CD were then gel-extracted using the Qiagen Gel Extraction Kit (Qiagen). The amount of DNA from the gel extraction was

measured using a spectrophotometer, and 60 ng/µl of both AB and CD were used as template in a subsequent PCR reaction conducted with primers A and D.

The resulting product was gel extracted and digested with New England Biolabs restriction enzymes and appropriate buffers. Vector pBJ113, illustrated in FIGURE I.2.1 (108) was also digested with the same enzymes, and both samples were run on agarose gels and extracted. The vector was dephosphorylated using calf alkaline phosphatase (Roche) and then ligated with the PCR product using the Roche DNA ligation kit. 2-5 µl of the ligation was used to transform *E. coli* Top 10 (Invitrogen) cells by heat shock. The cells were plated on LB agar plates containing 100 µg/ µl kanamycin and incubated at 37 °C overnight. The resulting colonies were checked for plasmid insertion by PCR. Appropriate colonies were picked and 5 ml of cultures were grown overnight. The plasmids were extracted from the cells using the Qiagen Miniprep Kit and sent for sequencing using an Applied Biosystems 3730xl DNA analyzer at the Johns Hopkins University Synthesis and Sequencing Facility.

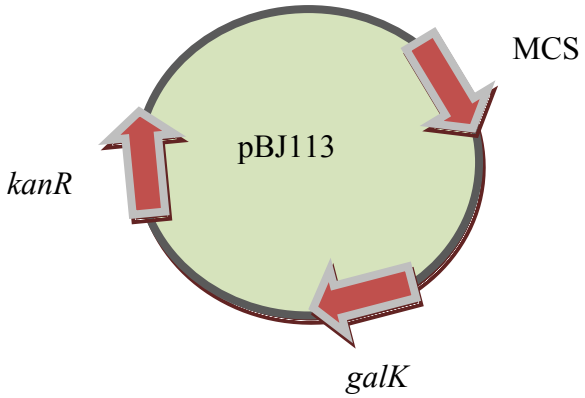

FIGURE I.2.1: Map of the pBJ113 plasmid used for gene deletion by homologous exchange. The multiple cloning site contains restriction endonuclease sequences in order to clone the gene deletion cassette into the plasmid. The plasmid also contains a kanamycin resistance (*kanR*) gene and the galactose kinase (*galK*) gene for positive/negative selection of deletion clones (108).

Construction of deletion mutants in M. xanthus

In-frame markerless deletion mutants were constructed as described previously (110). Deletion in *M. xanthus* is made through allelic exchange via homologous recombination upon insertion of plasmids containing homologous sequences to the genes of interest, into the appropriate locations on the genome. Positive and negative selection is used for screening for deletions, since the plasmid pBJ113 contains a kanamycin resistance cassette and the gene encoding galactose kinase, an enzyme that kills the cells in the presence of galactose (FIGURE I.2.1). Specifically, the plasmids with the correct DNA sequences were used to transform electrocompetent *M. xanthus* cells, prepared by repeated washing with water. The cells were electroporated at 400 Ω, 25 μFD, and 0.65kV using 1 mm electroporation cuvettes from BioRad. After electroporation, 1 ml of CTTYE was added sterile to the cells, which were allowed to recover at 32 °C, 250 rpm

for 5 h. The cells were plated on CTTYE agar plates containing 40 µg/µl kanamycin, by mixing 100 µl, 300 µl and 600 µl of cells with 3 ml of CTTYE 0.5% agar +kanamycin and pouring the mixture on top of CTT agar+kanamycin plates. The plates were incubated at 32 ℃ incubator for 5 days, and kanamycin resistant colonies were picked and plated on fresh CTT agar+ kanamycin plates. The clones were then grown in liquid CTT, and different amounts of the culture were plated on CTTYE plates with 2.5% galactose by mixing with CTTYE 0.5% agar + 2.5% galactose. The resulting colonies were screened for sensitivity for kanamycin, and kanamycin-sensitive, galactose-resistant clones were 3-way PCR screened for deletions, using an upstream primer to primer sequence A, a downstream primer to primer sequence D and a primer annealing to an internal sequence of the gene.

Construction of complemented strains

Complementation was attempted either at the native locus using homologous recombination or at the extrachromosomal phage attachment locus *attB* using site-specific recombination. For native locus complementation plasmid construction, a PCR product was generated using genomic DNA as template which spanned a sequence ~500 base upstream to ~500 bp downstream of the gene of interest, using a set of primers listed in TABLE I.2.1. The product was then digested and ligated into the pBJ113 vector and the plasmid obtained was electroporated into the relevant strains. Positive/negative selection using kanamycin and galactose was used to finally isolate the complemented strains.

For complementation from the phage attachment *attB* site, the entire gene of interest was amplified either from the gene start site or ~300 base pairs upstream from the start site to allow transcription either from a *pilA* promoter or the native promoter of the gene, respectively. The PCR product was digested and cloned into the pSWU30 vector (FIGURE I.2.2), containing the gene encoding the phage integrase, and the *pilA* promoter upstream of the multiple cloning site. Cells were electroporated with the 1 μg of plasmid DNA, and grown in CTTYE agar + 15 μg/ml oxytetracycline. Oxytetracycline-resistant clones were analyzed for complementation of the phenotype observed for the deletion strain.

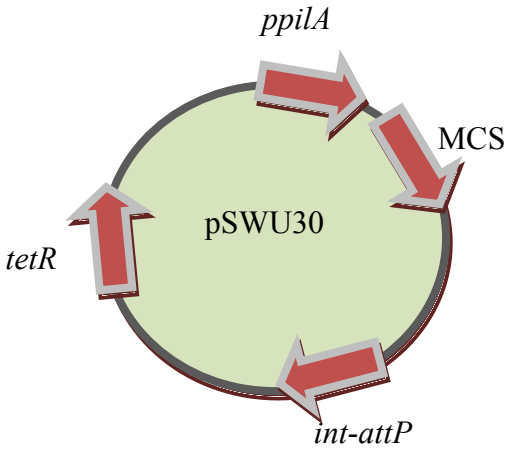

FIGURE I.2.2: Plasmid map of the pSWU30 plasmid used for complementation of deletion mutants. The plasmid has been modified to include a *pilA* promoter sequence upstream of the multiple cloning site (MCS) in order to constitutively express the desired protein under the *pilA* promoter. The plasmid also has a phage attachment site along with the integrase gene sequence (*int-attP*), which mediates plasmid integration into the phage attachment site *attB* located on the *M. xanthus* chromosome, via site specific recombination. Lastly, the plasmid encodes a tetracycline-resistance gene for selection of clones with integrated plasmid.

Tagging of PilY proteins in M. xanthus

To generate PilY1 containing a C-terminal FLAG tag, the *pilY1* gene was amplified with a reverse primer annealing to the end of the gene containing a FLAG sequence overhang. To generate PilY2 and PilY3 with N-terminal myc or FLAG tags splicing by PCR overlap was used. Since these proteins possess leader peptides that are posttranslationally removed the tags were placed after the leader peptide. Primers A, B, C, and D were made (TABLE I.2.1). Forward primer A annealed to the gene start site,

reverse primer B annealed to the end of the sequence - encoding the signal peptide possessing the DNA sequence of the myc or FLAG overhang. Forward primer C annealed to the gene sequence after the signal sequence, and contained a 5' end complementary sequence to the primer B overhang. The reverse primer annealed to the end of the gene. A two-step PCR was used to construct the full length gene containing the myc or FLAG sequence after the signal sequence and the entire product was cloned into the pSWU30 vector using electroporation of the relevant strains.

Alternatively, site directed mutagenesis was used to insert the DNA sequence for the FLAG and myc tags into the pSWU30::*pilY* plasmids. For this purpose, primers were designed to anneal upstream of the signal sequence at the 5' end, followed by the DNA sequence encoding the tag, followed by the 3'end of the primer annealing downstream of the signal sequence. Site directed mutagenesis was conducted as specified by Agilent QuickChange Site-Directed mutagenesis manual. Specifically, a PCR reaction was carried out with the plasmid to be mutated as template. The melting temperature was calculated by the following equation. T_m=81.5+0.41(%GC)-(675/N), where N was the primer length in bases. The extension time was estimated using the 1 min/kb rule, and 18 cycles of PCR were run. The resulting product was digested with *dpnI*, and *E.coli* top 10 cells were transformed with the resulting plasmid.

Construction of E.coli over-expression plasmids

DNA sequence encoding fragments of PilY1 (amino acids 23-329, amino acids 23-196) were amplified by PCR using *M. xanthus* genomic DNA. The PCR products,

along with relevant expression plasmids, pET28a, pET32b, pGEX were digested, followed by ligation and transformation of *E.coli* Top 10 cells. For expression, isolated plasmids were used to transform *E.coli* BL21 cells. To check protein expression, 50 ml of LB containing the appropriate antibiotic were inoculated with a BL21 colony and grown at 37 °C overnight. The culture was diluted 1:100 in fresh LB medium, and allowed to grow at 37 °C until it reached a density of OD_{600} of 0.4-0.7. At this point, 100 µl of the uninduced culture was saved for SDS-PAGE analysis, and the rest of the culture was induced for expression of the protein by adding IPTG at a final concentration of 1 mM and further culture for 5 hours. 50 µl of the induced culture was saved for analysis by SDS-PAGE. 1 ml of the culture was pelleted using a benchtop centrifuge (Eppendorf Model 5417R), and resuspended in 500 µl of Tris/HCl buffer pH 7.6. The sample was sonicated for 30 pulses at a power level 3 with a 30% duty cycle (Branson Sonifier). This was followed by centrifugation for 10 minutes to separate cellular debris from the cytoplasmic supernatant. All four samples, uninduced, induced, pellet and supernatant, were resuspended in equal amounts of Novex Tris-Glycine 2X SDS sample buffer containing 10 mM DTT, boiled in water for 10 minutes and loaded on a 4-20% precast Novex Tris-Glycine gel. The gel cassette was inserted into a XCell SureLock Mini-Cell Electrophoresis system and run at 109 V. The gels were then stained overnight using colloidal Coomassie (Invitrogen) and destained with water the next day.

Pilus shear assay

The pilus shear assay was performed as described previously (109). All strains were grown in CTT medium overnight to a cell density of OD_{600} of 1.0. Cells were harvested by centrifugation and resuspended in 400 µl of a 10 mM Tris buffer, followed by vortexing for 2 minutes at maximum speed using a table- top vortexer (Fisher Scientific). The sample was then centrifuged for 1 min at 14,000 rpm using a table-top centrifuge (Eppendorf). The supernatant was transferred into a fresh tube and the sample was centrifuged for another 5 min at 14,000 rpm. The supernatant was transferred into another fresh tube and 100 mM $MgCl_2$ was added to precipitate the pili overnight at 4 °C. The sample was centrifuged in the morning for 15 min at 14,000 rpm and the supernatant was discarded and the pellets (often not visible) were resuspended in 30 µl of sample buffer (Novex).

Western blot

All protein samples and lysates were prepared by boiling in water for 10 minutes in Novex 2X sample buffer with 10mM DTT.10 µl of protein standard maker (Invitrogen) was lodaded on a precast tris-glycine gel (Invitrogen). 30 µl of boiled samples were also loaded onto the wells of the gel for electrophoresis. The gel was then set up with a nitrocellulose membrane and the proteins were transferred on the membrane in an XCell sure lock mini cell electrophoresis blotting system. The membrane was then incubated in 5% fat free milk for 2 hours at room temperature or overnight at 4°C. Rabbit serum raised against purified T4P fibers was used at a concentration of 1:10,000. Goat anti-rabbit antibody was used at a concentration of 1:25,000.

Exopolysaccharide analysis using calcoflour white staining

Calcoflour white binding assays were performed as described (111). Sterile-filtered calcoflour white (Sigma) was made as a stock solution containing 15 mg/ml. This solution was added to CTT plates containing 0.5% agar at a final concentration of 15 μg/ml. For the assay various strains were grown in liquid CTT culture overnight to mid-log phase. 1 ml of each culture was pelleted and resuspended at a concentration of $5x10^9$ cells/ml. 10 μl of these cell suspensions were spotted in the center of a calcofluor white-containing CTT agar plate, allowed to dry, and incubated at 32 °C for 6 days. A handheld long-wave UV light source (Entela) was used to visualize the calcofluor white-binding pattern, and the image was captured with a digital camera.

Motility assays on agar

All motility assays on agar were performed using standard methods (112). The strains were grown overnight in liquid CTT media culture to mid log phase and 1 ml of a culture containing $4x10^8$ cells/ml were centrifuged and resuspended into TPM medium to a density of $4x10^9$ cells/ml. 10 ul of cells of these suspensions were plated on either 1.5% (hard) agar or 0.5% (soft) agar, as needed. The plates were incubated at 32 °C and the colony diameter was measured after 5 days. To record images an inverted microscope TE800 equipped with a digital camera was used.

Fruiting body assay

Fruiting body assays were performed as described in the literature (106). 1 ml of vegetative culture at $4x10^8$ cells/ml was centrifuged and resuspended in TPM medium at a density of $4x10^9$ cells/ml. 4 ul of the cell suspension was plated on 1.5% TPM agar plates and incubated at 32 °C for 5 days. Images of the fruiting bodies were taken using an inverted microscope TE800 (Nikon) equipped with a digital camera.

Aggregation assay

Aggregation assays were performed according to standard protocols (109, 113). 10 ml of exponentially growing cells was added to glass test tubes. The OD_{600} was measured of each culture at 0 minutes. Then the cultures were allowed to sit on the bench at room temperature. 1 ml of the suspensions was drawn from the top of the test tube every 0.5 hours for 3 hours and OD_{600} was measured using a spectrophotometer (BioRad). The final OD measurement was subtracted from the initial OD and divided by the initial OD, then multiplied by 100 to give the aggregation index in % (105).The results were normalized to the data from the wild type cells.

Percent Aggregation index = [OD_{total}-$OD_{supernatant}$ /OD total] x 100

Hemagglutination assay

Hemagglutination assays were performed as described previously (114). 5 ml of guinea pig blood was added to 95 ml of PBS. The suspension was centrifuged at 5000 x g for 5 min to pellet the erythrocytes and the weight of the cells was measured. The supernatant as well as the surface layer containing the white blood cells were aspirated without disturbing the erythrocyte pellet. The pellet was then washed five times with 100 ml of PBS, followed by centrifugation and aspiration. The final pellet was resuspended to make a 3% erythrocyte suspension in PBS. 25 µl of this suspension along with 20 µl of PBS were placed in each well. Various *M. xanthus* strains starting at $5x10^{7}$ cells/ml were serially diluted into the wells containing the erythrocyte and PBS mix. 1 mg/ml concanavalin A was used as a positive control and 10 mM potassium phosphate buffer pH 7.4 as negative control. The plate was sealed with parafilm, agitated for 1 min followed by an incubation for 4 h at 22 °C. Images of the plates were recorded using a Nikon digital camera.

Crystal violet assay

1 ml of a vegetative culture containing $4x10^{8}$ cells/ml was centrifuged and resuspended into TPM medium to give an OD_{600} of 0.5. 100 µl of this suspension for each strain was then added to a 96 well, non-tissue culture treated microtiter plate. The cells were incubated for 2 h at 32 °C without shaking. The plate was patted on paper towels to remove any non-attaching cells and the wells were rinsed with 100 µl water. The wells

were then stained with 150 µl of a 0.41% crystal violet solution for 10 min. The plate was again patted on a paper towel and washed with water. 200 µl of 95% ethanol was added to each well for 10 min and 100µl of this solution was transferred to a new 96 well plate. The absorbance was measured using the Molecular Devices VMax Kinetic ELISA microplate reader at OD_{595} and analyzed using the SoftMax® pro software. The data from each strain was normalized to the wild-type.

FLAG agarose pull-downs

A DK1622::$pilY1_{C\text{-}FLAG}$ culture was grown for 2 days in two flasks containing 400 ml CTT. The cells were pelleted by centrifugation for 10 min at 9,000 rpm using a Sorvall RC-5C centrifuge. To crosslink the interacting proteins, the lipophilic, membrane-permeable cross-linker DSP was used. For this purpose, the cell pellets were re-suspended to transfer the cells into the reaction buffer (phosphate buffered saline PBS, 0.1 M phosphate, 0.15 M NaCl, pH 7.2) and to remove any remaining media. The cells were washed once more with PBS and the cross-linker was added at a final concentration of 1-2 mM. To prepare the cross-linker solution dry DSP powder was added to DMSO at a concentration of 10 mM. The cells were incubated in the reaction mixture on ice for 2 h. 1 M Tris, pH 7.5 was added for 15 min at a final concentration of 10 mM to stop the reaction.

Upon cross-linking, the cells were lysed, according to the manufacturer's recommendation for usage with ANTI-FLAG M2 affinity gels (Sigma). Therefore, the cells were frozen at -20 °C, followed by resuspension in 10 ml of lysis buffer (50 mM

Tris HCl, pH 7.4, 150 mM NaCl, 1 mM EDTA, and 1% Triton X-100) per gram of cells. The cells were stirred with the lysis buffer for 15 min to fully extract the cross-linked proteins and the samples were centrifuged at 21,000 x g for 15 min.

1 ml of the supernatant was loaded onto the FLAG resin, which had been equilibrated with TBS buffer overnight (50 mM Tris HCl, 150 mM NaCl, pH 7.4). The resin was then washed 3 times with 10 ml of 0.1 M glycine HCl, pH 3.5 buffer to elute unspecifically bound proteins. The sample containing the FLAG- tagged PilY1 was incubated with the resin, and the unbound material was extracted as flow through by gravity. The column was then washed 10 column volumes of TBS.

The agarose was then mixed with 500 µl of sample buffer containing 10 mM DTT, boiled for 10 min, and 40 µl of each sample was loaded on two separate SDS-PAGE gels. One gel was used for staining with colloidal blue and the other one was blotted onto a nitrocellulose membrane, blocked with 5% not fat milk and incubated for 2 h with the primary anti-FLAG M2 antibody at a dilution of 1:1000 in 1xPBS containing 0.05% Tween-20. The membrane was washed three times for 10 min each in PBS with 0.05% Tween-20 and then incubated for 1 h with anti-mouse secondary antibody at a concentration of 1:25,000. Finally, the membrane was washed three times for10 min, incubated for 10 min with the chemiluminescent reagent (Thermo Scientific) and exposed to an autoradiography film. All films were developed in a FUJI film processor.

Electron microscopy

A 2 µl drop containing purified pili was placed onto of piece of parafilm. Carbon-coated copper or gold electron microscopic grids (EMS) were placed on top of the drop for 2 min before washing the grid twice with water for 30 seconds and placing it on top of a drop of unbuffered 2% uranyl acetate for 1 min. The negatively stained grids were allowed to dry and analyzed under the electron microscope. Pictures were taken with an AMT ER50 5 megapixel CCD camera and analyzed using the AMT Image Capture Engine software.

Trypan blue assay

Trypan blue assays were performed as described in the literature (115). Strains were grown in CTT medium to an OD of $5x10^8$ cells/ml, harvested by centrifugation, and re-suspended in TPM to $5x10^8$ cells/ml. A stock solution of trypan blue was made containing 100 µg/ml of the dye and 1 ml aliquots of cells were mixed with this solution to give a final concentration of the dye of 10 µg/ml. Cell-free TPM buffer containing 15 µg/ml trypan blue was used as a negative control. All samples were incubated at 32 °C for 30 min. The cells were then pelleted in a table-top centrifuge for 5 min at 12,000 RPM. The supernatant was pipetted into disposable spectrophotometer cuvettes (Fisher Scientific) and the OD was measured at 585 nm.

List of Primers used in this study

Primer Name	Sequence	Description
SA01	ATTAAAGCTTGCTAGCCATCATGACCCACT	1365 deletion A
SA02	GCTGTCAGGGTGGAGAAGAG	1365 deletion B
SA03	TGCTCCAGAACGTGTACGAG	1365 deletion C
SA04	CACGTCCATGTTGTCCTCAAGAATTCATTA	1365 deletion D
SA05	GCGCGCGGGGTTGAGCAG	1365 deletion test internal
SA06	ATTAAAGCTTCCTTGACCTCTCGTTGAG	0362 deletion A
SA07	CCATCAGCAGGATGGCCAGATGAGGGTGCG CATCAC	0362 deletion B
SA8	GTGATGCGCACCCTCATCTGGCCATCCTGCT GATGG	0362 deletion C
SA9	TAATGAATTCGCAGTGGCAATCATCACC	0362 deletion D
SA10	CCTGGCCCGACTCAG	0362 deletion test forward
SA11	CCCGGTGACCTGCGC	0362 deletion test reverse
SA12	CGAGCTGGTTTTCGCACA	0362 deletion test internal
SA13	ATTAAAGCTTGGCGTGCCCTGGCGA	1020 deletion A
SA14	GGAACCTGCGCCGGTCGGTGCTTCAGGGCC	1020 deletion B
SA15	GGCCCTGAAGCACCGACCGGCGCAGGTTCC	1020 deletion C
SA16	TAATGAATTCTGGCGTGGGGAAGCG	1020 deletion D
SA17	CTGCCCGACGTCGCC	1020 deletion test forward
SA18	GCGCACCGGGCTCTT	1020 deletion test reverse
SA19	CGCCACTGCCCGTGT	1020 deletion test internal
SA20	ATTAAAGCTTACGGGTGACAACCCAGAC	0361 deletion A
SA21	GATGGCGCGTCAAAGTCGTCTTGCGGCATCC TCCCGTCC	0361 deletion B
SA22	GGACGGGAGGATGCCGCAAGACGACTTTGA CGCGCCATC	0361 deletion C
SA23	TAATGAATTCGGGCGAGGGATTCTCAAC	0361 deletion D
SA24	CCGGTGCTGGCGCTCTT	0361 deletion test internal
SA25	ATTAAAGCTTCACCCTGATTGCCCTGAC	1365 native promoter complementation native locus 5’
SA26	TAATGGATCCCACGTCCATGTTGTCCTCAA	1365 native promoter complementation

		native locus 3’
SA27	ATAGCCGGATCCATGTTCGCGGCTGAAGGTG TT	1365 native promoter complementation attB site 5’
SA28	ATAGCCGAATTCCCCGTCTTCTAACGCCAGA C	1365 native promoter complementation attB site 3’
SA29	ATTAAAGCTTCCTTGACCTCTCGTTGAG	0362 native promoter complementation native locus 5’
SA30	TAATGGATCCGCAGTGGCAATCATCACC	0362 native promoter complementation native locus 3’
SA31	ATAGCCTCTAGAATGGCAAGCTCGCCTTCGA GA	0362 native promoter complementation attB site 5’
SA32	ATAGCCGGATCCACCTCCAGGAGCGTGATG	0362 native promoter complementation attB site 3’
SA33	ATTAAAGCTTAGAGCTCATTCCCCAGACG	1020 native promoter complementation native locus 5’
SA34	TAATGGATCCCTCTTCCATCCAGCTCACG	1020 native promoter complementation native locus 3’
SA35	ATAGCCGGATCCATGCTCCGTCGAAATCAAC GAC	1020 native promoter complementation attB site 3’
SA36	ATAGCCGAATTCCGATGGTCTCCAGGATGC	1020 native promoter complementation attB site 3’
SA37	ATAGCCAAGCTTGTGAAGACCCGTGCTGCG	pilA promoter in pSWU30 5’
SA38	ATAGCCTCTAGAGGGGGTCCTCAGAGAAGG	PilA promoter in pSWU30 3’
SA39	ATAGCCGGTACCATGAAGGCACTCTTCTCCA CC	1365 attB pPilA complementation 5’
SA40	ATAGCCGAATTCTCACGGCAGGCAACTGGC	1365 attB pPilA complementation 3’
SA41	ATAGCCTCTAGAGTGATGCGCACCCTCATC	0362 attB pPilA complementation 5’
SA42	ATAGCCGGATCCTCACTGCGGCATCCTCCC	0362 attB pPilA complementation 3’
SA43	ATAGCCTCTAGAATGCGCTGGACTCGAACC	1020 attB pPilA complementation 5’

SA44	ATAGCCGGATCCTCATGGCACCACCTCCTG	1020 attB pPilA complementation 3’
SA45	ATAGCCGGTACCATGATGAAGGCACTCTTCTCCACC	1365 C-term FLAG tag 5’
SA46	ATAGCCGAATTCTCACTTGTCATCGTCATCCTTGTAATCCGGCAGGCAACTGGCCGC	1365 C-term FLAG tag 3’
SA47	ATAGCCGGATCCATGTTCGCGGCTGAAGGTGTT	1365 N-term HA tag A attB site native promoter
SA48	AGCGTAGTCTGGGACGTCGTATGGGTACGCGAGCGCGCCAGG	1365 N-term HA tag B attB site native promoter
SA49	TACCCATACGACGTCCCAGACTACGCTCAGGACCCGGCGTCT	1365 N-term HA tag C attB site native promoter
SA50	ATAGCCGAATTCCCCGTCTTCTAACGCCAGAC	1365 N-term HA tag D attB site native promoter
SA51	GGCGCGCTCGCGTACCCATACGACGTCCCAGACTACGCTCAGGACCCGGCG	1365 N-term HA tag site directed mutagenesis 5’
SA52	CGCCGGGTCCTGAGCGTAGTCTGGGACGTCGTATGGGTACGCGAGCGCGCC	1365 N-term HA tag site directed mutagenesis 3’
SA53	ATAGCCAAGCTTATGGCAAGCTCGCCTTCGAGA	0362 N-term myc tag A attB site native promoter
SA54	CAGATCTTCTTCAGAAATAAGTTTTTGTTCCATGGCGGAGGCCAACGG	0362 N-term myc tag B attB site native promoter
SA55	ATGGAACAAAAACTTATTTCTGAAGAAGATCTGCAGACCACGCCGGAG	0362 N-term myc tag C attB site native promoter
SA56	ATAGCCGGATCCACCTCCAGGAGCGTGATG	0362 N-term myc tag D attB site native promoter

SA57	CCGTTGGCCTCCGCCGAACAAAAACTTATTTCTGAAGAAGATCTGCAGACCACGCCGGAG	0362 N-term myc tag site directed mutagenesis 5’
SA58	CTCCGGCGTGGTCTGCAGATCTTCTTCAGAAATAAGTTTTTGTTCGGCGGAGGCCAACGG	0362 N-term myc tag site directed mutagenesis 3’
SA59	ATAGCCGGATCCATGCTCCGTCGAAATCAACGAC	1020 N-term FLAG tag A attB site native promoter
SA60	CTTGTCATCGTCATCCTTGTAATCGGCGAGCACGGCTCC	1020 N-term FLAG tag B attB site native promoter
SA61	GATTACAAGGATGACGATGACAAGCAAAGTCCCGGCGGC	1020 N-term FLAG tag C attB site native promoter
SA62	ATAGCCGAATTCCGATGGTCTCCAGGATGC	1020 N-term FLAG tag D attB site native promoter
SA63	ATAGCCGGTACCATGAAGGCACTCTTCTCCACC	1365 N-term HA tag A attB site pilA promoter
SA64	AGCGTAGTCTGGGACGTCGTATGGGTACGCGAGCGCGCCAGG	1365 N-term HA tag B attB site pilA promoter
SA65	TACCCATACGACGTCCCAGACTACGCTCAGGACCCGGCGTCT	1365 N-term HA tag C attB site pilA promoter
SA66	ATAGCCGAATTCTCACGGCAGGCAACTGGC	1365 N-term HA tag D attB site pilA promoter
SA67	ATAGCCTCTAGAGTGATGCGCACCCTCATC	0362 N-term HA tag A attB site pilA promoter
SA68	CAGATCTTCTTCAGAAATAAGTTTTTGTTCCATGGCGGAGGCCAACGG	0362 N-term HA tag B attB site pilA promoter

SA69	ATGGAACAAAAACTTATTTCTGAAGAAGATC TGCAGACCACGCCGGAG	0362 N-term HA tag C attB site pilA promoter
SA70	ATAGCCGGATCCTCACTGCGGCATCCTCCC	0362 N-term HA tag D attB site pilA promoter
SA71	ATAGCCTCTAGAATGCGCTGGACTCGAACC	1020 N-term HA tag A attB site pilA promoter
SA72	CTTGTCATCGTCATCCTTGTAATCGGCGAGC ACGGCTCC	1020 N-term HA tag B attB site pilA promoter
SA73	GATTACAAGGATGACGATGACAAGCAAAGT CCCGGCGGC	1020 N-term HA tag C attB site pilA promoter
SA74	ATAGCCGGATCCTCATGGCACCACCTCCTG	1020 N-term HA tag D attB site pilA promoter
SA75	GGAGCCGTGCTCGCCGATTACAAGGATGAC GATGACAAGCAAAGTCCCGGCGGC	1020 N-term FLAG tag site directed mutagenesis 5’
SA76	GCCGCCGGGACTTTGCTTGTCATCGTCATCC TTGTAATCGGCGAGCACGGCTCC	1020 N-term FLAG tag site directed mutagenesis 3’
SA77	ATATATCATATGGCGCAGGACCCGGCG	pET281365 His tag F aa 23-196
SA78	ATATATGAGCTCCTAGGCGCACGCCTCTGC	pET281365 His tag R aa23-196
SA79	ATATATGCGGCCGCGCGCAGGACCCGGCG	pET32 1365 His tag F aa 23-196
SA80	ATATATGAGCTCCTAGGCGCACGCCTCTGC	pET32 1365 His tag R aa 23-196
SA81	ATATATGCGGCCGCGCGCAGGACCCGGCG	pET32 1365 His Tag F aa 23-329
SA82	ATATATGAGCTCCTAGCAGGTGGCGGCTCGT CC	pET32 1365 His Tag R aa 23-329
SA83	ATATATGCGGCCGCGCGCAGGACCCGGCG	pGTK 1365 GST tag F aa 23-196
SA84	ATATATGTCGACCTAGGCGCACGCCTCTGC	pGTK 1365 GST tag R aa 23-196

SA85	ATATATGCGGCCGCGCGCAGGACCCGGCG	pGTK 1365 GST tag F aa 23-329
SA86	ATATATGTCGACCTAGCAGGTGGCGGCTCGTCC	pGTK 1365 GST tag R aa 23-329
SA87	ATATATGGCCGCCAGGACCCGGCGTCTTGCAGC	pET21 1365 C-His tag F 23-510 aa
SA88	ATATATATCTCGAGGAGGCGGGCGACATGCGCGG	pET21 1365 C-His tag R 23-510 aa
SA89	ATATATGGCCGCCAGGACCCGGCGTCTTGCAGC	pET21 1365 C-His tag F 23-658 aa
SA90	ATATATATCTCGAGATGTCGTTCACCCAGGTCT	pET21 1365 C-His tag R 23-658 aa

TABLE 3.1: List of primers used in study described in chapter I.

I.3 RESULTS

Using a novel isolation method, type IV pili were purified from the hyper-piliated M. xanthus ΔdifE and ΔpilT strains that contained a PilY1 homolog

We accomplished for the first time large-scale isolations and purifications of the type IV pilus of *M. xanthus* to apparent homogeneity as judged by electron microscopy and SDS-PAGE by developing a new isolation protocol in our laboratory. So far, researchers had only used the pilus shear assay (described in the Materials and Methods section) to detect pili. Although this assay uses very few cells, it is not sensitive enough to detect low abundance proteins like minor pilins (109). In fact, the shear assay results in the isolation of so few pili that in Coomassie-stained SDS gels the PilA band cannot be directly visualized but has to be detected using Western blots and an anti-PilA antibody. Because potential accessory proteins of the type IV pilus in *M. xanthus* are likely present in substantially lower abundance than PilA, we decided to isolate large quantities of pili for protein gel electrophoresis and Coomassie staining. Our protocol enabled us to isolate sufficient amounts of ultrapure pili that allowed us to detect a minor protein that consistently co-purified with PilA and therefore is highly likely a *bona fide* minor pilin (FIGURE I.3.1). To isolate the pili, *M. xanthus* cells from hyper-piliated strains such as *ΔdifE* or *ΔpilT* were grown to a late log phase in 8 flasks containing 400 ml of CTT medium. The cells were harvested by centrifugation at 11,000 rpm using a Sorvall floor

centrifuge and an SLA3000 rotor and the culture supernatants were pooled. The supernatant was then centrifuged for 10 min in an SS34 rotor at 20,500 rpm and collected in a beaker. 150 mM NaCl (Sigma) and 2% PEG 20K (Alpha Aesar) were added to the supernatant and the solution were allowed to stand overnight at 4 °C. The chilled solution was then centrifuged for 15 min in an SS34 rotor at 20,500 rpm and the small whitish pellets were retained. The pili-containing pellets were re-suspended in 8 ml of a 10 mM Tris buffer pH7.5 containing 2 mM $MgSO_4$. This solution was allowed to settle for 30 min to sediment the struvite crystals (inorganic magnesium phosphate crystals that are formed by the cells), and centrifuged for another 6 min at 4,000 rpm in an HB6 rotor. The supernatant was poured off into a fresh tube to which 150 mM NaCl was added. The solution was re-centrifuged at 10,000 rpm for 6 min to obtain a clear supernatant. 2% PEG 20K was added to this solution and dissolved. The solution was allowed to settle overnight at 4 °C and was then centrifuged at 8,000 rpm for 10 min, followed by the analysis of the small white pellets by electron microscopy and SDS-PAGE. An average isolation from 8x400 ml culture supernatant resulted in the purification of ca. 5-10 mg purified pili.

Using this method, the following results were obtained. As FIGURE I.3.1 shows, the pili had been purified to homogeneity based on electron microcroscopic images that showed no other structures than pili being present in these purified samples. When analyzed on SDS-PAGE one major and very few minor bands were visible after staining with colloidal Coomassie. Mass spectrometry showed that all of these bands were composed of PilA, the major pilin, except one high molecular weight band running between the 98 kDa and 250 kDa marker bands. This protein band was identified as the

hypothetical protein MXAN_1365, which had a calculated molecular weight of about 160 kDa. Why PilA runs at multiple molecular weights is currently unclear, but one possibility is that the higher molecular bands of the protein correspond to multimers such as dimer, trimers, etc. The more pronounced lower molecular weight band of PilA appeared to be a modified version of the protein according to our mass spectrometry data.

A

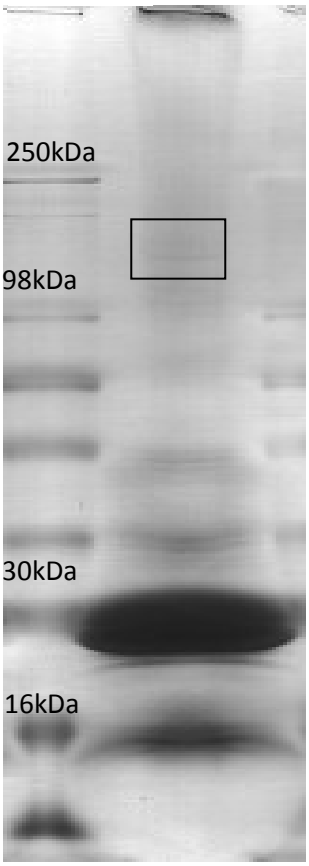

B

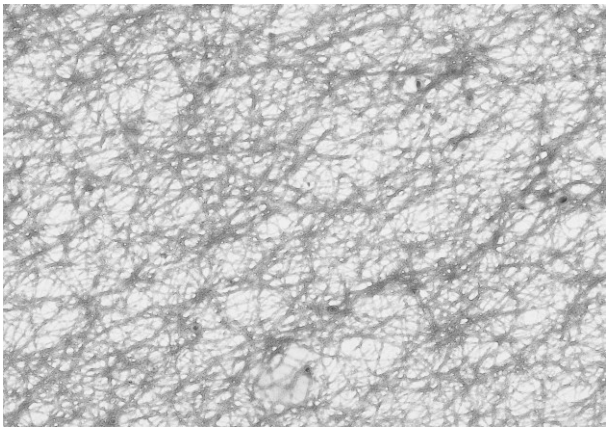

FIGURE I.3.1: A: Coomassie stained SDS-PAGE of purified pili from *ΔdifE*. The dominant and all other minor bands were identified by MALDI-TOF MS as PilA. The only exception was a high molecular weight band around 160 kDa (marked with a box), which is the hypothetical protein MXAN_1365. B: Electron micrograph showing uranyl acetate negatively stained pili of a representative isolation at low magnification. Note, the picture shows no other structures than pili demonstrating the purity of the preparation (courtesy of Dr. Egbert Hoiczyk).

Bioinformatics analysis

MXAN_1365 is a homolog of the P. aeruginosa minor pilin PilY1, and the Neisseria spp. PilC, and genetic analysis suggests that the genome contains two further genes encoding paralogs

MXAN_1365 is a hypothetical protein according to the annotation of the NCBI database and shows homology to the *P. aeruginosa* PiY1 and the *Neisseria* PilC minor pilins. Genetic analysis of the *M. xanthus* genome revealed the presence of two further open reading frames (ORFs), *MXAN_0362* and *MXAN_1020* coding for two potential paralogs of MXAN_1365 (FIGURE I.3.2, I.3.3, TABLE I.3.1).

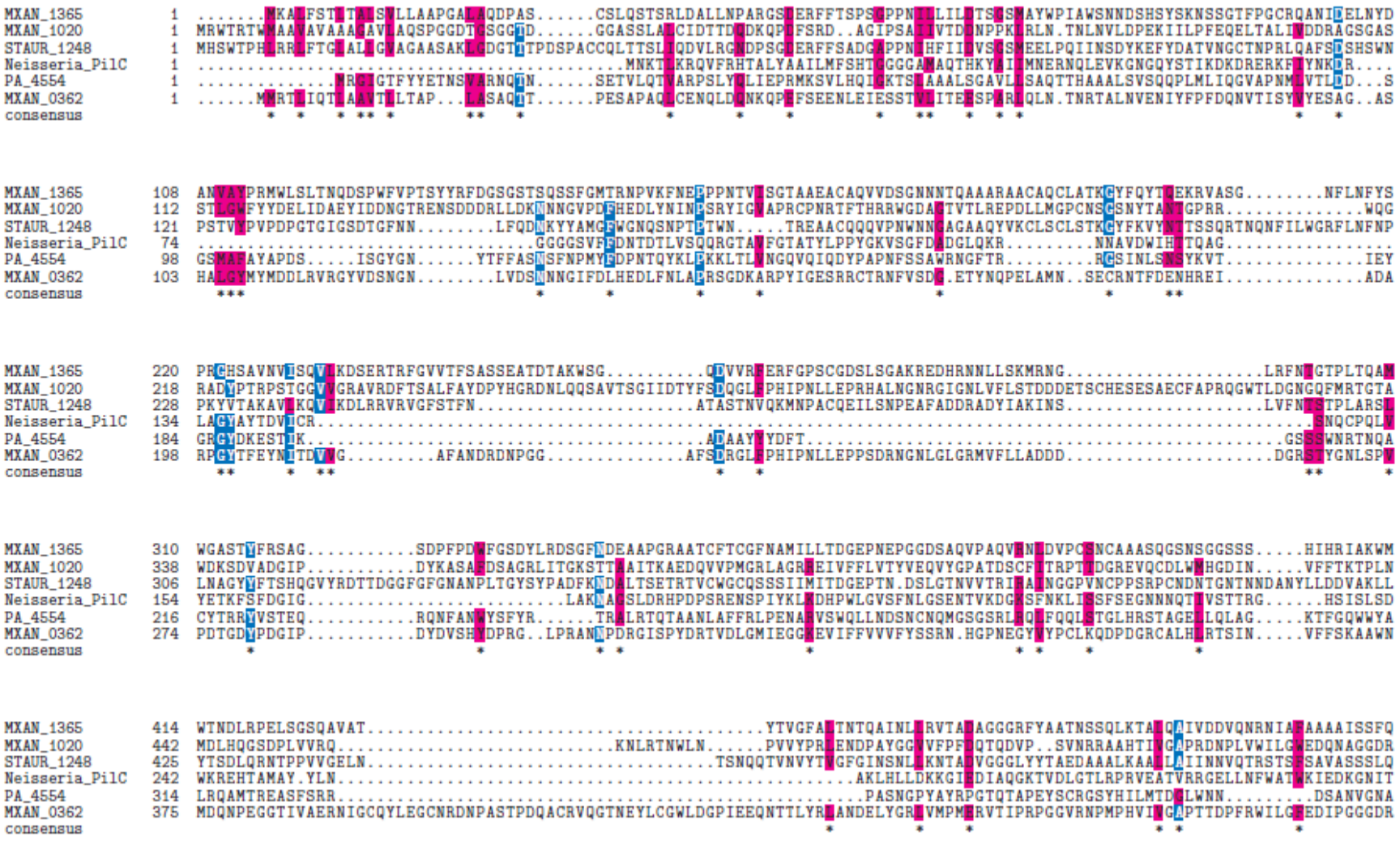

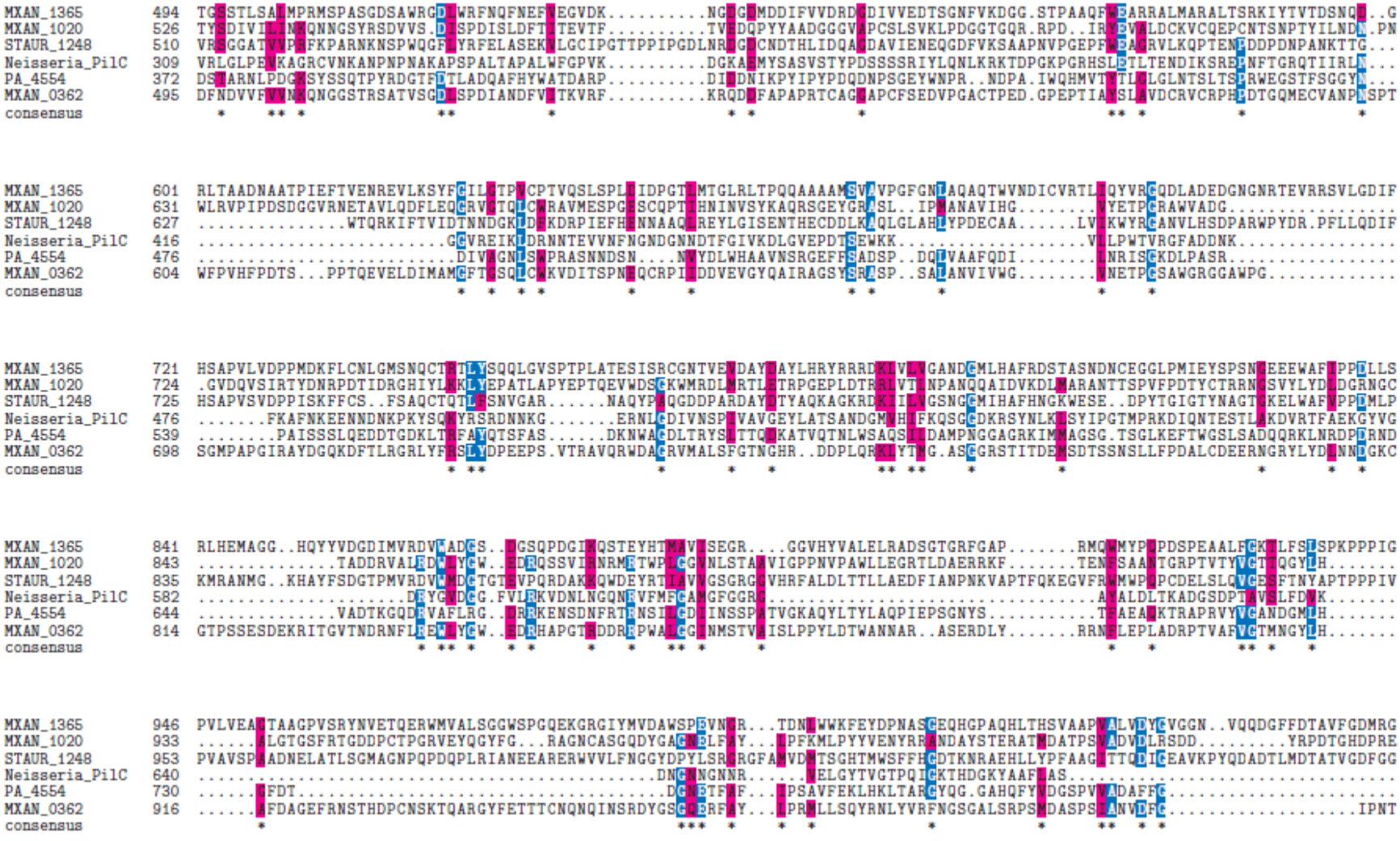

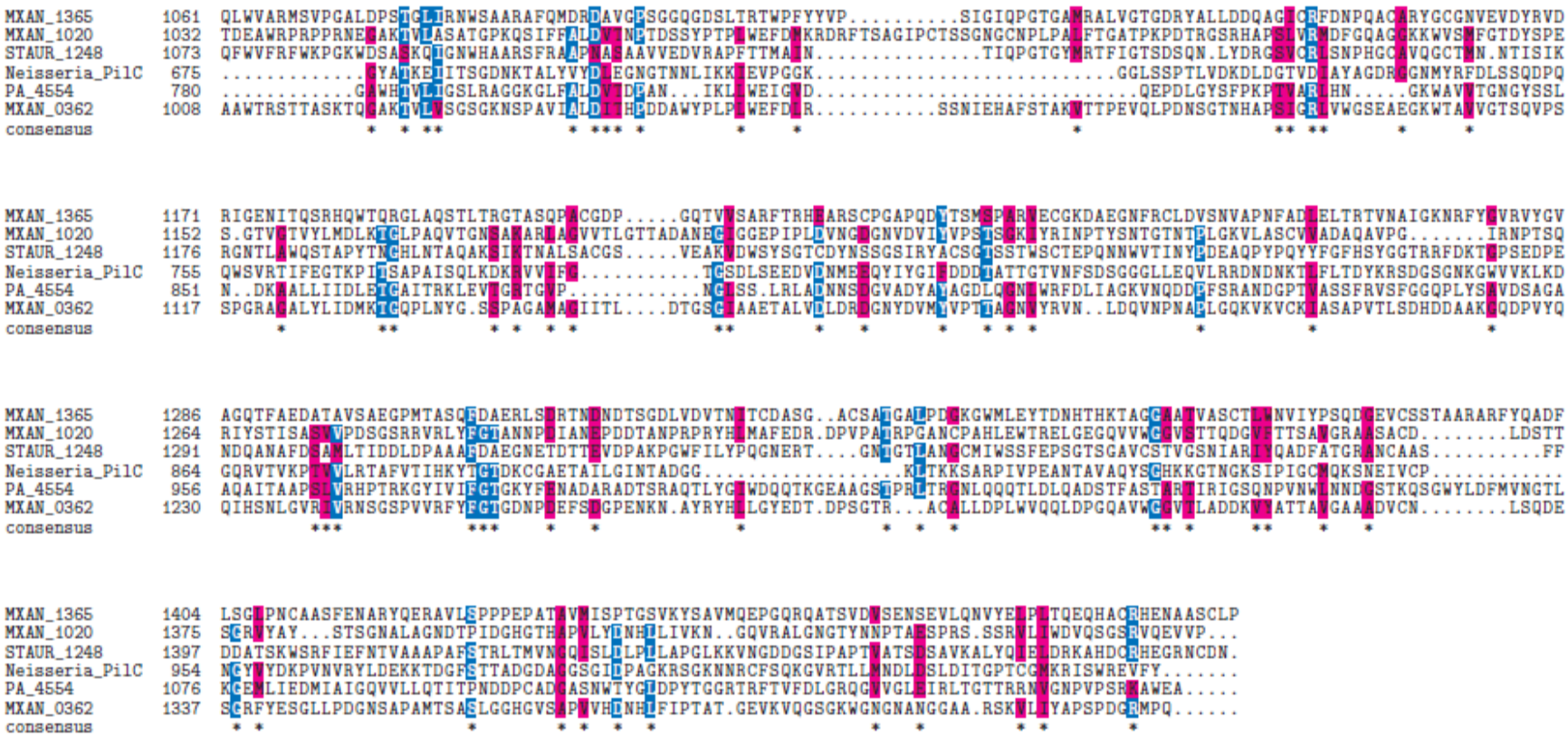

FIGURE I.3.2: Alignment of the full length protein sequences of the *M. xanthus* proteins MXAN_1365, MXAN_1020, and MXAN_0362 together with *P. aeruginosa* PilY1 (PA_4554), *N. gonorrhoeae* PilC and *Stigmatella aurantiaca* STAUR_1248. Dark shade indicates similar amino acids while light shade indicates more than 50% conservation in amino acid homology.

Proteins	% identity
PilY1 and MXAN_1365	27
PilY1 and MXAN_0362	25
PilY1 and MXAN_1020	22
MXAN_1365 and MXAN_0362	26
MXAN_1365 and MXAN_1020	28
MXAN_0362 and MXAN_1020	36
MXAN_1365 and PilC1	25
MXAN_0362 and PilC1	23
MXAN_1020 and PilC1	22

TABLE: I.3.1 Percent identity between various PilY proteins.

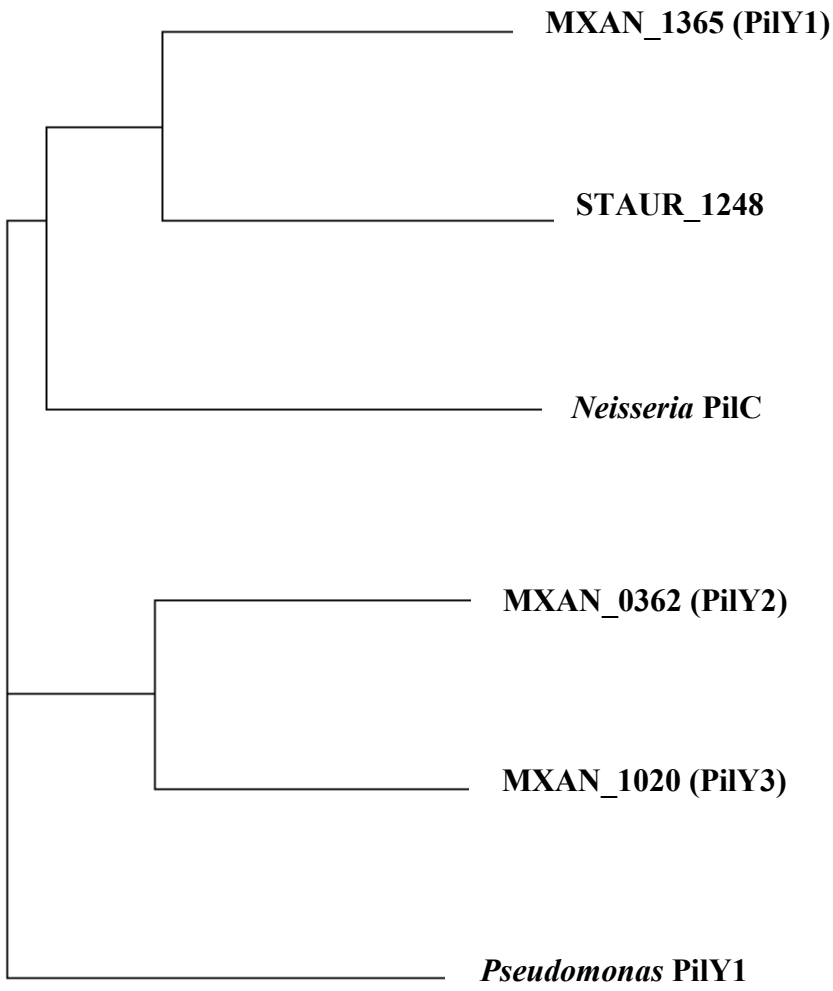

FIGURE I.3.3: Phylogenetic tree of *M. xanthus, P. aeruginosa, S. aurantiaca* and *Neisseria* PilY proteins, based on protein sequence alignments.

MXAN_1365 contains a predicted N-terminal integrin domain, while MXAN_0362 encodes a predicted N-terminal lectin domain

MXAN_1365 encodes a protein of 1494 amino acids length that we decide to rename PilY1. Its N- terminal contains a predicted integrin alpha M domain[2] (TABLE I.3.2). Interestingly, PilY1 of *P. aeruginosa* and MXAN_1365 are very similar structurally sharing 9 out of the top 10 predicted hits with respect to their N-terminal domain (TABLE I.3.3). MXAN_1365 also has a predicted signal peptide (FIGURE I.3.4),

[2] HHPRED server is used to evaluate predicted domains in the protein. A predicted hit is considered reliable if it has (1) >50% probability, or (2) >30% probability and is among the top three hits. The *E-value* is also an alternative measure of statistical significance. It indicates how many chance hits with a score better than this would be expected if the database contained only hits unrelated to the query. At E-values below one, matches start to get marginally significant. Contrary to the probability, when calculating the E-value HHpred does not take into account the secondary structure similarity. Therefore, the probability is a more sensitive measure than the E-value.

indicating that the protein is secreted. In contrast, MXAN_0362 encodes a 1419 amino acids long protein that we re-named PilY2 and that contained a predicted lectin-like domain in its N-terminus (TABLE I.3.4). Like MXAN_1365, MXAN_0362 is likely to be secreted because it also contains a predicted signal peptide (FIGURE I.3.5). Finally, MXAN_1020 encodes a 1456 amino acids long protein re-named PilY3 which possesses a predicted signal peptide but lacks any other easily detected structural known domains (FIGURE I.3.6). Phylogenetic analyses suggest that PilY2 and PilY3 are more closely related to each other than they are to PilY1 (FIGURE I.3.7).

TABLES I.3.2-I.3.5 list the N-terminal predicted domains of PilY1, *P. aeruginosa* PilY1 PA_4554, PilY2 and PilY3.

Number	Hit	Probability	P-value	E-value	Template
1	Aerotolerance related membrane protein	99.8	1.3E-24	3.9E-20	7-211
2	VON willebrand factor type A	99.8	1.1E-23	3.4E-19	74-260
3	Complement factor B; VON willebrand factor	99.7	9.3E-20	2.8E-15	12-223
4	Complement C2;C3/C5	99.6	2.5E-19	7.6E-15	5-210
5	Magnesium-chelatase 60 kDa subunit	99.6	2.3E-21	7E-17	7-187
6	Anthrax toxin receptor 2	99.6	6.9E-19	2.1E-14	5-181
7	Complement factor B	99.6	1.9E-18	5.7E-14	2-201
8	SPRPN10, 26S proteasome regulatory subunitRPN10	99.5	4.3E-18	1.3E-13	4-181
9	Anthrax toxin receptor 1	99.5	2.9E-18	8.6E-14	6-184
10	Integrin alpha M; cell adhesion	99.5	2.4E-18	7.1E-14	2-194

TABLE I.3.2: Predicted N-terminal domains of MXAN_1365, PilY1.

Number	Hit	Probability	P-value	E-value	Template
1	VON willebrand factor type A	99.3	1.6E-15	4.7E-11	94-;'p[261
2	Aerotolerance-related membrane protein	99.2	5.9E-15	1.8E-10	26-211
3	Complement factor B; VON willebrand factor	98.9	9.2E-13	2.8E-08	30-218
4	Complement C2; C3/C5 convertase	98.9	8.9E-13	2.7E-08	24-210
5	Complement factor B; BB, hydrolase	98.7	7.3E-12	2.2E-07	16-202
6	Anthrax toxin receptor 2	98.5	5.5E-11	1.7E-06	20-181
7	SPRPN10, 26S proteasome regulatory subunit RPN10	98.4	7.4E-11	2.2E-06	20-181
8	Complement factor B; serine protease	98.4	2.1E-10	6.4E-06	254-447
9	Integrin alpha M; cell adhesion	98.4	2.8E-11	8.5E-07	20-189
10	Cell WALL surface anchor family protein; VWFA fold	98.3	5.8E-11	1.8E-06	32-373

TABLE I.3.3: Predicted N-terminal domains of *P. aeruginosa* PA_4554 (PilY1).

Number	Hit	Probability	P-value	E-value	Template
1	Lectin, BCLA sugar binding protein bacterial lectin, oligosaccharides	34.3	0.00087	26	105-124
2	Protein RSC3288, lectin sugar-binding protein, D-mannose	34.3	0.0011	33	84-110
3	Pseudomonas aeruginosa lectin II; fucose, calcium; HET	33.1	0.0012	35	84-110
4	Lectin, CV IIL; mannose	32.3	0.0012	37	83-109
5	Lectin, sugar binding protein	27.5	0.0015	46	88-112
6	PTU-1 Ca Channel	23.5	0.00095	29	7-18
7	Heparan sulfate D-glucosaminyl 3-O- sulfotransferase 3A1		0.00087	26	1-27
8	IGG1 intact antibody	18.8	0.003	90	42-122
9	DNA polymerase III	18.2	0.004	1.2E2	68-101
10	Next to BRCA gene 1 protein	18.0	0.00062	19	13-52

TABLE I.3.4: Predicted N-terminal domains of PilY2.

Number	Hit	Probability	P-value	E-value	Template
1	Probable resuscitation-promoting factor RPFB	61.6	5E-05	1.5	10-48
2	OMCI, complement inhibitor	36.5	0.001	32	83-119
3	Protein RSC3288; lectin, sugar-binding protein, D-mannose	33.1	0.0012	36	84-110
4	Lectin, BCLA; sugar binding protein, bacterial lectin, oligosaccharides	31.6	0.001	31	105-124
5	Pseudomonas aeruginosa lectin II	31.4	0.0013	40	84-110
6	Lectin CV-IIL; mannose	30.5	0.0014	43	83-109
7	UNDA; beta-barrel, C-type cytochrome, electron transport	28.7	0.00041	12	2-33
8	YCF48-like protein	26.6	0.0015	46	225-312
9	KIAA1568 protein	26.3	0.0038	1.1E+02	36-106
10	Lectin; sugar binding protein	26.0	0.0017	51	88-112

TABLE I.3.5: Predicted N-terminal domains of MXAN_1020, PilY3.

Top 10 hits as predicted by HHPRED with respect to the N-terminal amino acid sequences of the *M. xanthus* proteins PilY1, PilY2, and PilY3 as well as for *P. aeruginosa* PA_4554 PilY1. The shared hits between MXAN_1365 (PilY1) and PA_4554 are highlighted in yellow.

All three PilY proteins are secreted

All three *M. xanthus* proteins, PilY1, PilY2, and PilY3 are predicted to be secreted, as determined by the presence of canonical Gram-negative signal peptides at their N-termini. The SignalP server at the University of Denmark Odenske was used for the analysis of the sequences. The length of the predicted signal peptides of about 20 amino acids is in good agreement with the length of other determined signal peptides for secreted proteins such as the secretin PilQ.

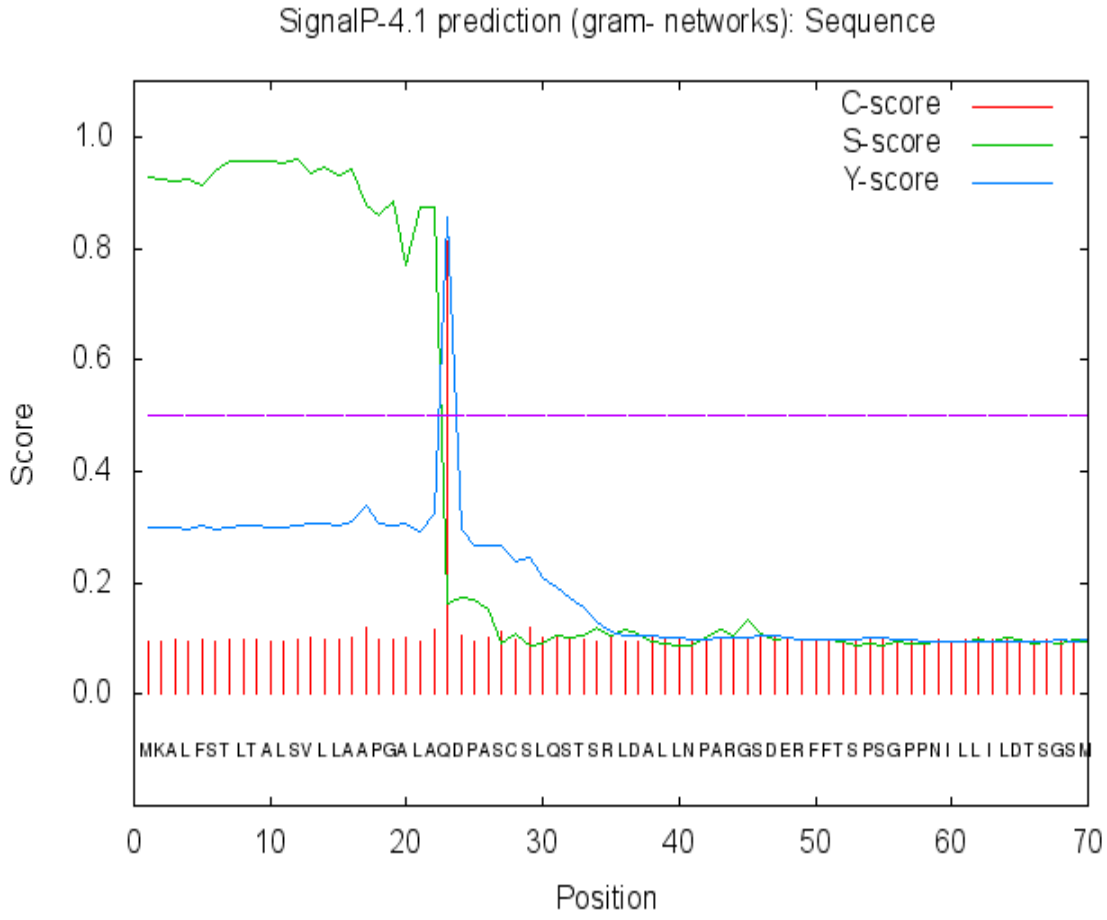

FIGURE I.3.4 SignalP results for the predicted signal peptide of PilY1. The signal peptide is predicted to be cleaved between amino acid number 22 and 23.

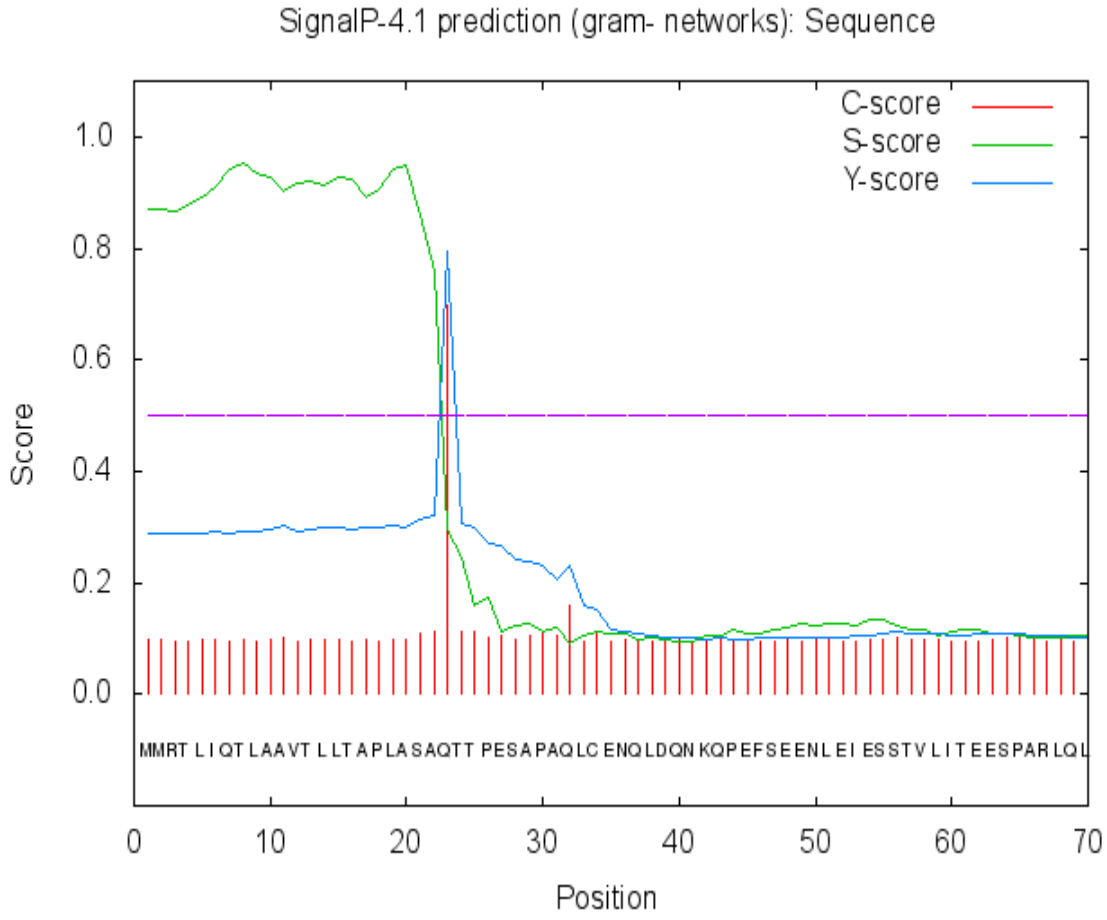

FIGURE I.3.5 SignalP results for the predicted signal peptide of PilY2. The signal peptide is predicted to be cleaved between amino acid 22 and 23.

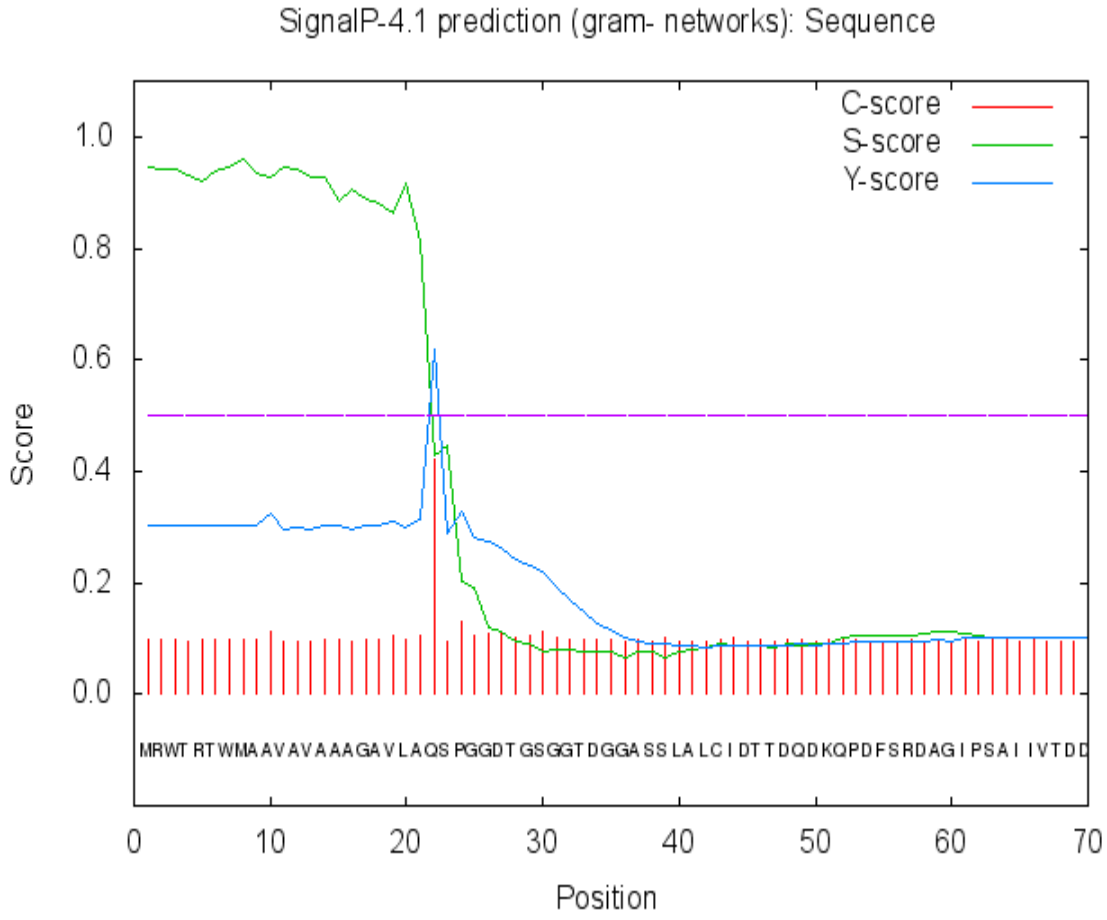

FIGURE I.3.6 SignalP results for the predicted signal peptide of PilY3. The signal peptide is predicted to be cleaved between amino acid 21 and 22.

PilY1: MXAN_1365: type IV pilus assembly protein PilY1-1494aa

PilY2: MXAN_0362: type IV pilus assembly protein PilY2-1419aa

PilY3: MXAN_1020: hypothetical protein PilY3- 1456aa

FIGURE I.3.7 Schematic representation of predicted domains of PilY1, PilY2, and PilY3. (SP- Signal Peptide)

The three genes encoding the PilY homologs of *M. xanthus* are flanked by other ORFs that encode proteins with predicted homology to minor type IV pilins. A comparison of the operon encoding *pilY1* in *P. aeruginosa* with that encoding MXAN_1365, MXAN_0362, and MXAN_1020 in *M. xanthus* reveals many genes that encode homologous minor pilin proteins, which are conserved between these two species (FIGURE I.3.8). Moreover, several genes in the operons containing *MXAN_1365*, *MXAN_0362*, and *MXAN_1020* are paralogs, as well as have homology to *pilY1* operon genes.

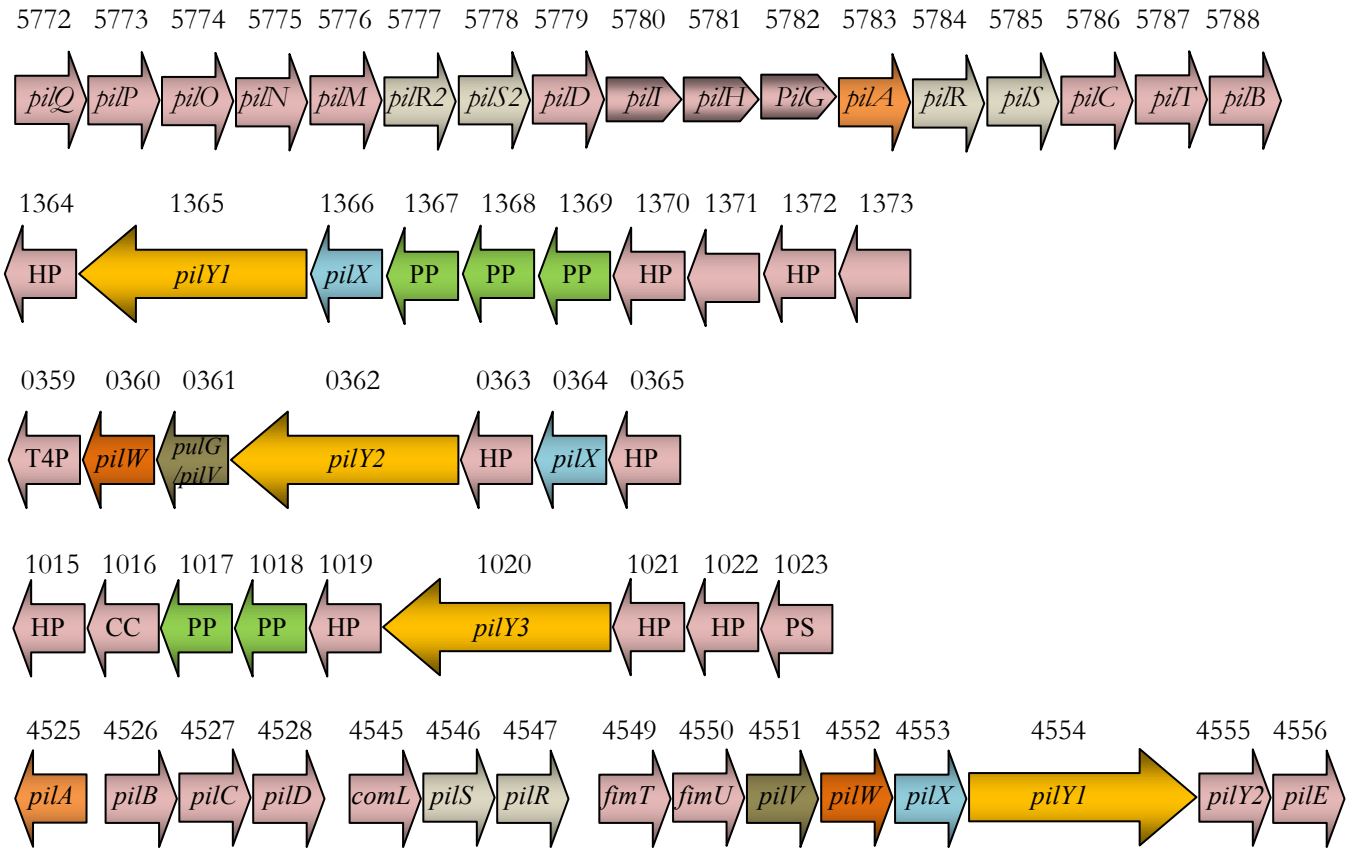

FIGURE I.3.8: Predicted structures of the operons containing *P. aeruginosa pilY1* (*PA_4554*) as well as *M. xanthus MXAN_1365* (*pilY1*), *MXAN_0362* (*pilY2*), and *MXAN_1020* (*pilY3*). The operon encoding most of the canonical pilus proteins in *M. xanthus* is also shown. Predicted homologous proteins are indicated by the same color. HP: hypothetical protein; PP: prepilin-type N-terminal cleavage/methylation domain-containing protein; T4P: type IV pilus biogenesis protein; CC: cytochrome C family protein; PS: prystinamycin I synthase 3.

PilY1, PilY2 and PilY3 influence social motility

Because PilY is important for twitching motility in *Pseudomonas*, I reasoned that *M. xanthus* PilY1, PilY2 and PilY3 may also be important for type IV pilus-mediated motility. In order to determine their biological function, I made therefore in-frame deletions of all three genes encoding these proteins initially in the wild-type background. Moreover, because of the possibility that these proteins may have similar functions I also generated double and triple deletions as to examine the effects of these manipulations on motility, piliation and cell aggregation and swarming. To assess the effect on motility, I performed motility assays with all strains by spotting 10 µl of concentrated cells in the middle of a media petri dish containing 0.5% or 1.5% agar to monitor the effect on S- and A-motility.

Surprisingly, deletion of the pilus-tip protein encoding gene *pilY1*in the wild-type background had no discernible effect on S-motility. The diameter of swarm colonies measured after six days of swarming were similar to that of the original wild-type strains (FIGUREs I.3.9 B, I.3.12). Moreover, the colony edge of these swarms looked comparable to the ones of the wild-type when viewed under an inverted microscope at 10x magnification (FIGUREs I.3.10 B, I.3.11 B).

More surprisingly, deletion of *pilY2* in the wild-type background reduced the efficiency of S-motility by about 30 percent, as determined by the swarm diameter of actively spreading colonies at the end of six days (FIGURE I.3.9 C, I.3.12). Intriguingly,

the swarm edges of these mutant colonies looked less contiguous and the cells have less contact than cells at the edge of typical wild-type swarms when viewed at 10x magnification. Often could flares of cells as well as individuals cells be seen separating from the swarm edge indicating that these cells aggregated less than the wild-type (FIGURE I.3.10 C, I.3.11C). Thus, I hypothesized that the product of *pilY2* is needed for the cohesiveness of the cells, a phenomenon intimately linked to efficient swarming.

Deletion of *pilY3* in a wild-type background resulted in a phenotype that looked similar to that of Δ*pilY1* or original wild-type phenotype. Likewise, the colony diameter and swarm edges of this strain did not show any apparent differences when compared with these two strains (FIGUREs I.3.9 D, I.3.12, I.3.10 D, and I.3.11 D).

I next examined double and triple deletion strains. A striking swarming defect was observed for the strain carrying a double deletion of *pilY1* and *pilY2*. The swarm diameter of this strain was comparable to the one observed for the Δ*pilA* strain, cells that lack pili and therefore are unable to move by S-motility (FIGUREs I.3.9E, I.3.12). Inspection of the swarm edge at higher magnification confirmed that these cells even at the colony level looked and behaved like Δ*pilA* cells *(*FIGURE I.3.9F, I.3.10 I*),* with very little cohesiveness among the cells and only a few flares and individual cells leaving the swarm (FIGURE I.3.10 E, I.3.11 E). From these observations, I hypothesized that PilY1 and PilY2 together are needed for proper type IV pilus biogenesis. When *pilY3* was deleted in the background of a *pilY1* deletion, no apparent defect could be detected and the cells swarmed similar to the parental Δ*pilY1*mutant or the wild-type (FIGUREs I.3.9 G, I.3.12). Similarly, the edge of the swarms of this double mutant looked cohesive and

smooth like the one observed for the parental or wild-type strain (FIGURE I.310 F, I.3.11 F).

Finally, I generated the third combination of deletions: a *pilY3* deletion in a Δ*pilY2* deletion background. Surprisingly, the deletion of *pilY3* in this background appeared to improve swarming as indicated by a 20% increased diameter of the swarms after six days on soft agar (FIGURE I.3.9 H, I.3.12). Inspection of the swarm edge, however, did not reveal any significant difference when compared to the parental strain even after magnification (FIGURE I.3.10 G, I.3.11 G). Lastly, we deleted *pilY2* in the double deletion background of *pilY1* and *pilY3*. This strain behaved exactly like the double deletion parent strain, being deficient (FIGURE I.3.9 F, I.3.12) in swarming with a non-cohesive swarm edge (FIGURE I.3.10 I, I.3.11 I)

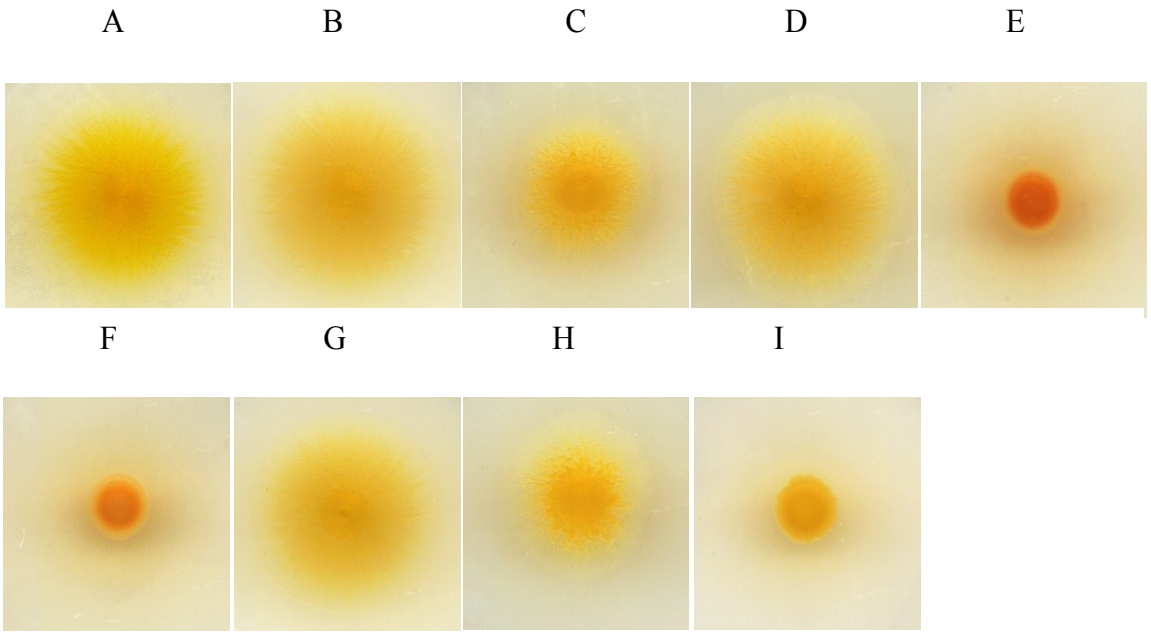

FIGURE I.3.9: Macroscopic pictures of swarm patterns of various *pilY deletion* mutants. The swarm diameter is compared to the wild-type DK1622 strain and the S-motility deficient Δ*pilA* strain. A: wild-type; B: Δ*pilY1;* C: Δ*pilY2;* D: Δ*pilY3;* E: Δ*pilA;* F: Δ*pilY1*Δ*pilY2;* G: Δ*pilY1*Δ*pilY3;* H: Δ*pilY2*Δ*pilY3;* I: Δ*pilY1*Δ*pilY2*Δ*pilY3.*

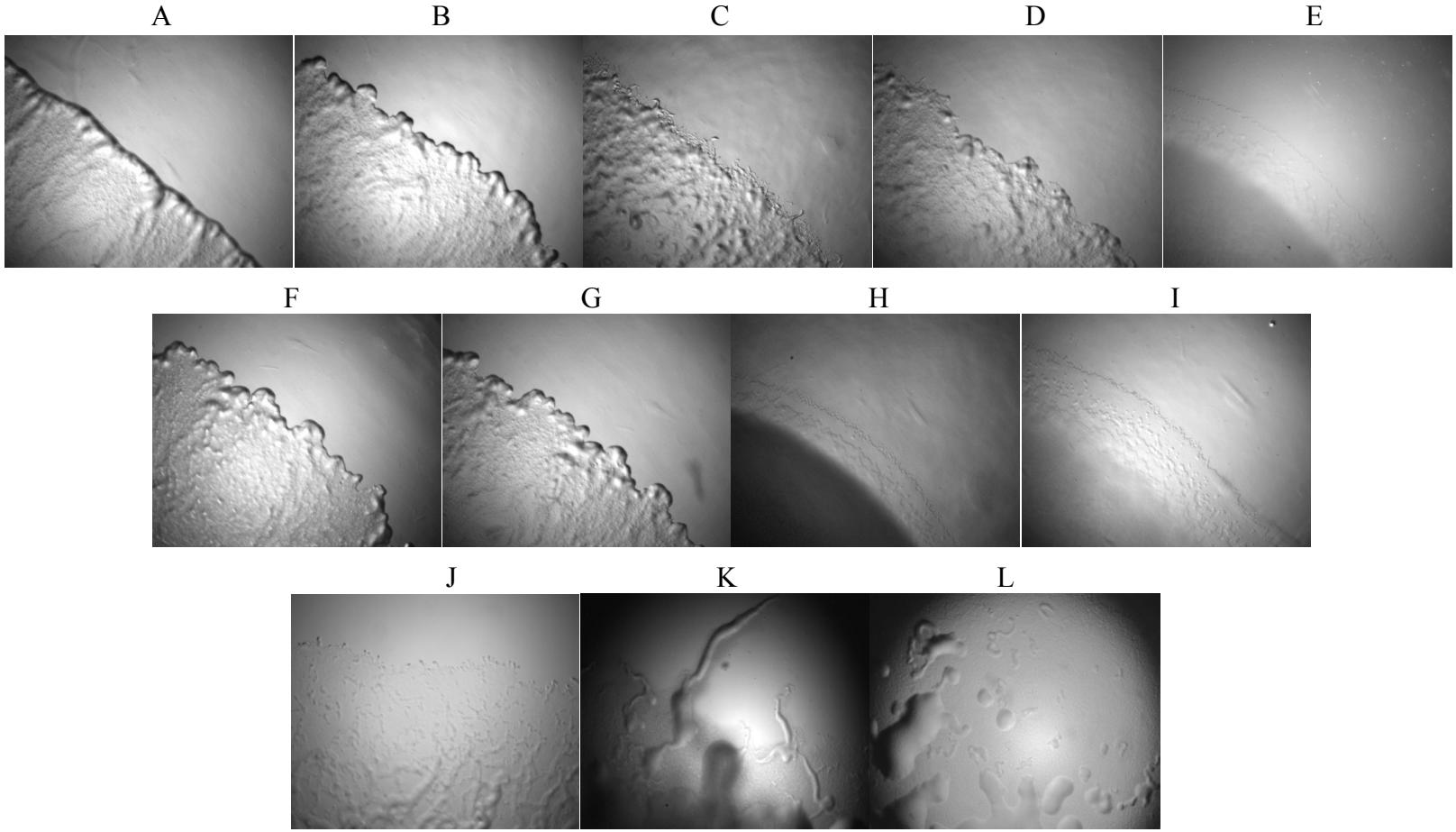

FIGURE I.3.10: Light microscopic pictures of swarm edges of various *pilY* deletion mutants at 2x magnification. The swarms are on the left, and the agar surface is seen on the right of each picture. A: wild-type; B: Δ*pilY1;* C: Δ*pilY2;* D: Δ*pilY3;* E: Δ*pilY1*Δ*pilY2;* F: Δ*pilY1*Δ*pilY3;* G: Δ*pilY2*Δ*pilY3;* H: Δ*pilY1*Δ*pilY2*Δ*pilY3;* I: Δ*pilA; J:* Δ*pilY1*Δ*pilY2*Δ*pilY3::pilY1*$_{C\text{-}FLAG}$*;* K: Δ*pilY1*Δ*pilY2*Δ*pilY3::pilY2*$_{N\text{-}myc}$*;*L:Δ*pilY1*Δ*pilY2*Δ*pilY3::pilY2*

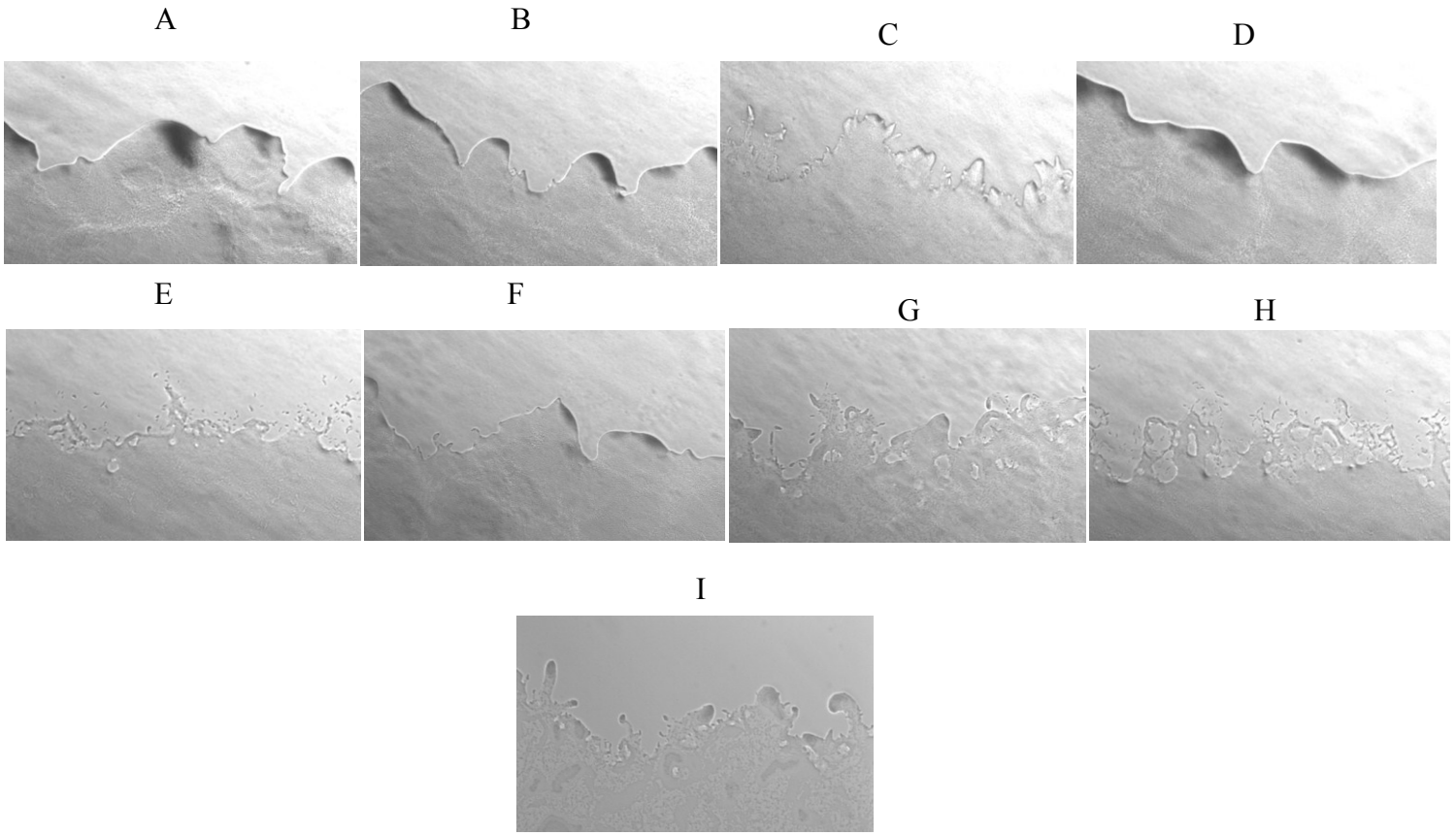

FIGURE I.3.11: Swarm edge of each deletion strain at 10x magnification. A: wild-type; B: Δ*pilY1;* C: Δ*pilY2;* D: Δ*pilY3;* E: Δ*pilY1*Δ*pilY2;* F: Δ*pilY1*Δ*pilY3;* G: Δ*pilY2*Δ*pilY3;* H: Δ*pilY1*Δ*pilY2*Δ*pilY3;* I: Δ*pilY1*Δ*pilY2*Δ*pilY3::pilY1*$_{C\text{-}FLAG.}$

For the quantification of the motility, each assay was performed three times in triplicates and the diameter of the swarms were measured after 5 days and plotted on a graph after normalization to wild-type. (FIGURE I.3.12)

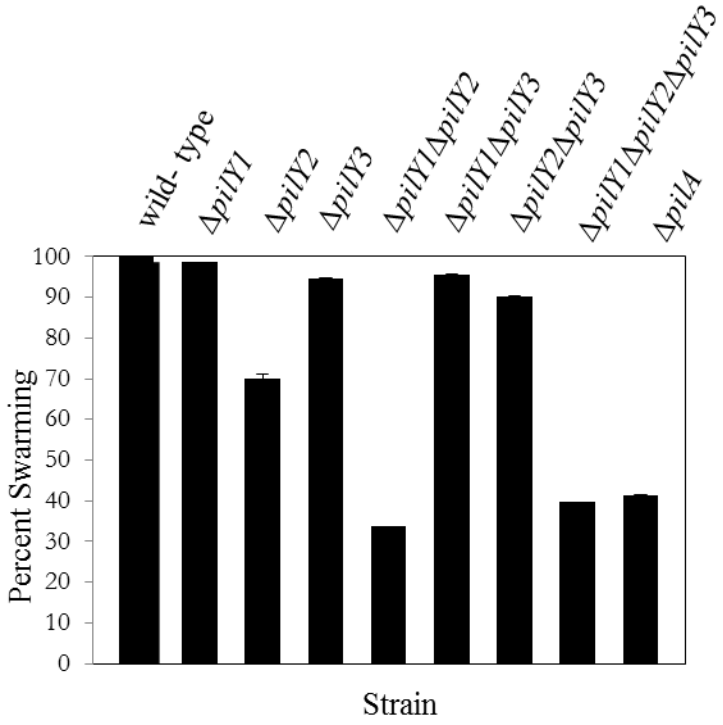

FIGURE I.3.12: Diameter of the swarms for each strain measured after 6 days, normalized to wild-type level swarming.

To confirm that these observed phenotypes of these mutants were truly caused by the loss of the various *pilY* genes, all strains were complemented by expressing the deleted proteins under control of the *pilA* promoter from the chromosomal *attB* phage attachment site. For these experiments, both the wild-type PilY proteins as well as those containing C-terminal or N-terminal (after the signal peptide) tags were expressed (FIGURE I.3.10 J-L). As can be seen even the triple deletion strain complemented with

pilY1, *pilY1* C-terminal FLAG tag, and *pilY2* with N-terminal myc tag (after the signal peptide) was able to regain motility on soft agar albeit to varying degrees (FIGURE I.3.10 J-L , I.3.11 I).

I also investigated the role of these proteins in adventurous motility, or gliding on 1.5% agar media petri dishes. All mutants generated retained their ability to glide on hard surface (FIGURE I.3.19), as visualized by magnification of the swarm edges at 10x using an inverted light microscope. Thus, it appears that the PilY proteins specifically influence gliding on soft agar exerting their influence via type IV pilus-dependent swarming motility and not via effects on adventurous motility.

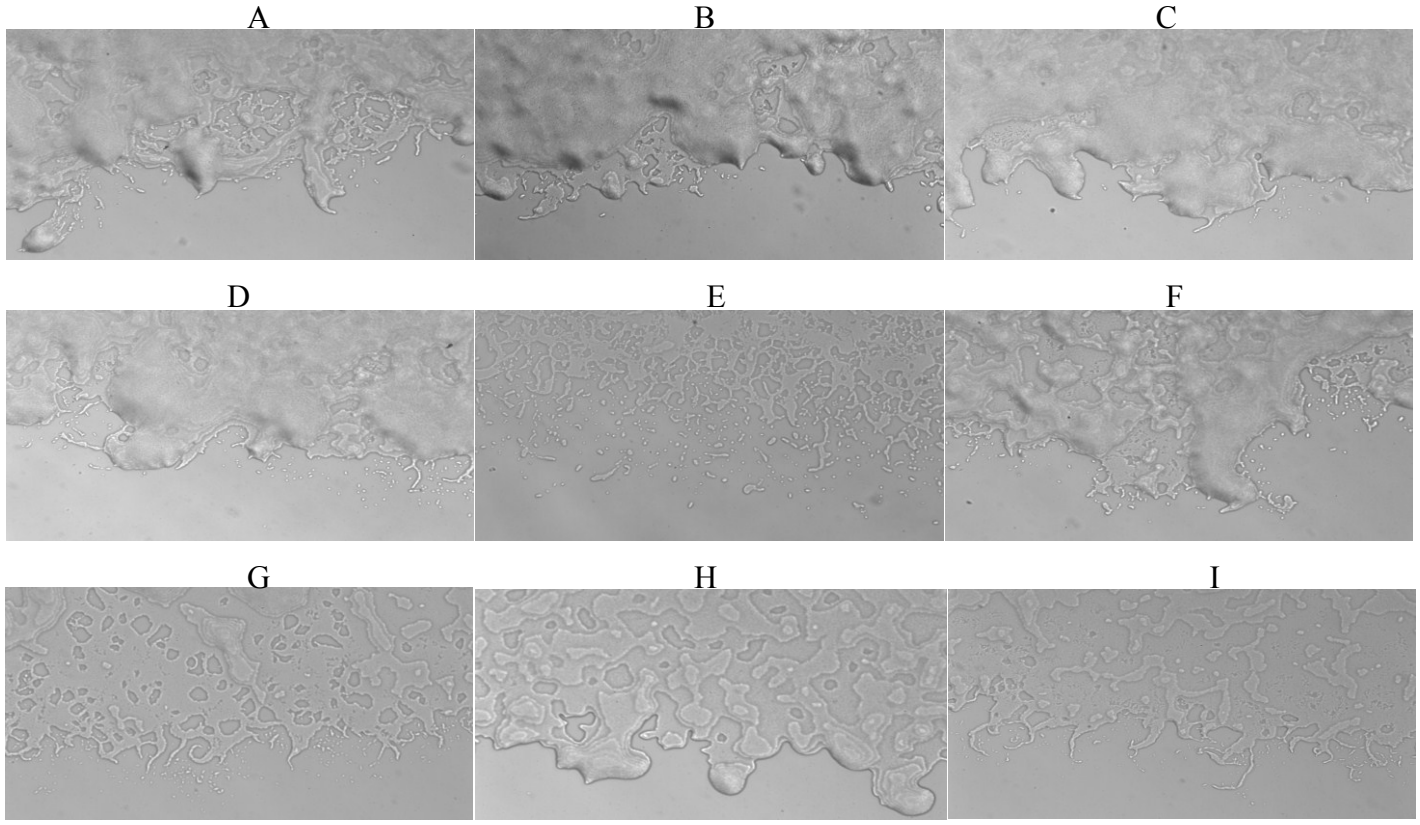

FIGURE I.3.13: Swarm edges of the various mutant strains on 1.5% hard agar at 10x magnification. From top left: A: wild-type; B: Δ*pilY1;* C: Δ*pilY2; D:*Δ*pilY3;* E: Δ*pilY1*Δ*pilY2;* F: Δ*pilY1*Δ*pilY3;* G: Δ*pilY2*Δ*pilY3;* H: Δ*cglB;* I: Δ*pilY1*Δ*pilY2*Δ*pilY3.*

PilY1 and PilY2 influence the aggregation of cells

Several of the generated strains showed differences in cultures, in terms of aggregation and cohesiveness. Compared to the wild-type cells that easily clump when grown in liquid culture, some mutants seemed more dispersed in culture (FIGURE I.3.14 B). Therefore, aggregation assays were performed with the mutants to determine the differences in the aggregation behavior of the strains, relative to the behavior of the wild-type cells. Analysis of these assays showed that the deletion mutants *pilY2*, the double deletion mutant *pilY1pilY2,* and the triple deletion mutant *pilY1pilY2pilY3* aggregated less strong than wild-type; with Δ*pilY2* aggregating about 30% less, and the double and triple deletions about 90% less. For these experiments was the non-aggregative strain Δ*pilA* used as a control (FIGURE I.3.14A). Moreover, the complemented strains confirmed these analyses as the triple deletion strain complemented with *pilY1* and *pilY1* C-terminal FLAG tag was able to regain aggregation (FIGURE I.3.14 B).

A

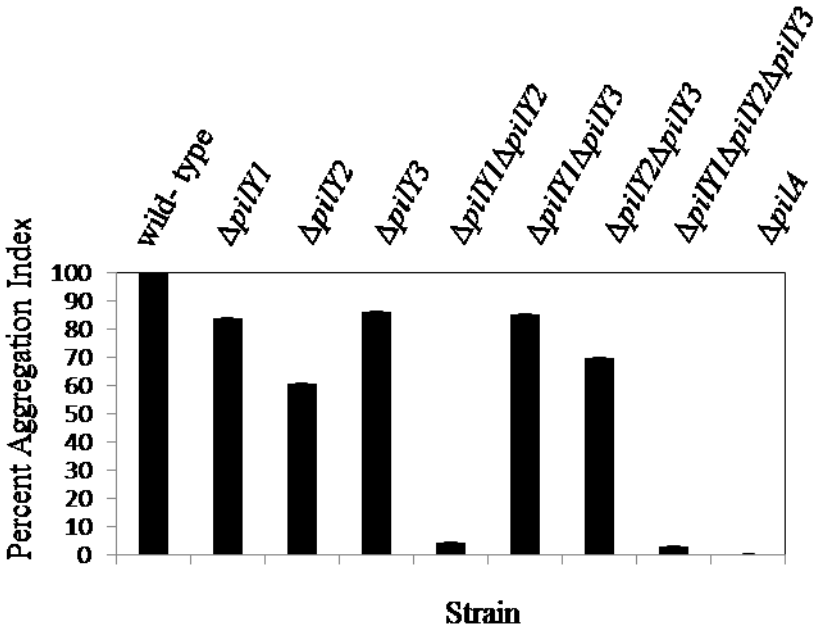

B

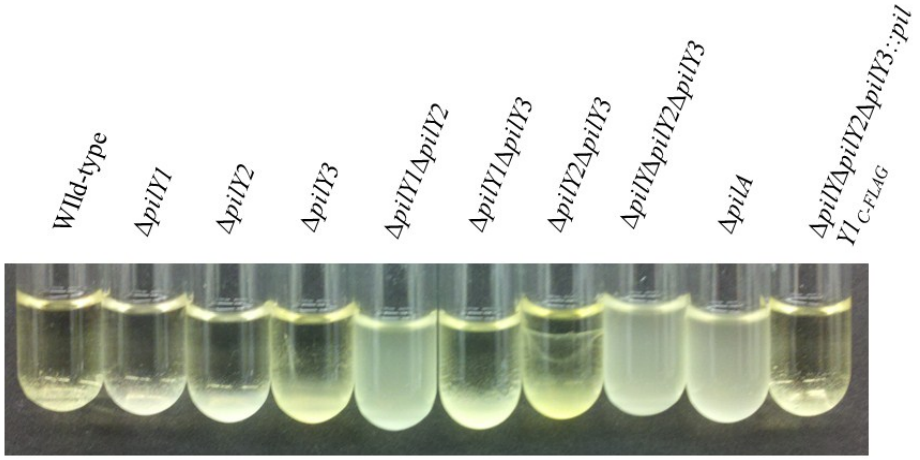

FIGURE I.3.14: A: Percent aggregative indices of the mutants relative to wild-type cells. B: Aggregative versus dispersed liquid cultures of various Δ*pilY* strains, compared to the wild-type strain.

Aggregation of cells is normally the result of complex interactions between polymers such as EPS and LPS with protein structures such as pili and adhesins. Consequently, mutant strains that lack these polymers such as the Δ*difE* and Δ*pilA* strain grow usually non-aggregative in culture. Thus, I reasoned that the lack of aggregation in my mutant strains, as well, the observed deficiency in swarming could be due either to changes in the piliation of the cells, or in the production of EPS. Therefore, both of these factors were separately investigated.

Both PilY2 and PilY3 are needed for cell-surface type IV pilus assembly

As had been reasoned the observed lack of aggregation and social motility in the double knockout strain Δ*pilY1*Δ*pilY2* could be due either to a lack of T4P or a lack of extracellular polysaccharide, both of which are necessary for aggregation and social motility. Since the two proteins are homologs of the type IV pilus accessory protein, PilY of *P. aeruginosa*, which is known to be involved in T4P biogenesis, we hypothesized that the double deletion strain may no longer assemble pili. To test this hypothesis pilus shear assays were performed by vigorous vortexing the cells of the strain to shear off any surface pili and precipitating them from solution using $MgCl_2$. The results of these experiments confirmed our hypothesis showing that the double deletion strain had no longer assembled pili on its cell surface, even though all strains expressed PilA (FIGURE I.3.15).

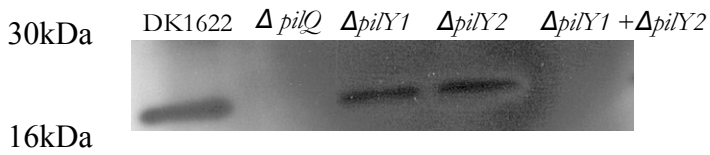

FIGURE I.3.15: Western blot of pili fractions obtained after shearing surface pili from each strain. The PilA antibody was generated using our purified pili and was used to detect the presence of PilA in these assays. The Δ*pilQ* strain was used as a control to ensure that no lysis of the cells had occurred during the process (this strain lacks surface pili because it lacks the secretin gate, but still expresses the protein and would therefore release cytoplasmic PilA when lysed).

All three PilY proteins are needed for proper EPS localization.

Although the lack of surface pili explained the phenotype of the Δ*pilY1*Δ*pilY2* strain, it did not explain the 30% reduced swarming and aggregation defect observed in Δ*pilY2* strain, which obviously properly assembled pili. Therefore, I hypothesized that the EPS assembly in these strains might be altered, since PilY1 is a T4P biogenesis protein, and pili and EPS formation and regulation are coupled processes. Therefore, calcoflour white binding assays were performed to visualize the EPS in these strains. All these mutant strains showed calcoflour white-binding patterns that were different from the ones observed with the wild-type strain. Calcoflour white, a UV-excitable fluorescent dye that binds glucose fibrils such as cellulose, predominantly stains the periphery of wild-type swarms after 6 days. However, the mutant strains showed staining throughout the entire swarms (FIGURE I.3.16). Most notable were mutants Δ*pilY2*, Δ*pilY3 and* Δ*pilY2*Δ*pilY3*, the last of which displayed a reproducible and consistent swirl pattern throughout the

swarm. The double and the triple deletion strains showed no calcoflour white-binding, similar to the control Δ*difE* strain that is defective for EPS production. This was not surprising, since the pilus shear assay indicated that these strains lacked surface piliation.

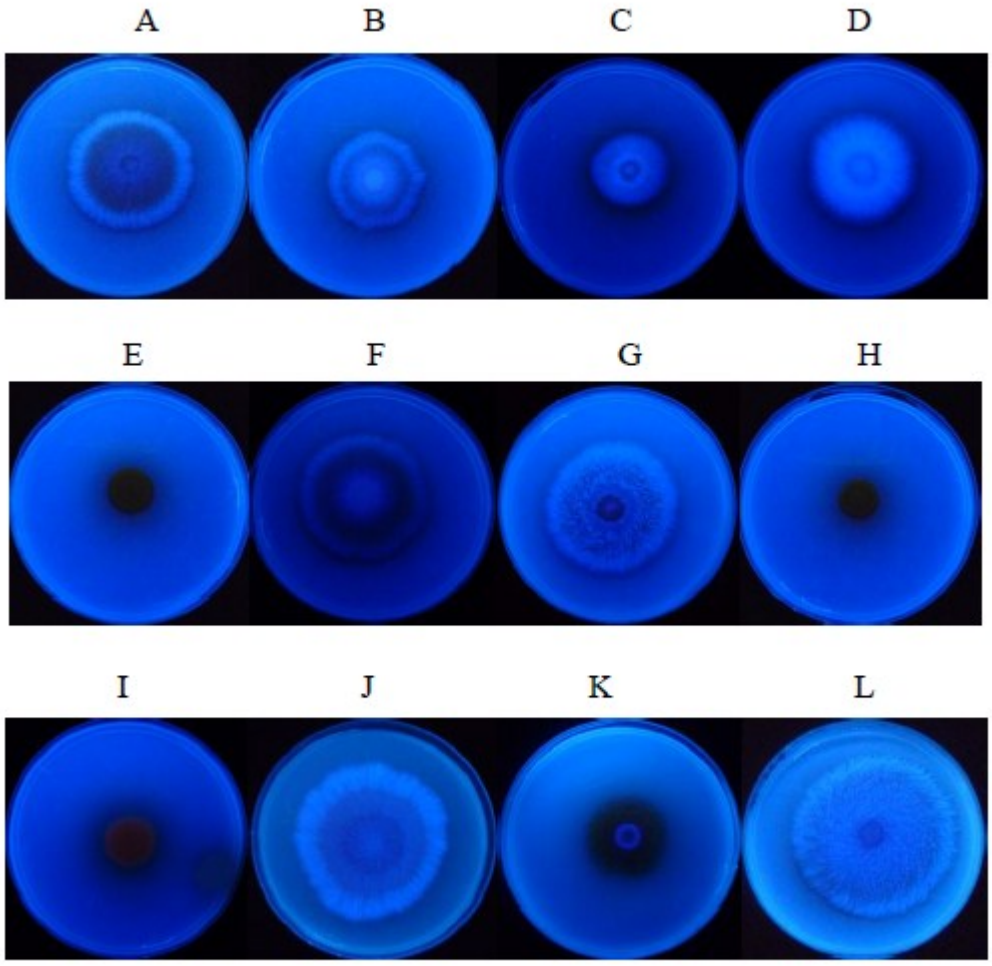

FIGURE I.3.16: Calcoflour binding patterns of various *ΔpilY* mutants. From top left: A: wild-type; B: Δ*pilY1;* C: Δ*pilY2;* D: Δ*pilY3;* E: Δ*pilY1*Δ*pilY2;* F: Δ*pilY1*Δ*pilY3;* G: Δ*pilY2*Δ*pilY3;* H: Δ*pilY1*Δ*pilY2*Δ*pilY3;* I: Δ*difE;* J: Δ*pilY3::pSWU30pilY3;* K: Δ*pilY1*Δ*pilY2*Δ*pilY3::pSWU30pilY1;* L: Δ*pilY1*Δ*pilY2*Δ*pilY3::pSWU30pilY1*$_{C\text{-}FLAG}$.

Because the Calcoflour white-binding patterns in all mutant strains were dispersed throughout the swarm in contrast to the wild-type, which only had binding at the colony periphery, we wondered whether these mutants produced more EPS than the wild-type. Therefore trypan blue binding assays were performed to quantify the amount of EPS produced by each mutant strain. According to these assays, the amount of EPS in the

deletion strain Δ*pilY2* was reduced by 40%, which mirrors the observed reduction in motility, and aggregation defect of this strain (FIGURE I.3.17). Also notable was the fact that the Δ*pilY2*Δ*pilY3* double deletion strain bound substantially more trypan blue than Δ*pilY2* alone, also mirroring the difference between the two strains in motility and aggregation. The Δ*difE* strain was used as a negative control, since it has been reported to lack EPS production. Based on these assays, it was concluded that the mutant strains have defects both in the localization as well as the amount of EPS fibrils confirming the role of piliation in the control of these processes.

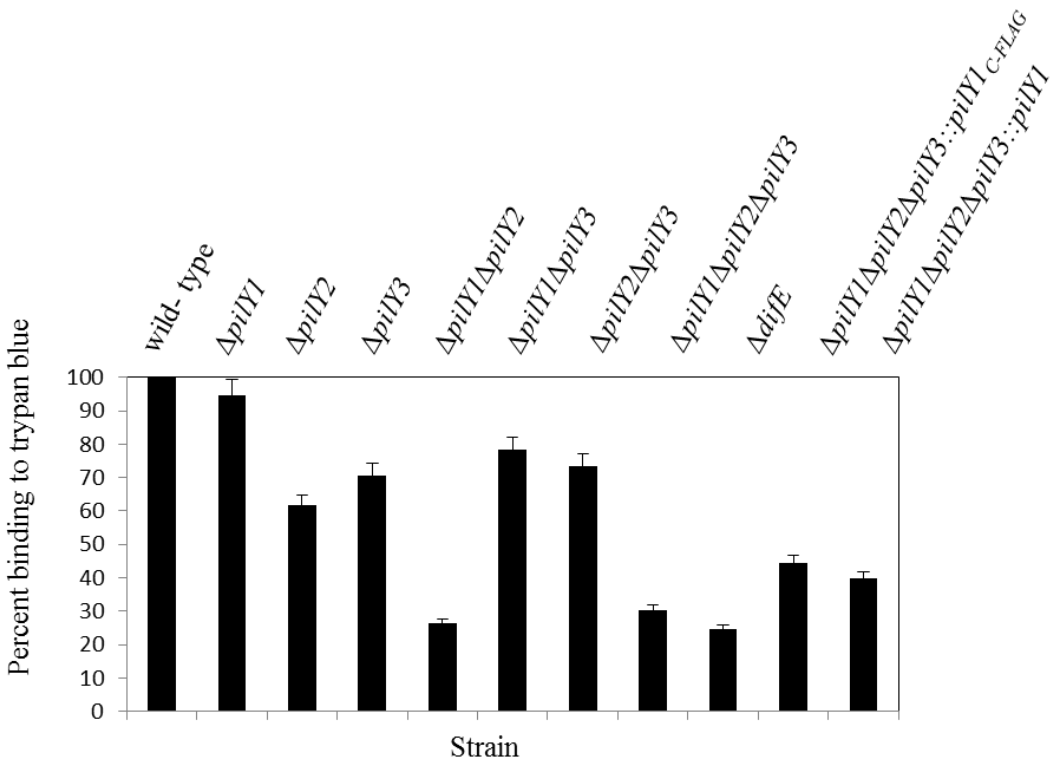

FIGURE I.3.17 Trypan blue binding results of all mutant strains, in comparison to wild-type.

PilY1, PilY2, and PilY3 influence fruiting body formation of cells

Motility is not only important for swarming and aggregation but also for fruiting body formation. Thus, I tested whether the deletion strains that were unable to swarm would also be incapable of forming proper fruiting bodies. To test this hypothesis fruiting body assay were used, which showed that the strains did in fact have various degrees of fruiting body formation defects that mirrored their piliation and EPS defects. Overall, the fruiting body phenotypes of each strain were consistent with that of the swarming phenotype, with the Δ*pilY2* strain having a severe fruiting body defect like the double and triple deletion strains, which had only very few not darkened mounds that are indicative of immature fruits. Fruiting bodies of the Δ*pilY3* and Δ*pilY1*Δ*pilY3* double deletion strains made normal darkened fruits. However, they were more densely packed together and smaller in size than that of the wild-type (FIGURE I.3.18).

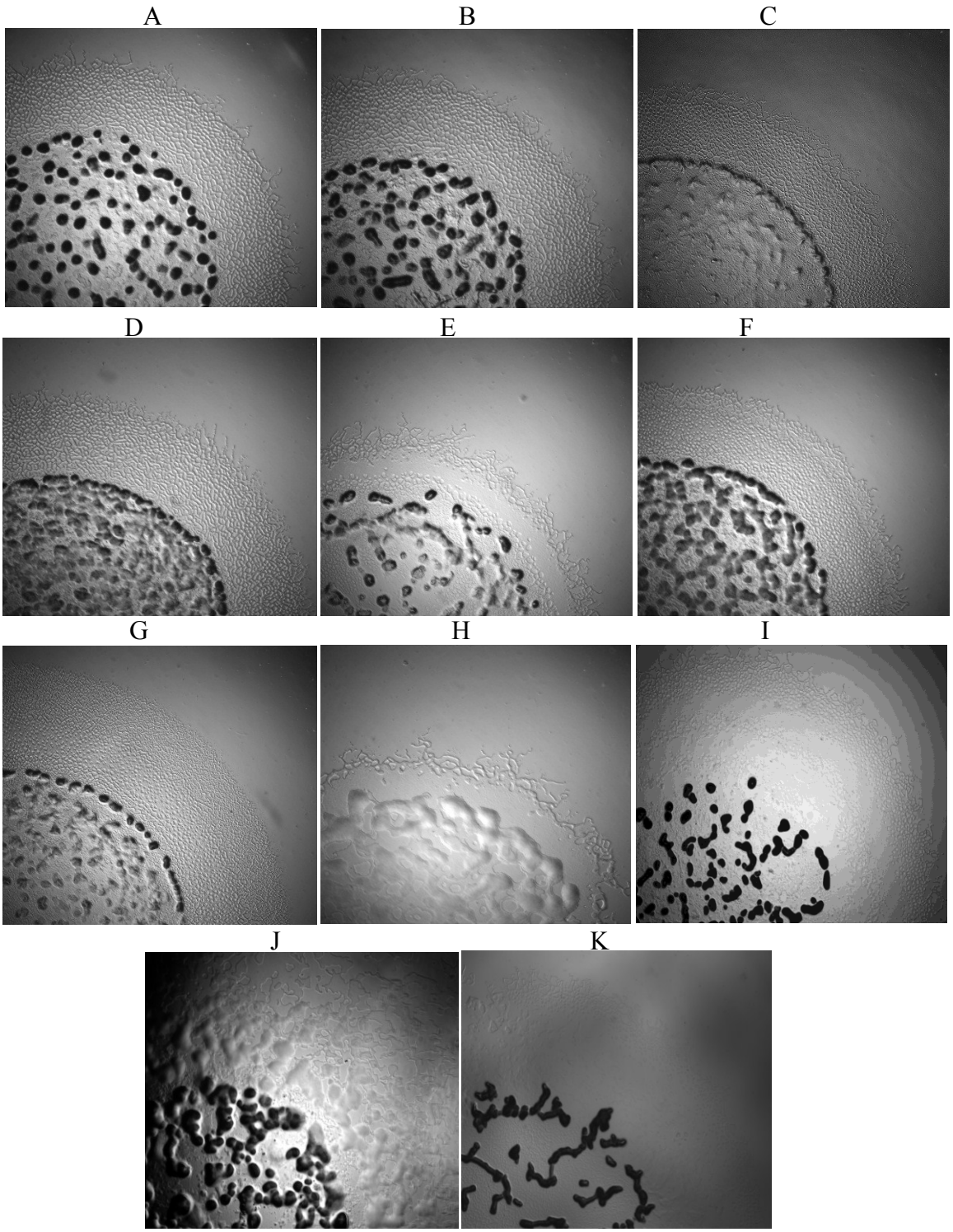

FIGURE I.3.18: Fruiting bodies of the various mutant strains in comparison to wild-type cells. From top left: A: wild-type; B: Δ*pilY1;* C: Δ*pilY2;* D: Δ*pilY3;* E*:* Δ*pilY1*Δ*pilY2;* F*:* Δ*pilY1*Δ*pilY3;* G: Δ*pilY2*Δ*pilY3;* H: Δ*pilY1*Δ*pilY2*Δ*pilY3;* I: Δ*pilA,* J: Δ*pilY1*Δ*pilY2*Δ*pilY3::pilY2;* K: Δ*pilY1*Δ*pilY2*Δ*pilY3::pilY1.*

Exploring the role of PilY2 as a lectin

When allowed to stand, *M. xanthus* liquid cultures form a thin film of sticky cells at the bottom of the flask, which dislodges easily upon swirling of the flasks. In comparison the mutant strains that did aggregate, Δ*pilY2* made a film of cells on the bottom of the flask that came off upon swirling even more readily than the wild-type or cells of the Δ*pilY1* and Δ*pilY3* strains. This led to the hypothesis that the three PilY homologs of *M. xanthus* might engage in different binding functions of the type IV pilus. PilY1 could be involved in attaching to other cells in the swarm, which would be consistent with the integrin αM protein-protein interaction domain in its N-terminus. In contrast, PilY2 could be involved in attachment to the extracellular matrix because of its lack of cohesiveness in the swarm, as well as the loosely adhering films the cells form on the bottom of the culture flask, despite having surface pili. This observation would also be consistent with the predicted lectin-like domain in the N-terminus of PilY2.

To test the hypothesis that PilY2 might be involved in the attachment to the extracellular matrix, I performed the following experiments.

Crystal violet assay

The first experiment utilized the crystal violet assay to determine differences in the ability of the strains to attach to a surface, in this case a 96-well non-tissue culture treated plate (FIGURE I.3.19B). The results of this assay mirrored that of the aggregation

assay (FIGURE I.3.19A). However, the Δ*pilY2* mutant strain did not show any difference in attachment to the surface compared to wild-type cells.

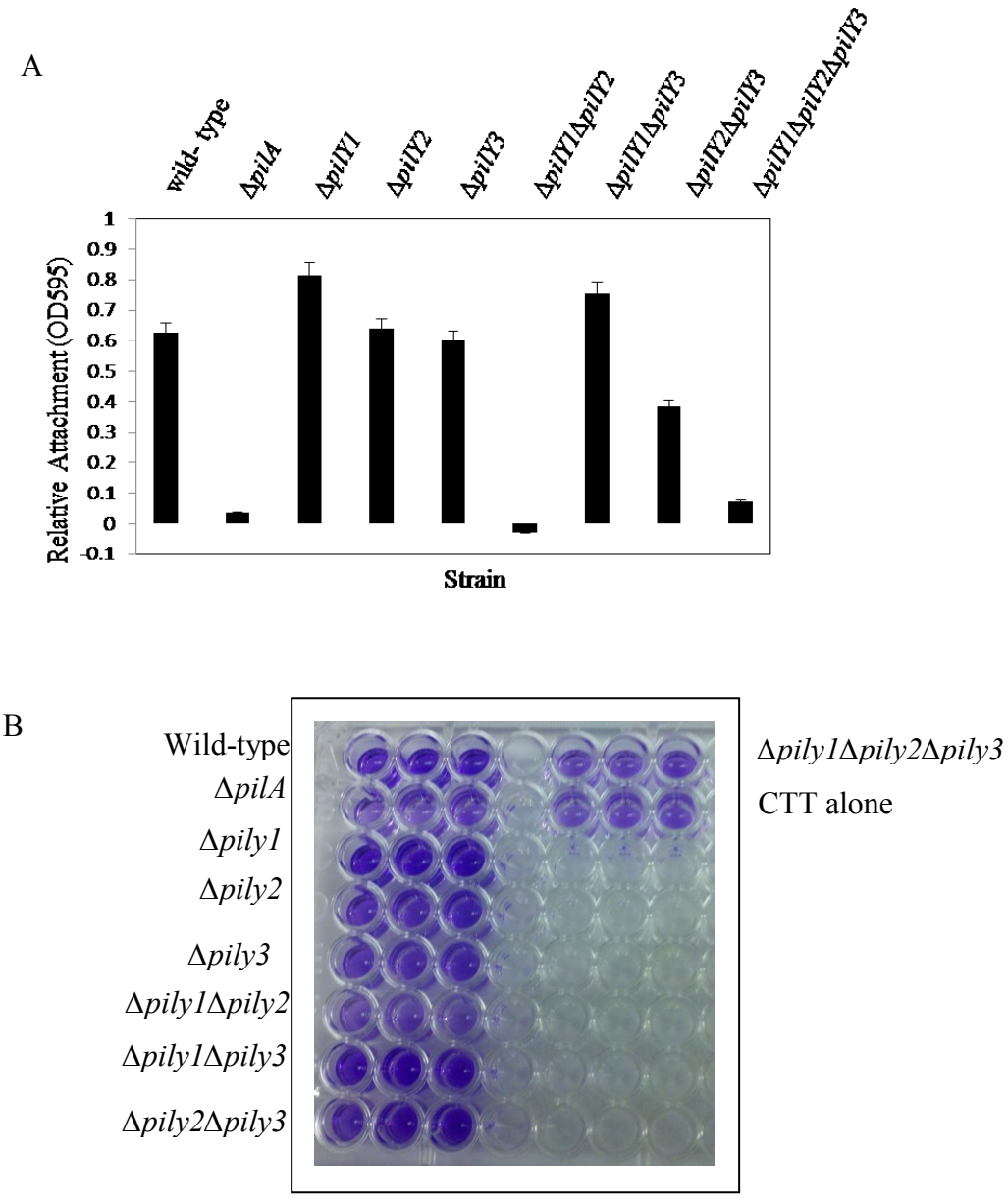

FIGURE I.3.19: A: Bar graph showing the attachment of different mutant strains to the surface of a 96-well plate, in comparison to wild-type cells. B: Crystal violet binding of the mutant strains in comparison to wild-type. Strains that do not attach to the surface bind less crystal violet, which can be measured in a spectrophotometer (A).

Hemagglutination assay

The putative lectin-like activity of PilY2 was also explored using a hemagglutination assay. *M. xanthus* displaying correctly polymerized pili have been shown to possess the ability to agglutinate guinea pig erythrocytes, a phenomenon, which can be inhibited by mannose, N-acetyl-D-galactosamine, and to a lesser degree by fructose, raffinose, melibiose, and α-methyl-D-mannoside (114). Thus, guinea pig erythrocytes were incubated with the different *M. xanthus* mutant strains following the hypothesis that Δ*pilY2* and perhaps Δ*pil3* (which has a weaker predicted lectin domain) will be unable to agglutinate erythrocytes, when compared with wild-type. The lectin concanavalin A was used as a positive control. However, all *M. xanthus* strains tested, including wild-type failed to agglutinate guinea pig erythrocytes, while concanavalin A did (FIGURE I.3.20) indicating that there may be differences between our strains and the strains that had been previously used for these assays.

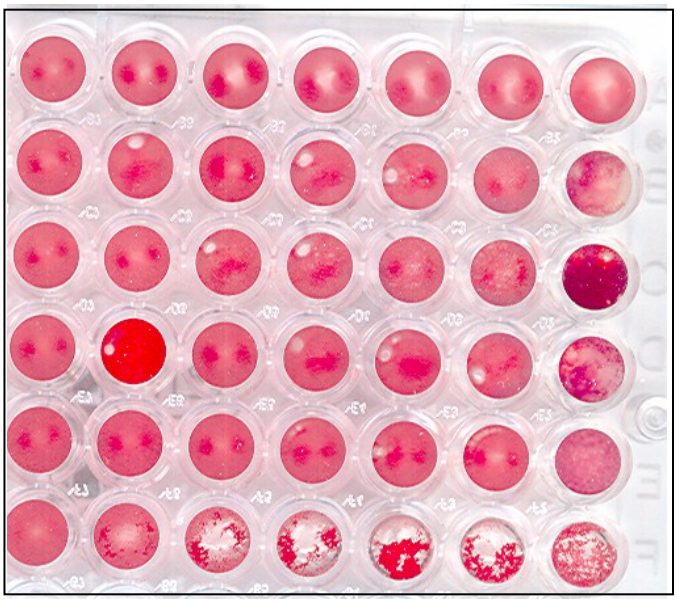

FIGURE I.3.20: Guinea pig erythrocyte agglutination assay: the erythrocytes were incubated with the different mutant strains of *M. xanthus*.

Concanavalin A was able to agglutinate guinea pig erythrocytes, while even piliated *M. xanthus* strains did not. Since pili can be removed from the cell surface by shear forces, it could have been possible that the pili had been lost during the handling. Alternatively, it could be possible that the lectin-like domain of PilY2 does not recognize the sugars that are present on the erythrocyte surface, molecules that these soil-dwelling microbes never encounter. Therefore, it would be interesting to test other erythrocytes for their agglutination ability or to repeat the assay using isolated pili rather that whole bacteria to enhance the interaction of the pili with their potential binding partner on the erythrocyte surface.

Isolation of PilY proteins under different conditions

One of the unsolved questions is why *M. xanthus* possesses three different PilY proteins, that all play roles in either swarming, aggregation, piliation and/or EPS localization. Based on the results it was known that PilY1 is consistently copurified with type IV pili isolated from liquid cultures of the hyerpiliated strains Δ*difE* and Δ*pilT*. It was also known that the deletion of *pilY2* resulted in a swarming defect on soft agar. Thus, I hypothesized that T4P may be accessorized by different PilY proteins under different conditions. According to this hypothesis, PilY1 may be the accessory protein in liquid culture, while PilY2 or PilY3 may be the dominant accessory protein on soft or hard agar. One reason that no defect in motility is observed for the Δ*pilY1* strain could be that in the absence of PilY1, PilY2 simply compensates for the lack of the latter. To test this hypothesis, I attempted to identify conditions under which PilY2 or PilY3 would co-purify with the pili. Thus, I used large amounts of wild-type cells or the various *pilY* mutants grown on either soft or hard agar, to isolate T4P in order to see whether we could detect a high molecular weight band corresponding to the PilY proteins in these isolates. However, no pili isolations from wild-type or the mutant strains were as pure or as abundant as the ones from the hyper-piliated strains grown in liquid cultures (FIGURE I.3.21) and therefore I was unable to detect unique bands on the SDS-PAGE that correspond to these two PilY proteins.

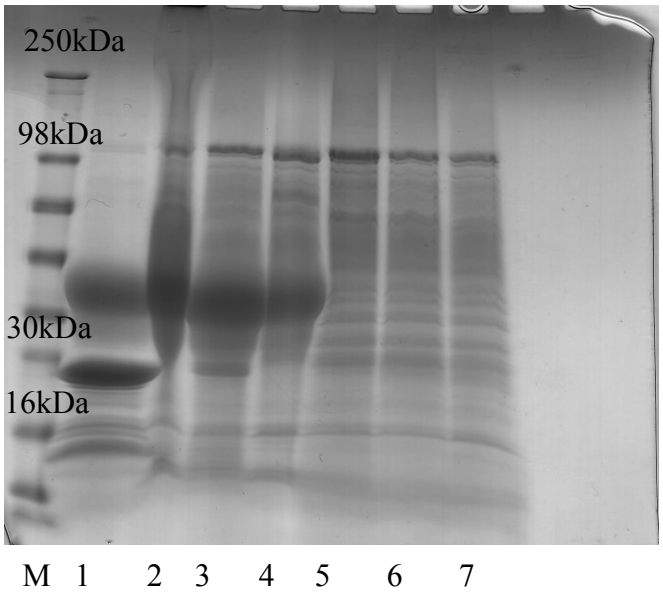

FIGURE I.3.21: SDS-PAGE of T4P isolated from different strains under different conditions. The proteins are visualized by colloidal Coomassie. M. Molecular weight marker 1. Δ*difE* liquid culture 2. Wild-type liquid culture 3. Wild-type 0.5% CTT agar 4. Δ*pilY2* liquid culture 5. Δ*pilY2* 0.5% CTT agar 6. Δ*pilY1*Δ*pilY2* 1.5% CTT agar 7. Δ*pilY1* 1.5% agar.

To potentially generate a hyper-piliated Δ*pilY1* mutant which would facilitate pilus isolation, I generated a deletion of *pilY1* in a Δ*difE* strain background. The objective of making this strain was to be able to address the following questions: 1. Does the deletion of *pilY1* in a hyper-piliated strain cause a reduction in piliation? 2. Does a deletion of *pilY1* result in a substitution by *pilY2*, so that the latter replaces the former as tip protein? If so, having a hyperpiliated strain would facilitate detection of PilY2. 3. Can I complement the double deletion strain with a tagged version of PilY1 to determine whether the protein is indeed on the tip of the pilus, using immunogold labeling in conjunction with electron microscopy and western blotting.

Once I was able to delete *pilY1* in the Δ*difE* background, pili were isolated using the established method to test whether a new high molecular weight band in SDS-PAGE

appeared in place of PilY1. In the SDS-PAGE, however, no high molecular band was found to replace PilY1 (FIGURE I.3.22A). Moreover, the amount of pili obtained from this mutant strain seemed similar to that of a Δ*difE* strain. When the deletion strain was complemented with PilY1 expressing a C-terminal FLAG tag, it was observed that the PilY band reappears in the expected size, and when probed with anti-FLAG M2, the FLAG tag is at the height of the full length PilY protein (FIGURE 3.22 B). Thus, it is plausible that the tag gets incorporated in the pilus, and the strain can be used for immunogold electron microscopy, in order to determine the location of the protein.

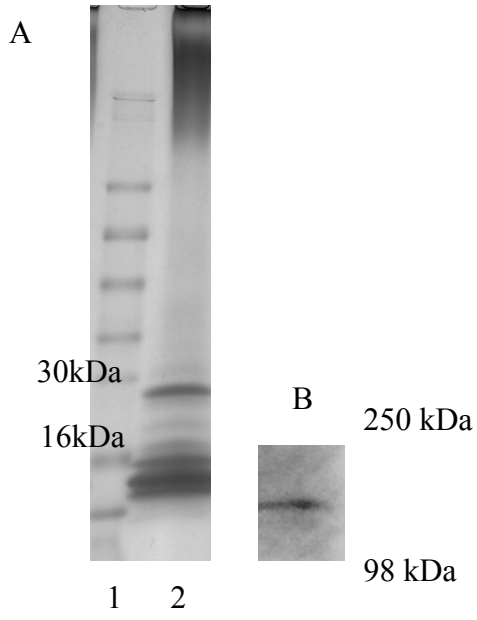

FIGURE I.3.2. A. SDS-PAGE of a pilus preparation from the Δ*difEΔ1365* strain. 1. Molecular weight marker 2. Pilus isolation; major pilin PilA band is around 30 kDa. The three smaller bands around 16kDa also are PilA, as determined by MALDI-MS. B. Western blot of pilus prep from the complemented strain, probed with a mouse anti FLAG M2 antibody. The FLAG signal is at the same height as full length MXAN_1365, thus the tagged protein is associated with the pili.

Identifying the binding partner of PilY1

The N-terminus of PilY1 contains an integrin αM-like domain, a putative protein-protein interaction motif. Thus, I hypothesized that PilY1 on the pilus tip may be involved in making cell-to-cell contacts by interacting with a receptor protein on the cell surface. Therefore, a number of approaches were used to identify this potential binding partner. The first approach was to express a recombinant His-tagged N-terminus of PilY1 in *E.coli* and using the purified protein as a bait to capture any interacting proteins from a *M. xanthus* cell lysate. I tried expressing various fragments of the full length protein, with GST or His tags under different promoters using various expression vectors (FIGURE I.3.23). However, the protein fragments were only recovered as inclusion bodies upon expression and did not fold properly.

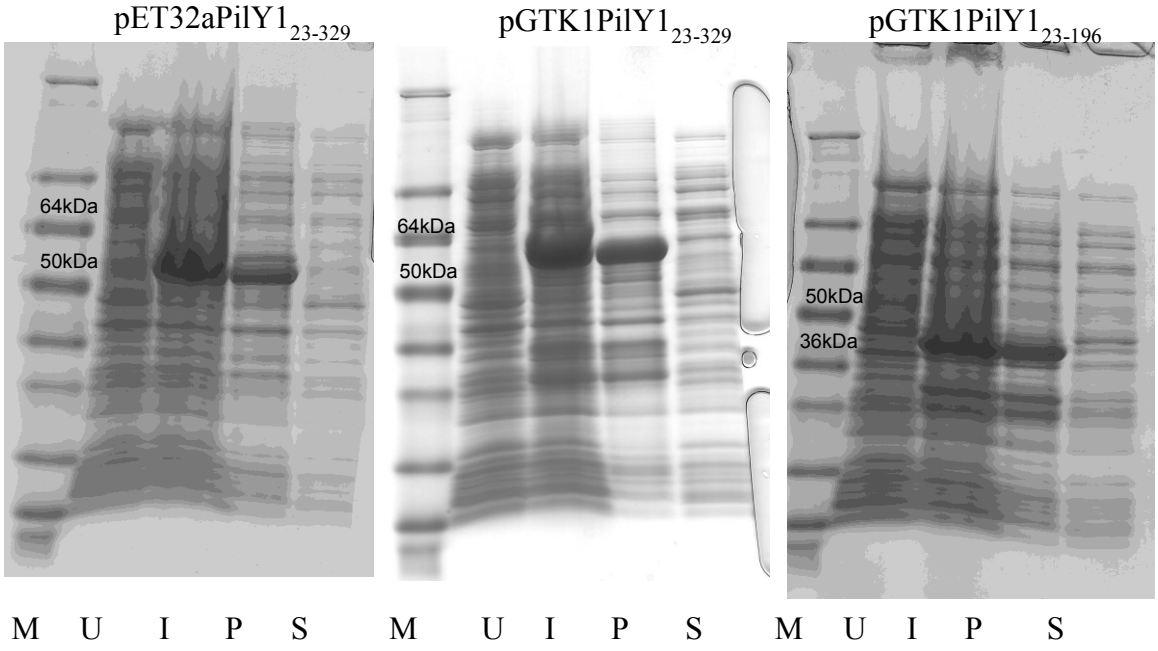

FIGURE I.3.23 Expression of PilY1 fragments in *E.coli.* M: molecular weight marker; U: un-induced lysate; I: IPTG-induced; P: pellet of lysate; S: supernatant of lysate.

Because I was unable to express a soluble N-terminal fragment of the full-length protein, I decided to take another approach to identify the binding partner. Therefore, I attempted to generate an antibody against PilY1 for pull-downs by isolating the protein in the way we discovered it: from Coomassie-stained protein gels. In order to isolate large amounts of proteins, I did 14 large scale pilus isolations and confirmed the successful purification with transmission electron microscopy (FIGURE I.3.24 B). Precast, single well prep gels were used to separate the denatured PilY1 from the rest of the PilA protein bands (FIGURE I.3.24 A). Afterwards the right size protein band was cut out from the

prep gels, confirmed by mass spectrometry, and sent for immunization of a rabbit to induce the production of polyclonal antibodies against the protein. Unfortunately, the resulting antibody did not recognize the full-length protein from the pilus preps nor two recombinant fragments expressed in *E.coli* (FIGURE I.3.24 C).

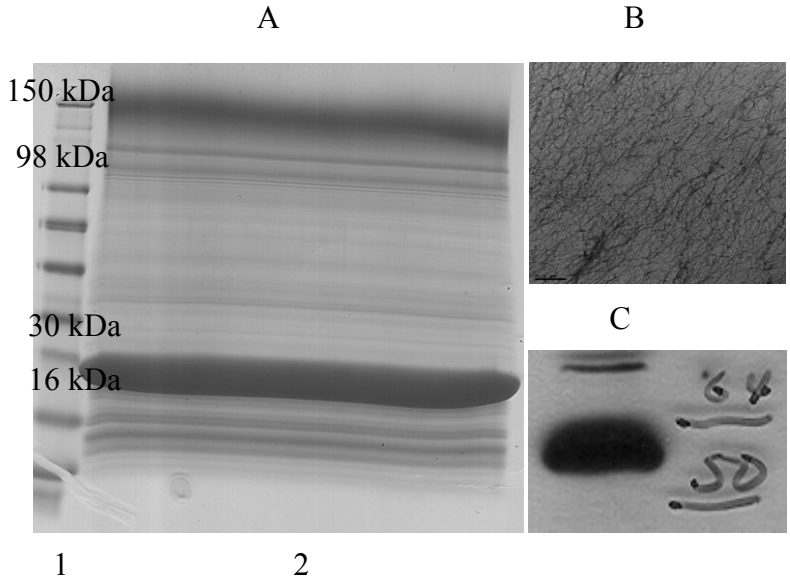

FIGURE I.3.24 A: Coomassie stained SDS-PAGE of a pilus isolation using a preparatory gel. 1. Molecular weight marker 2. Protein bands from pilus isolation. The major band between 30 and 16 kDa is PilA, and the two major bands between 160 and 98 kDa are PilY1. The two bands were cut out and sent for antibody production. B: TEM of isolated pili negatively stained with uranyl acetate. C: Western blot of *M. xanthus* lysate probed with the serum generated from the rabbit. The serum recognizes proteins around 50 and 64 kDa, but not at the size of full length PilY1 protein.

Therefore a new attempt was made to generate antibodies against the three PilY proteins. For this, specific peptides were synthesized that were selected based on the likelihood of immunogenicity in the rabbit using a proprietary software (GenScript®). The final bleed was tested against wild-type lysate and relevant deletion lysates (FIGURE

I.3.25). The serum reacted non-specifically to the lysate, and even after immunodepletion against the deletion lysate, remained nonspecific.

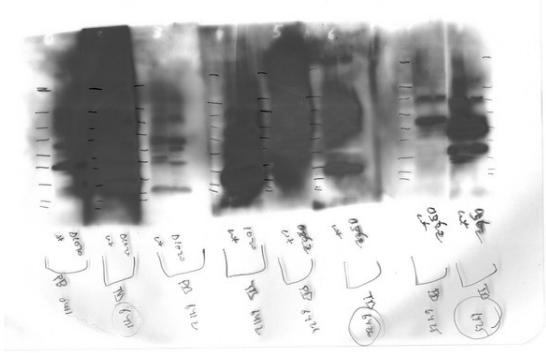

FIGURE I.3.25 Sera generated against the three PilY proteins were used to probe the deletion and wild-type lysates.

I also tried to non-specifically label the cysteines in the PilY1 protein isolated from pilus preps using sulfydryl-reacting biotin, in order to tag the protein for pull-down assays. However, the sulfydryl-reacting biotin labeled the two cysteines of PilA, and did not label any of the more numerous cysteines of PilY1 as can be seen from the Western blots with Streptavidin-HRP (FIGURE I.3.26B). The reason for this may be that the PilA protein is present in such high amounts that it simply exhausts the reagent before any label reacts with the cysteines present in the few PilY molecules.

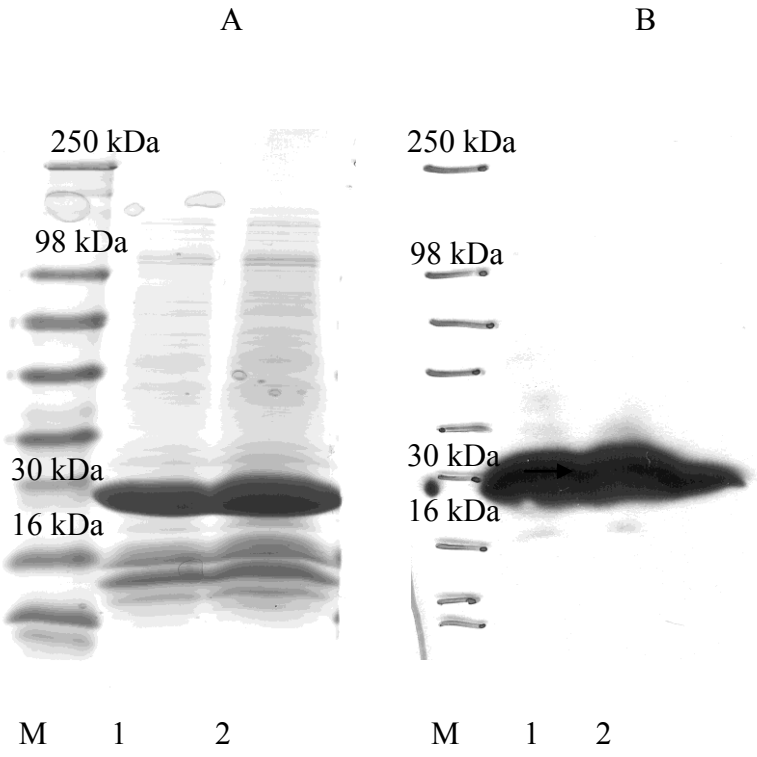

FIGURE I.3.26 Sulfydryl-reacting biotin labeling of purified type IV pili. A: Coomassie stained pili from a pilus isolation. M: molecular weight marker 1. And 2: Different amounts of protein from the pilus isolation were loaded into the two wells. The top most band between 250 and 98 kDa is PilY1; the dominant band between 30 kDa and 16 kDa is PilA. B: Western blot of the pili from the pilus prep after labeling with sulfydryl-reacting biotin, probed with streptavidin-HRP. Biotin labeling was successful for PilA cysteines, but failed for PilY1.

As my next approach I expressed a C-terminal FLAG-tagged full length PilY protein from the phage attachment *attB* site of *M. xanthus* using site-specific recombination. To increase expression, the protein construct was placed under the control of the constitutively expressed *pilA* promoter. Using this construct, I was able to express the full length FLAG-tagged protein (FIGURE I.3.27).

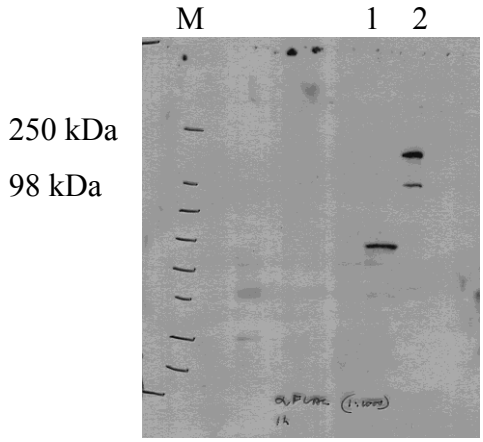

FIGURE I.3.27 Western blot of wild-type lysate expressing full-length PilY1 C-FLAG from the *attB* site. 1. Positive control, purified FLAG-tagged protein; 2: Wild-type::*pilY1* C-FLAG lysate. (The lanes between the marker lane and lane 1 were used for an unrelated experiment).

I then attempted a pull down experiment using *M. xanthus* lysate from the C-terminal FLAG-tagged strain together with FLAG agarose beads. The lysate was incubated with lysate of wild-type cells, cross-linked with a membrane-permeable cross-linker, and possible protein complexes were captured using anti-FLAG M1 agarose affinity gel. As control, lysate without FLAG-tagged PilY1 was used. The agarose was boiled in sample buffer and an aliquot was run on SDS-PAGE to be stained with Coomassie and blotted with anti-FLAG M2 antibody (FIGURE I.3.28 A, B). When analyzed with Coomassie, several unique bands appeared in the lane with FLAG tagged PilY1 protein. However, the blot revealed that there was degradation of the full-length protein, which resulted in several smaller FLAG-tagged protein species (FIGURE I.3.28B). Thus, the bands seen in the Coomassie gel may not be proteins that were pulled down specifically with PilY1, but may be the PilY1 protein itself or degradation products. Moreover, it was determined that it would be more appropriate to repeat the experiment with lysate from a Δ*pilY1::pilY1C-FLAG* strain, since in this strain the FLAG-tagged

protein does not compete with the biological normal protein that is still present and expressed.

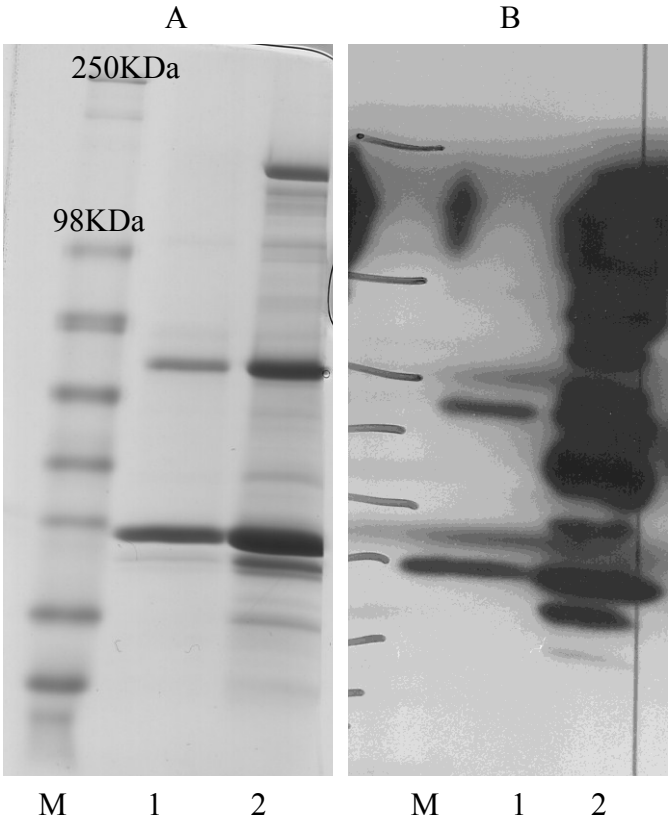

FIGURE I.3.28: Pull-down of potentially interacting proteins using a wild-type cell lysate of PilY1C-FLAG. M: molecular weight marker; 1: Boiled agarose with FLAG M1 incubated with wild-type lysate 2. Boiled agarose with FLAG M1 incubated with wild-type::PilY1C FLAG lysate. A: Coomassie stained B. Western blot.

Role of PilQ

Since PilY1 is obviously on the tip of the protein, it possibly could interact with PilQ to initiate the assembly of the pilus. Thus, I made a number of other deletion strains in a Δ*pilQ* background. The resulting strains Δ*pilQ*Δ*pilY2* and Δ*pilQ*Δ*pilY3* showed a surprising and interesting phenotype. While Δ*pilQ* is deficient in swarming motility on soft agar, strains Δ*pilQ*Δ*pily2* and *pilQ*Δ*pilY3* showed motility on soft agar. This observed motility did not resemble wild-type swarming, but rather appeared to be a different, novel form of motility. Interestingly, these strains were also able to form fruiting body mounds, while Δ*pilQ* alone is completely deficient for aggregation (FIGURE I.3.29).

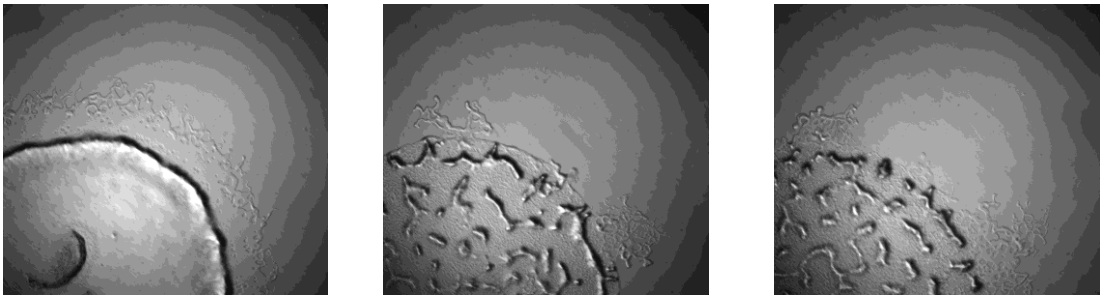

Δ*pilQ* Δ*pilQ* Δ*pilY*2 Δ*pilQ* Δ*pilY*3

FIGURE I.3.29 Fruiting body assays with various *ΔPilQ* mutant strains. Note, the fruiting body-like aggregates of Δ*pilQ* Δ*pilY*2 and Δ*pilQ* Δ*pilY*3.

I.4 DISCUSSION

At the beginning of this thesis project, it was known that *M. xanthus* possesses T4P and that the bacterium uses these structures for S-motility, a form of surface-associated locomotion that is predominantly used on soft, moist surfaces. Despite repeated attempts from various research groups, no one, however, had been able to isolate these pili to either characterize their composition or to use them to generate antibodies that could detect the assembled structure (the only antibody used in this field of research is suitable for Western blots but does not recognize the assembled structure, which makes the *in situ* detection of assembled pili impossible). During my thesis project, I developed a novel isolation method that allowed the isolation and purification of sufficient quantities of pili. With this method in hand, I was able to demonstrate for the first time that *M. xanthus* T4Ps contain a minor tip protein and the bacterium's genome contains two further paralogs. Using genetic, biochemical and behavioral assays, I then dissected their roles in S-motility, piliation, and EPS production. Interestingly, one of the three proteins, PilY2 had been identified before in genetic screens aimed at dissecting motility, however its true function was unknown. Moreover, no information existed for PilY1 and PilY3.

According to the first study, disruption of the gene *MXAN_0358* by transposon insertion leads to impairment in social motility. MXAN_0358 is a predicted isoleucine tRNA synthetase, and is significant because it is adjacent to genes that are homologs *of P. aeruginosa fimT, pilW, pilV*, and *pilY1* (79). The study predicted that the impairment in S-motility could either be a direct effect of the disruption of *MXAN_0358*, or it could be due to changes in the expression rate of the adjacent genes *MXAN_0359-MXAN_0362*. Of

these genes, *MXAN_0359* encodes a putative type IV pilus biogenesis protein, *MXAN_0360* encodes a PilW homolog, *MXAN_0361* a type II secretion pseudopilin PulG homolog, as well as a T4P minor pilin PilV homolog. Finally, *MXAN_036*2 encodes a PilY1 homolog (79). I have found in my study that deletion of this gene, *MXAN_0362*, results in a 30% reduction of swarming and aggregation as well as defects in fruiting body formation. Thus, it is highly likely that the disruption of swarming seen in the transposon insertion screen of *MXAN_0358* is due to polar effects changing the expression of *MXAN_0362*. Moreover, newer experiments conducted by me (not included in this thesis) show that the Δ*pilY1*Δ*0361* double deletion has the same phenotype in swarming as a Δ*pilY1*Δ*pilY2* double deletion. Since *MXAN_0362* encodes another minor pilin protein, it is likely that these proteins are also essential for S-motility. Analysis of *MXAN_0361* indicates that this gene encodes a major pseudopilin PulG homolog. Therefore, it is possible that MXAN_0361 polymerizes into a pilus-like structure, with MXAN_0362 encoding a tip adhesin on this structure. It is reported that overexpression of the major pseudopilin in other species can lead to the production of a pilus–like structure (126).

Interestingly, PilY2 (MXAN_0362) was also identified in another study. Microarray analysis of a deletion mutant of the *masABK* operon showed a change in the expression levels of several type IV pilus-associated genes (103). These genes are listed in TABLE I.4.1.

Genes with altered expression in Δ*mas* mutant compared to wild-type.		
Gene Locus	Gene function/ annotation	Fold decrease
MXAN_0360	Type IV pilus biogenesis operon protein	24
MXAN_0361	Type IV pilus biogenesis operon protein	46
MXAN_0362	Putative pilus biogenesis operon protein	23
MXAN_0363	Hypothetical protein	28
MXAN_0364	Hypothetical protein	26
MXAN_5780	Putative efflux ABC transporter/permease protein *pilI.*	23
MXAN_5781	Efflux ABC transporter/ATP-binding protein *pilH.*	26
MXAN_5782	Putative efflux ABC transporter accessory factor *pilG*	44
MXAN_5783	Pilin *pilA*	74

TABLE I.4.1: Microarray analysis results indicate changes in the expression of several type IV pilus-associated genes in a Δ*masABK* operon mutant, in comparison to wild-type (Adapted from 103).

The study reported that the products of *MXAN_0360*, *MXAN_0361*, and *MXAN_0362* are not known to function in *M. xanthus* S-motility, although the N-terminus of MXAN_0360 shares homology to PilW, a protein that belongs to the PulG family of proteins, predicting a putative role in pilus biogenesis or secretion. *MXAN_0361* encodes a PilV homolog, yet another protein that belongs to the PulG family. Finally, *MXAN_0362* encodes a *Neisseria* PilC homolog, MXAN_0363 is homologous to the *Sphingomonas* cytochrome C, and MXAN_0364 to PilX of *P. aeruginosa* (103).

Although both of these studies identify *MXAN_0362*, none actually assesses the role of MXAN_0362 in S-motility or in fruiting body formation. Therefore, the data presented here are the first that firmly establish the role of MXAN_0362 in *M. xanthus* S-motility. Moreover, the synergistic effect observed in the *MXAN_0362 MXAN_1365* double deletion that results in a complete loss of S-motility is also novel. Thus, this thesis has identified a new key factor important for S-motility in *M. xanthus.* Despite this progress there are still unanswered questions. One of these questions is why the deletion of *pilY2* leads to a partial loss in social motility, even though functional pili are still made in this case. One reason could be that the PilY proteins stabilize the pilus, so even though pili are made in the Δ*pilY2* mutant, they are not as competent for swarming due to unstable polymerization. The alternate scenario is that PilY1, PilY2 and PilY3 are all present on the pilus, but in different areas of the complex swarm structure. PilY2, which has a lectin-binding domain, may be binding the EPS on the outermost rim of the swarm, while PilY1, which has a protein-protein interaction domain, maybe present in the interior of the swarm. If this turns out to be the case, then the model of swarming would have to be modified from a simple scenario, in which the cells with pili bind to the EPS to a more complex picture, in which cells with pili possessing PilY2 on the tip bind to the EPS and act as pioneers expanding the edge of the swarm, while cells with pili possessing PilY1 on the tip remain in the interior of the swarm, and consolidate the swarm through an increased cohesiveness. This scenario is likely since the EPS localization in all the *pilY* mutant strains is altered, as can be seen from the calcoflour white binding. It is known that pili act as sensors for EPS, and thus, removal of the tip proteins may disrupt EPS sensing and thus alter the secretion pattern for EPS from the periphery to the interior

of the swarm. Calcoflour white staining used as an indicator for EPS is present primarily on the swarm periphery. This is also consistent with our hypothesis that PilY2 is present on the swarm periphery and binds the EPS. This could also mean that in theory the number of cells which would possess PilY2 pili would be minimal compared to cells with PilY1 pili, since presumably, only a single layer of cells would be all that would be needed to push the swarm forward by anchoring the cells to the EPS, while PilY1 pili cells would have to do the bulk of work of keeping the cells of the swarm together. This hypothesis would also explain why we have not found PilY2 in any of the pili preparations. One would have to do a very meticulous isolation of very few cells from the periphery of hundreds of swarms in order to isolate enough cells for a pilus preparation, in which the miniscule amount of PilY2 would be visible on an SDS-PAGE gel. To do this experiment is virtually impossible without having a hyperpiliated strain.

The other strategy for detection of PilY2, in the absence of an antibody, is to tag this protein in-vivo. I have constructed strains, which express the full length PilY2 from a chromosomal site, the *attB* site, possessing an N-terminal myc tag, following the signal peptide. I was able to complement the swarming defect of a triple *pilY* mutant by expressing this tagged protein from the chromosomal site, albeit, not at a high level (FIGURE I.3.10 K). In Western blots I was able to detect the myc tag in pili preparations, but the signal from the lysate of many cells was very weak, therefore, the number of pili is currently too low to attempt a direct isolation.

I have also constructed a triple deletion strain complemented with a PilY1C-FLAG-tag version of the gene expressed from an extrachromosomal site, and this strain complements the phenotype close to wild-type levels. Moreover, this tagged protein is

also expressed from the *attB* site of a Δ*difE*Δ*pilY1* strain, a hyperpiliated strain that should allow the isolation of sufficient quantities of pili. We are planning to use these pili to do immuno-gold electron microscopy in order to confirm the localization of this protein. We also have a Δ*pilY3* deletion mutant complemented at the *attB* site with *pilY3* carrying an N-terminal FLAG tag following the signal peptide. This strain complements the deletion mutant phenotype of Δ*pilY3*. Thus, I will soon be in a position to be able to potentially determine the location of each protein within the swarm.

Finally, I am in the process of overexpressing the PilY2 lectin domain in *E.coli* to potentially perform binding assays between *M. xanthus* EPS and the PilY2 protein. This experiment should allow me to discern whether PilY2 indeed binds the EPS component (I have EPS that was purified by a former Masters student, Elizabeth Stoneburner).

Like the lectin-like domain, the N-terminal integrin domain of PilY1 appears to be important since it is also present in the N-terminus of *P. aeruginosa* PilY1 (HHPRED). Interestingly, a similar integrin domain is also important for gliding motility in *Toxoplasma gondii* (104). This obligate intracellular pathogen possesses secretory organelles that include the micronemes, which secrete proteins containing adhesive motifs that resemble mammalian proteins. The secreted proteins include the TRAP proteins, which have an integrin α domain required for attachment and entry of the parasite into host cells (104).

Although the picture drawn here for the function of the three proteins appears to explain S-motility, piliation and EPS secretion, some unresolved questions remain. One of these questions is why we do not see a lack of aggregation in the ΔPilY1 mutant, if this protein as proposed is needed for cell-cell attachment. One explanation could be that

PilY2 can compensate the loss of PilY1, while PilY1 cannot do the same for a ΔPilY2 mutant.

CHAPTER II

CHARACTERIZATION OF A NOVEL CLASS OF OSMOREGULATED PERIPLASMIC POLYSACCHARIDES IN *MYXOCOCCUS XANTHUS*

I.1 INTRODUCTION

Bacterial polysaccharides

Slimes and capsules

Bacteria produce a number of different extracellular biopolymers which play various roles in bacterial growth and survival. These polymers include polysaccharides, inorganic polyanhydrides, polyesters, and polyamides (116). The majority of extracellular bacterial biopolymers are polysaccharides, which are classified based on their location relative to the cell.

Extracellular polysaccharides (EPS) that are covalently attached via the phospholipid or the lipid A molecules to the bacterial cell body are called capsules, while those that are loosely attached are called slime, or free EPS (FIGURE II.1.1) (118,119,121). This distinction, however, can become difficult when capsules gets disconnected from the cell and released into the medium. Similarly, slime can be very close to the cell, without an obvious anchor making the distinction between these two types of EPS sometimes appear artificial. Capsules and slime together or extracellular polysaccharides in general play roles in preventing desiccation, helping to evade the host

immune, or providing adherence to organic and inorganic substrates via dipole, steric or hydrophobic interactions and/or covalent or ionic bonds (119). These roles make bacterial extracellular polysaccharides key determinants of biofilms. An example of a capsule is the layer of hyaluronic acid that surrounds the cell bodies of *Steptococcus pyogenes* (122) (FIGURE II.1.1), while slime is often observed on cyanobacteria, and may be used for gliding (see chapter I; 9).

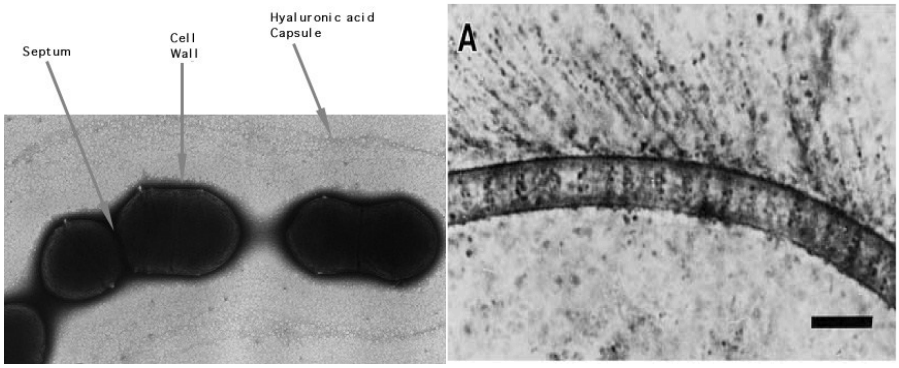

FIGURE II.1.1: Examples of capsule and slime layers of bacteria. Left: Electron micrograph of *Streptococcus pyogenes*, with the cells seen as dark bodies, and the hyaluronic acid capsule surrounding the cells visible as thin spread material (Picture Maria Fazio and Vincent A. Fischetti. Right: Light microscopic visualization of slime secretion using India ink. The bacterial cell body is the rod-shaped darker structure, and the slime is seen as extruding filaments pointing away from the cell body (9).

Lipopolysaccharide

Another important polysaccharide in bacteria is lipopolysaccharide (LPS), also known as endotoxin, a potent inducer of the host immune response (123). LPS is composed of three parts: Lipid A, core and O-antigen. Both the core and the O-antigen are composed of various monosaccharaides, while the Lipid A is the lipid moiety that

anchors the lipopolysaccharide to the bacterial outer membrane, making LPS a glycolipid. The O-antigen is diverse in different bacteria and plays an important role in the stimulation of the host immune response.

Peptidoglycan

The bacterial peptidoglycan is yet another major polysaccharide of bacteria. Chemically it is composed of long alternate chains of N-acetyl glucosamine and muramic acid, which are covalently linked thru short peptides. The main function of this chain link-like molecule is to function as cell wall mechanically supporting the bacterial cell against osmotic or mechanic challenges (124).

Osmoregulated periplasmic glucans

Osmoregulated periplasmic glucans are another class of bacterial polysaccharides that are found in the periplasmic space of Gram-negative bacteria. These poly-glucans are classified based on their respective glucose backbones, which show high structural variability depending on the species that produces them (117,120). Family I periplasmic glucans are heterogeneous in size, ranging from 5-28 glucosyl residues per molecule. Their linear backbone consists of β-1-2-linked glucosyl residues with branches of glucosyl units that are connected to the main molecule through β-1-6 bonds. Family I periplasmic glucans are found in many bacteria and have been studied in *E.coli, P. aeruginosa, P. syringae*, and *E. chrysanthemi.*

Family II periplasmic glucans consists of cyclic glucans backbones linked by β-1,2 glycosidic bonds. Cyclic β glucans were first discovered in 1942 in the culture supernatant of *Agrobacterium tumefaciens* cultures. Since then, cyclic glucans have been found in *Sinorhizobium, Mesorhizobium,* and *Brucella* species (117, 120).

Family III periplasmic glucans consists of cyclic glucans linked by β-(1,3) and β-(1,6) glycosidic bonds. These glucans are produced by *Bradyrhizobium* spp., *Azorhizobium caulinodans* and *Azospirillum brasilence*.

Finally, family IV periplasmic glucans consists of cyclic glucans linked by β-(1,2) bonds containing a single α-(1,6) glycosidic linkage (117, 120). They have so far been identified in *Ralstonia solanacearum*, *Xanthomonas campestris* and *Rhodobacter sphaeroides* (117).

In many bacteria these glycosidic backbones are modified by molecules that are scavenged from other sources of the cell such as outer membrane phospholipids and include phosphoglycerol, phosphoethanolamine, and phosphocholine, or are metabolic intermediates like acetyl, succinyl, and methylmalonyl groups. Substitution often depends on the growth state of the culture or the osmotic conditions of the medium (117).

Family	Species	Linkages	Substitution	Genes
I	*E. coli*	β-1,2 β-1,6	PG, PEA, Suc	*opgG, opgH, opgB, opgC, opgD*
	P. syringae	β-1,2 β-1,6	Suc, Ac	*opgG, opgH*
	P. pseudomonas	β-1,2 β-1,6	Suc	*opgG, opgH,*
	E. chrysanthemi	β-1,2 β-1,6	Suc, Ac	*opgG, opgH,*
II	*S. melitoti*	β-1,2	PG, Suc, MeMal	*ndvB, cgmB*
	M. huakuii	β-1,2	None	ND
	A. tumefaciens	β-1,2	PG	*chvB*
	B. abortus	β-1,2	Suc	*cgs, cgm*
III	*B. japonicum*	β-1,3 β-1,6	PC	*ndvB, ndvC*
	A. brasilense	β-1,3 β-1,4 β-1,6 α-1,3	Suc	ND
	A. caulinodans	β-1,3 β-1,6	None	ND
IV	*X. campestris*	β-1,2 α-1,6	PC	$opgH_{xcv}$, *opgB*
	R. solanacearum	β-1,2 α-1,6	Ac	*opgG, opgH*
	R. sphaeroides	β-1,2 α-1,6	Suc, Ac	*opgG, opgI, opgH, opgC*

TABLE II.1.1: Identified families of osmoregulated periplasmic glucans. Each glucan is listed along with the species that produce it, its linkages, and substitutions. The genes responsible for synthesis and regulation of these glucans are also listed. Abbreviations: PG: phosphoglycerol PEA: phosphoethanolamine, Suc: Succinate, Ac: acetyl, MeMal: methylmalonyl, PC: phosphocholine, ND: Not Detected (117)

II. 2 METHODS AND MATERIALS

Isolation of the periplasmic polysaccharide

As part of my thesis project I isolated a novel carbohydrate polymer from *M. xanthus* wild-type cultures. This polymer could be isolated from both liquid and agar-grown cells and is distinct from EPS because it can be isolated from a Δ*difE* strain, a cell line that is deficient in EPS production. To isolate the polymer, two flasks of 400 ml of CTT inoculated with cells from an agar plate were grown to log phase for two days by shaking at 250 rpm. This pre-culture was then expanded into 8 flasks of CTT, and allowed to grow overnight. To isolate from agar grown cells, the preculture were centrifuged and concentrated in CTT medium. The cells were then plated on large aluminum trays containing media (CTT with 1% agar) and allowed to dry. The trays were then incubated at 32 °C for 12-14 h. The cells were then harvested either by centrifugation (liquid culture) at 9,000 rpm in a Sorvall RC5+ centrifuge (Beckman) using a SLA3000 rotor or scraped off the gar using cell scrapers (tray cultures). The cell pellets were collected, transferred into a household blender, mixed with 120 ml extraction buffer (10 mM Tris/HCl buffer pH 8.0, 10 mM $MgCl_2$), and blended for 3 min. The blended cells were then centrifuged at 11,000 rpm for 10 min and the resulting supernatant was again centrifuged at 20,500 rpm for 10 min to remove cellular debris. The supernatant was pooled in a beaker and 20% (w/vol) ammonium sulfate was added and slowly dissolved by stirring. At this point, the polymer can be seen visually as bundle-forming precipitant. The sample was transferred to four SS34 tubes, and

centrifuged at 20,500 rpm for 15 min to pellet the precipitated polymer. The supernatant was discarded and the pellets were dissolved in 1 ml deionized water by shaking them overnight at 4 °C. After pooling, 0.05% dodecyl maltoside detergent was added to the dissolved polymer to solubilize contaminating membrane vesicles. Finally, 20% ammonium sulfate was added to re-precipitate the dissolved polymer. The sample was then transferred to one SS34 centrifuge tube, and centrifuged at 20,500 rpm for 15 min. The resulting pellet was dissolved in 1 ml deionized water and was used for all analyses.

Electron microscopy

2 µl of the isolated polymer was put directly on carbon-coated copper grids and allowed to dry. The grids were then washed three times for 30 seconds each, and placed for 1 min on top of a 20 µl drop of 2% phosphotungstic acid (pH 7.6). Upon drying, the grids were viewed in a Philips electron microscope (FEI), and images were taken with a digital CCD camera (Gatan).

Thin Layer Chromatography

500 µl of the isolated polysaccharide sample was hydrolyzed in sealed glass ampules using 50 µl 1 M sulfuric acid for 2 h at 100 °C. The hydrolyzed samples were evaporated to dryness, dissolved in a small amount of water and spotted on thin layer

chromatography (TLC) plates. After the plates were dried they were placed into a TLC chromatography tank containing 200 ml solvent (140 ml 1-propanol, 40 ml ethyl acetate, 20 ml H_2O) and left there until the solvent front reached the upper end of the plate (ca. 2 hours). The thin layer chromatograms were then removed from the tank, dried, and sprayed with the detection reagent (1.5 g α-naphthol dissolved in 6.5 ml H_2SO_4, 4 ml H_2O and 40 ml ethanol). The plates were heated at 70 °C in an oven and the visible spots were either scanned or photographed.

Generation of an antibody against the periplasmic polymer

Isolated purified periplasmic carbohydrate was injected into two rabbits to generate polyclonal antibodies according to standard protocols. The collected sera were tested for cross-reactivity using dot blots.

Dot blot

10 µl of 10 mg/ml of various monosaccharides were spotted onto a nitrocellulose membrane along with the polymer sample and allowed to dry. The membrane was then blocked first with 5% non-fat milk for 2 h, followed by a 2 h long incubation with the primary antibody (diluted at 1:1,000) and three washes with buffer (1xPBS +0.05% Tween 20). After the wash, the membrane was incubated with the secondary anti-rabbit antibody (diluted as 1:25,000) for 1 hour, washed three times more and incubated with the chemiluminescent reagents to visualize the spots.

Immuno-gold electron microscopy of thin sections

Immunogold-EM was done by Carol Cooke at Johns Hopkins Department of Cell Biology using standard methods.

Procedures performed at the University of Georgia

Size exclusion chromatography, GC-MS for glycosyl composition, linkage analysis, and NMR were performed by the University of Georgia Center for Carbohydrate Research as described below.

Dialysis

The polymer sample was suspended in nano-pure water and placed in 20,000 Da MWCO dialysis bag (*Pierce, Prod # 66012*) and dialyzed under running de-ionized water for 48 h. The dialyzed samples (~12 mg) free of lower MW fractions were freeze-dried for further analysis.

Partial hydrolysis

To 20 mg of the dialyzed and freeze dried polymer sample 5 ml of 0.1 M trifluoroacetic (TFA) solution was added and incubated at 80 °C for 2.5 h. The TFA was removed by evaporation under a dry N_2 stream and addition of methanol. The dried sample was

dissolved in de-ionized water and the solutions were filtered through a 0.22 μm filter for preparative size exclusion chromatography (SEC).

Size-exclusion high pressure liquid chromatography (SEC)

Column: Superdex Peptide GE-Amersham, optimal separation range 500-10,000 Da for dextrans, equilibrated with 50 mM ammonium acetate buffer pH 5.2

Detection: ELS detector (Agilent) was used for post-column detection of soluble components eluted from the column. Gain 9, filter 5, 70 °C

Flow rate: 0.5 ml/min.

Sample: 1 mg/ml solution in de-ionized water; 200 μg was loaded onto the column

Elution buffer: 50 mM ammonium acetate pH 5.2.

Data were collected and processed using the Agilent ChemStation software. MW standard dextrans with MW 40,000 Da, Maltoheptaose DP7, and Glucose were used to calibrate the column.

Glycosyl composition by GC-MS of TM- derivatives of methyl glycosides (TMS)

Glycosyl composition analysis was performed by combined gas chromatography/mass spectrometry (GC/MS) of the per-*O*-trimethylsilyl (TMS) derivatives of the monosaccharide methyl glycosides produced from the sample by acidic methanolysis.

An aliquot was taken from the sample and added to separate tubes with 20 μg of inositol as internal standard. Methyl glycosides were then prepared from the dry sample following the mild acid treatment by methanolysis in 1 M HCl/methanol at 80 °C (16 h), followed by re-*N*-acetylation with pyridine and acetic anhydride in methanol (for detection of amino sugars). The sample was then per-*O*-trimethylsilylated by treatment with Tri-Sil (Pierce) at 80 °C for 0.5 h. These procedures were carried out as previously described in Merkle and Poppe (1994) *Methods Enzymol*. 230: 1-15; York, et al. (1985) *Methods Enzymol.* 118:3-40. GC/MS analysis of the TMS methyl glycosides was performed on an Agilent 7890A GC interfaced to a 5975C MSD, using Agilent DB-1 fused silica capillary column (30 m × 0.25 mm ID).

Per-O-methylation and linkage analysis

For glycosyl linkage analysis, the sample was permethylated, depolymerized, reduced, and acetylated; and the resulting partially methylated alditol acetates (PMAAs) analyzed by gas chromatography/mass spectrometry (GC/MS) as described by York *et al* (1985) *Methods Enzymol.* 118:3-40.

Initially, the dry sample was suspended in about 200 μl of dimethyl sulfoxide and placed on a magnetic stirrer for 1-2 weeks. The sample was then permethylated by the method of Ciukanu and Kerek (1984) *Carbohydr. Res.* 131:209-217 (treatment with sodium hydroxide and methyl iodide in dry DMSO). The sample was subjected to the NaOH base for 15 min before methyl iodide was added and left for 45 min. More base was added for 10 min and, finally, additional methyl iodide was added for 40 min. This addition of more methyl iodide and NaOH base was to ensure complete methylation of the polymer. Following the sample workup, the permethylated material (PMAA) was hydrolyzed using 2 M TFA (2 h in sealed tubes at 121 °C), reduced with $NaBD_4$, and acetylated using acetic anhydride/TFA. The resulting PMAAs were analyzed on a Hewlett Packard 7890A GC interfaced to a 5975C MSD (mass selective detector, electron impact ionization mode EI-MS); separation was performed on a 30 m Supelco 2380 bonded phase fused silica capillary column.

NMR Spectroscopy

The sample was deuterated three times by lyophilization in D_2O, then re-dissolved in 0.5 mL D_2O and placed in a 5 mm NMR tube. 1-D proton and 2-D gCOSY, TOCSY, gHSQC, gHMBC, ROESY spectra were obtained on a Varian Inova 600 and 800 MHz spectrometer at 45 °C using standard Varian pulse sequences. Chemical shifts were measured relative to internal acetone (δ_H=2.22, δ_C=33 ppm).

II.3 RESULTS

Discovery of a novel carbohydrate polymer from M. xanthus

The observation that led to the discovery of a novel periplasmic carbohydrate from *M. xanthus* was an increase in viscosity of the culture supernatant upon vigorous shaking or vortexing of the cells. Initially, it was thought that this increase of viscosity was due to the release of DNA, however, when attempts to decrease the viscosity through DNAse treatment failed, a protocol was developed to isolate the released material. Through a serious of salt precipitation and centrifugation steps the material could be enriched and was finally pelleted from the solution through centrifugation at 20,500 rpm in a Sorvall SS34 rotor. The resulting jelly-like pellet could easily be dissolved in 1-5 ml of water and increased the viscosity of the solution in the same way the original culture supernatant behaved indicating that the material responsible for the change of viscosity had been purified (II.3.1 A, B, C). Upon lyophilization the polymer became a fluffy cotton-candy-like white powdery solid (FIGURE II.3.1.D).

The isolated polymer is viscous and makes a white powder

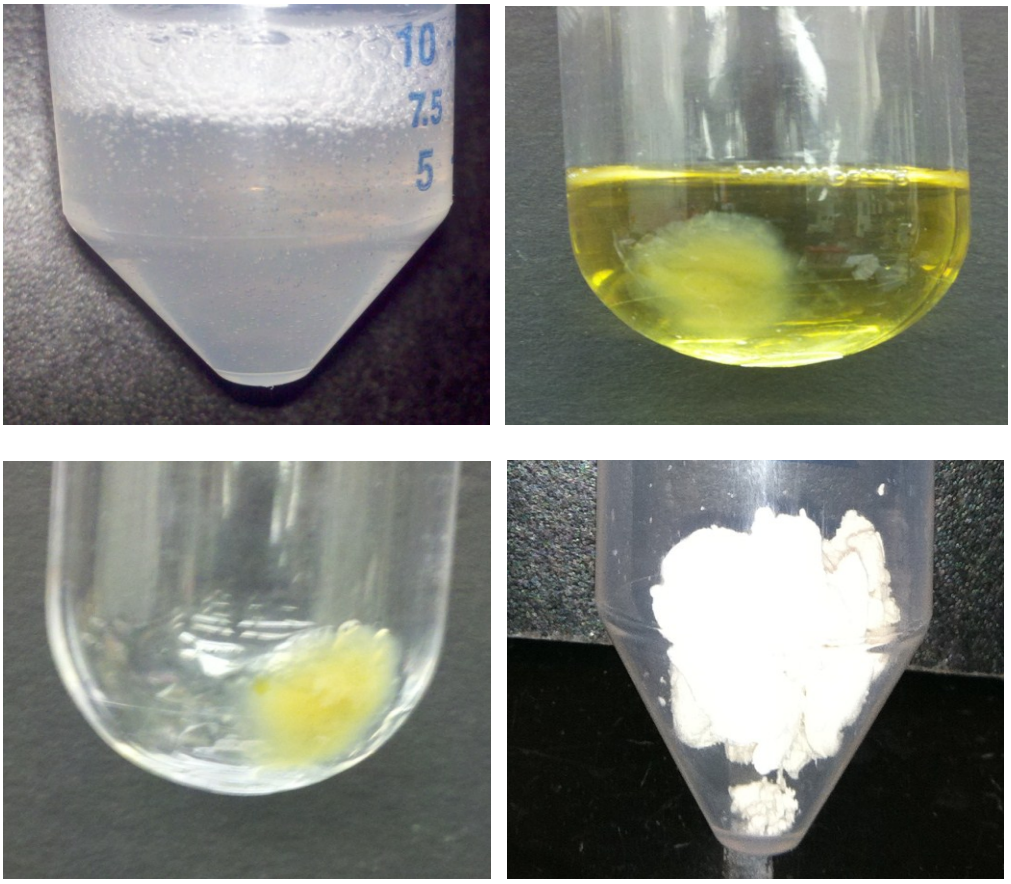

FIGURE II.3.1: Appearance of the carbohydrate polymer at various steps of the isolation procedure. From top left: 1. The polymer increases the viscosity of water. 2. The precipitated polymer in the culture supernatant. 3. A pellet of the carbohydrate polymer after centrifugation 4. Upon lyophilization the polymer becomes a white fluffy powder.

Because of its behavior it was hypothesized that the material was most likely a carbohydrate. To test this idea a number of treatments were performed to quickly identify the chemical nature of the substance. As it was insoluble in methanol or chloroform a lipid or wax-like nature could be ruled out. This was also confirmed by the observation

that the material was resistant to detergent treatment. Moreover, since the substance withstood prolonged incubation with proteinase K, it was also most likely not a protein. Finally, I confirmed its carbohydrate composition using a colorimetric anthrone test, and thin layer chromatography after acid hydrolysis (FIGURE II.3.2).

Thin layer chromatography of the polysaccharide after hydrolysis with TFA

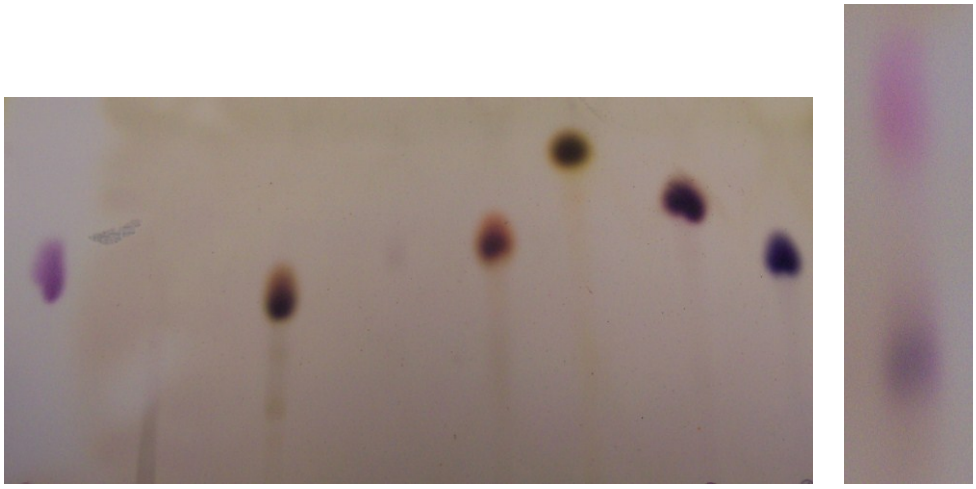

FIGURE II.3.2: Left picture: Top: TLC of various monosaccharaides and the isolated carbohydrate sample. All substances were visualized with naphthol-sulfuric acid. From Left: glucose (purple), glucosamine (grey), galactose (brownish), galactosamine (grey), mannose (purple), rhamnose (yellowish), xylose (dark purple), and fructose (bluish). Right picture: Enlarged TLC of the trifluoroacetic acid-hydrolyzed carbohydrate polymer reveals a purple spot at about the height of mannose or glucose.

The polymer is composed of bundles of fibers as visualized by transmission electron microscopy

To characterize the polymer further, we next examined its structure under the electron microscope. Since many carbohydrates such as cellulose form bundles, we wanted to determine whether the isolated material behaved similarly. Upon adsorption to the grid surface and staining, the material revealed a meshwork of fibers that was often composed of laterally associated bundles of fibers (FIGURE: II.3.3). This ultrastructural appearance further confirmed that the material was a carbohydrate and indicated that the substance was most likely formed by a high molecular-weight substance and therefore very different from the previously characterized periplamic glucans.

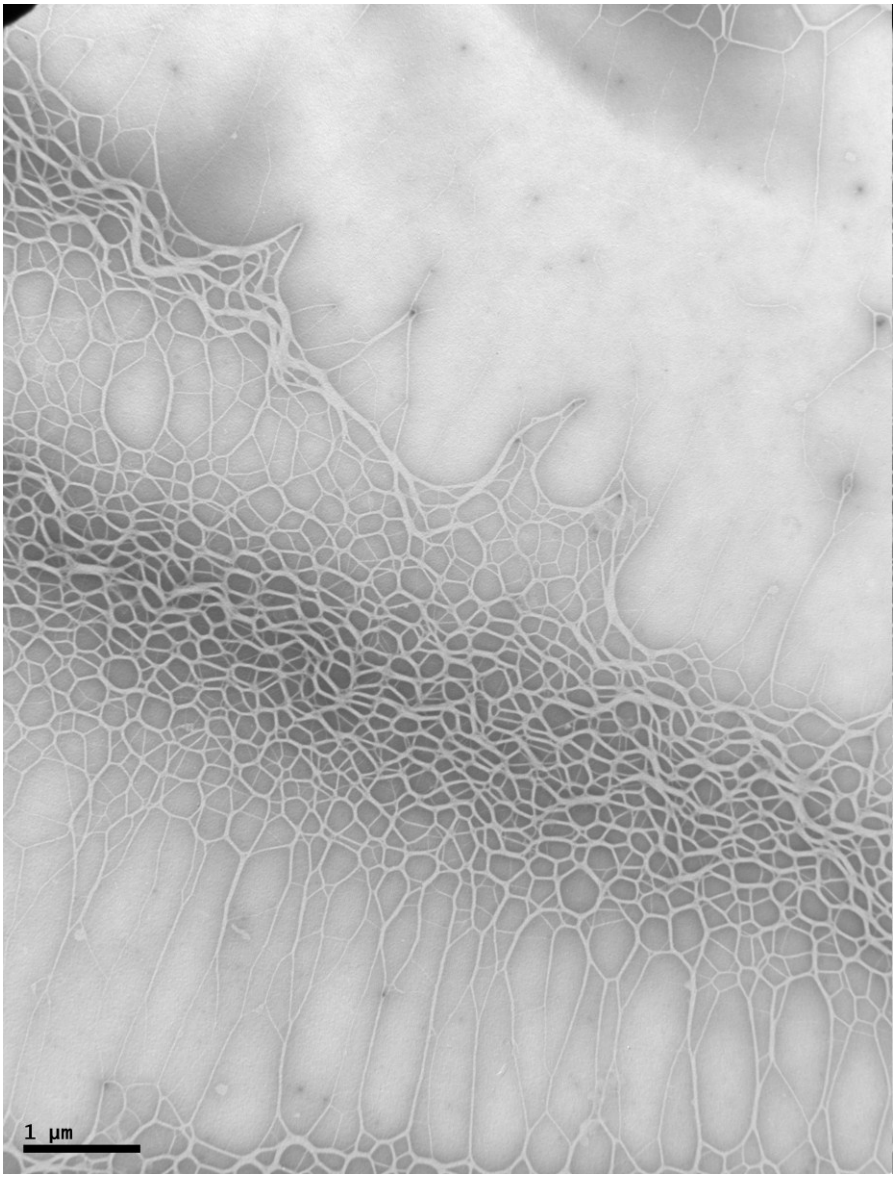
1 µm

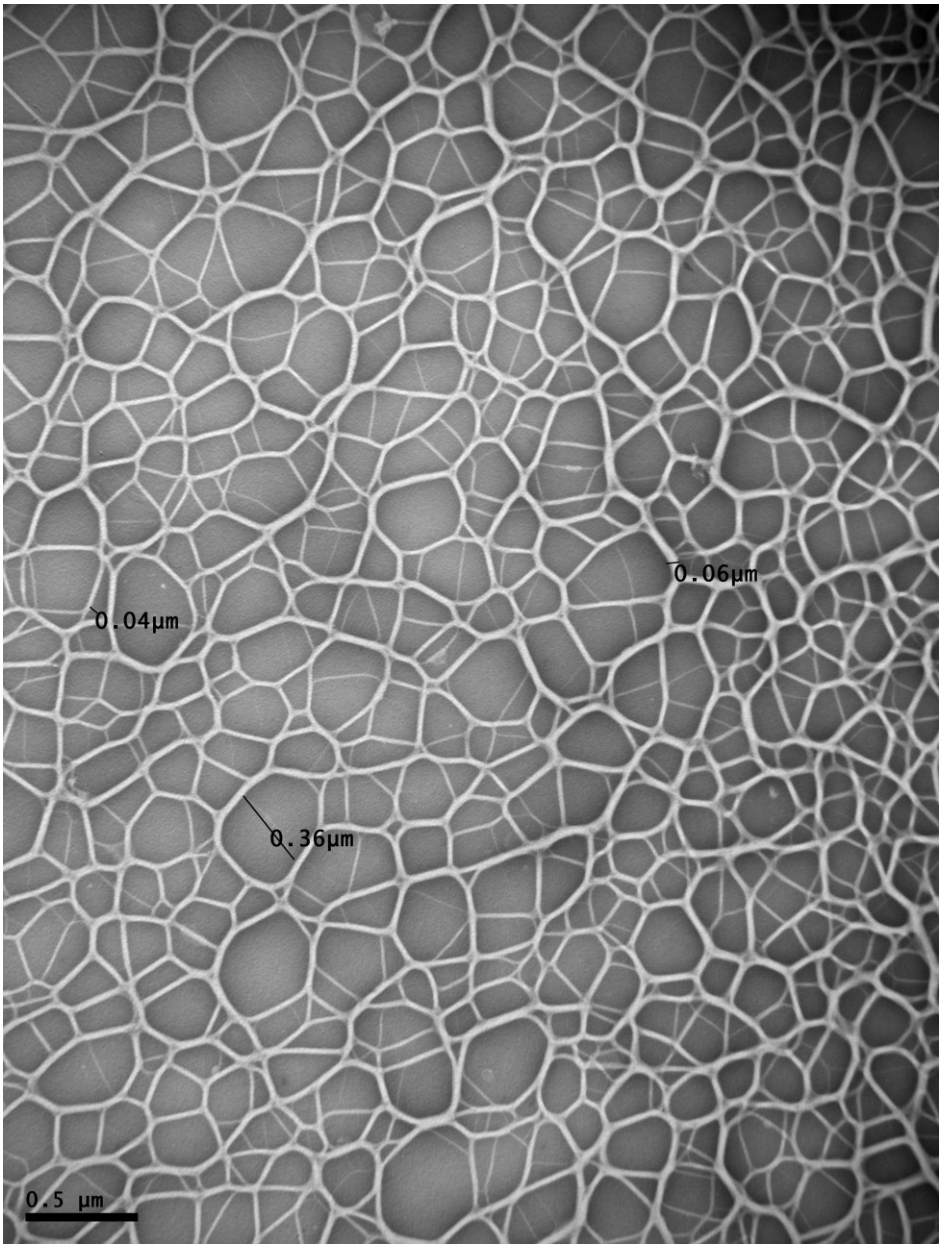

FIGURE: II.3.3: Transmission electron micrograph of the isolated polysaccharide sample.

Generation of an anti-fiber antibody

Based on the observation that the carbohydrate was only released from the cells upon vigorous shaking that also resulted in the breach of the cell envelopes, I hypothesized that the material was not associated with the surface of the cells but had to be released and therefore was most likely periplasmic. Moreover, to rule out that this material was EPS, we repeated our isolations using the Δ*difE* strain, which is deficient in EPS production. Since we could isolate the same amount of material from this strain the polymer was found to be distinct from EPS. To further study its cellular localization, we generated polyclonal antibodies and tested their specificity against the purified material and a number of test carbohydrates using a dot blot.

As expected, the antibody recognized the isolated polymer in a dot blot even when using a small amount of material (FIGURE II.3.4). Since we did not have a strain that failed to produce the material, we were unable to use a negative control for the dot blot. However, to show that the observed binding was indeed specific, we also tested the antibody against a panel of different polysaccharides of known composition.

The dot blot of this specificity test shows that the antibody recognizes starch as well as xanthan gum strongly, while agarose shows only weak cross reactivity. Since starch is a polyglucan and xanthan gum contains a high amount of glucose, in addition to mannose and glucaronic acid, their recognition by the antibody was not too surprising. In contrast, agarose is a polysaccharide made of repeat units of agarobiose, a disaccharide of D-galactose and 3,6-anhydro-L-galactopyranose. Thus, its failure to strongly cross-react was not surprising given its very different composition (TABLE II.3.1).

The antibody did not recognize chitin, a polymer of glucosamine or heparin, a polymer made of repeat units of glucosamine and uronic acid or galactose. This result was somewhat surprising since glucosamine is also present in the polymer and even at the same ratio as glucose (TABLE II.3.1). However, it could be possible that the glucose residues were more accessible and therefore more immunogenic.

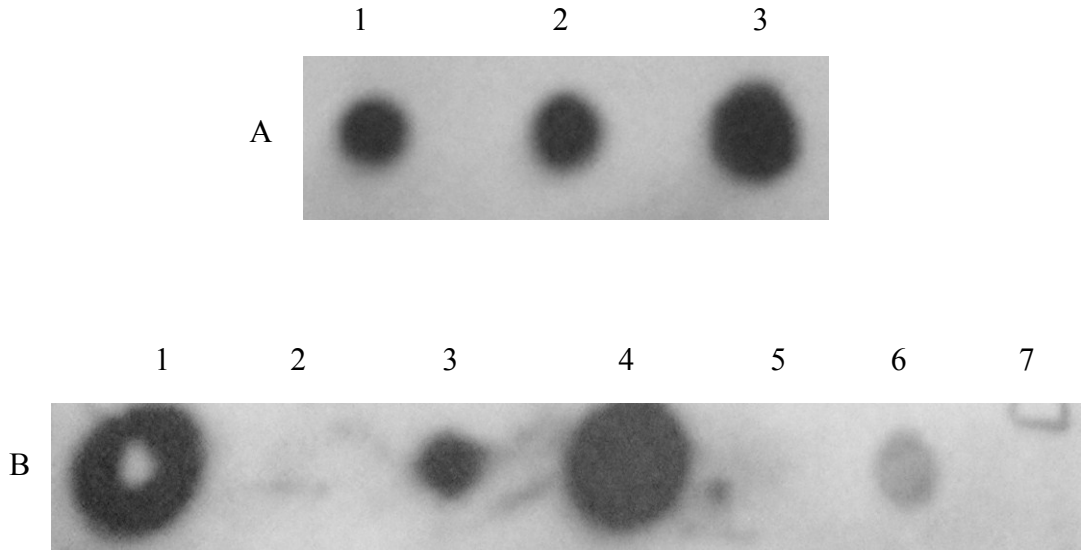

FIGURE II.3.4 Dot blot with polyclonal antibody generated against the isolated polysaccharide. A: Test of different amounts of the polysaccharide. 1. ~ 6 µg 2. ~10 µg 3. ~20µg. B: The antibody was tested for specificity by blotting against various known polysaccharides. 1. Isolated polysaccharide. 2. Chitin 3. Xanthum gum 4. Starch 5. Heparin 6. Agarose 7. TPM buffer.

The polymer is associated with the cell envelope of M. xanthus

We used the generated antibody to label thin sections of wild-type *M. xanthus* cells in order to determine the cellular location of the polysaccharide. Therefore cryo-thin sections were incubated with the antibody that then was detected using immuno-gold

labeling. As can be seen from the picture, the label was nearly exclusively associated with the cell envelopes of the cells confirming our hypothesis that the polymer is periplasmic and has to be released to be isolated (FIGURE II.3.5).

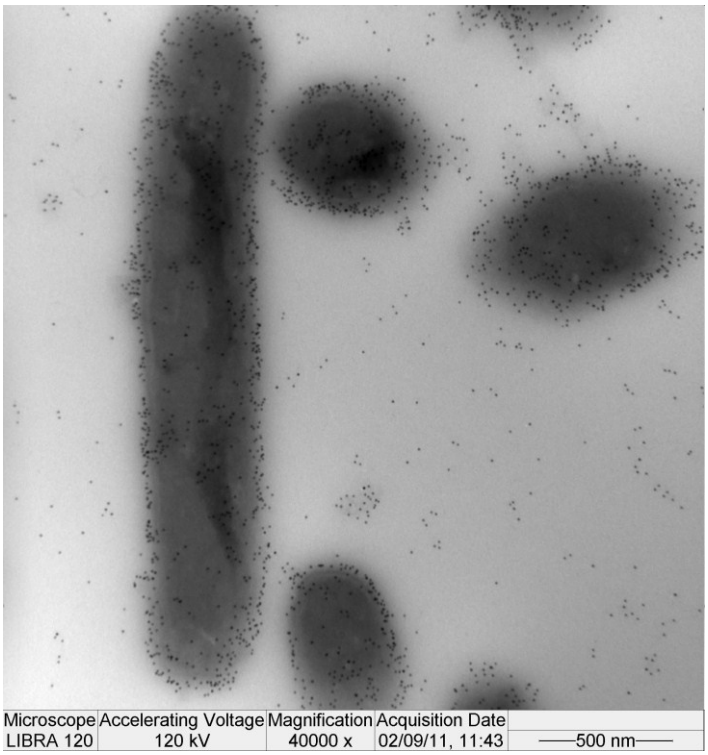

FIGURE II.3.5: Thin sections of DK1622 wild-type cells labeled with the serum containing the polyclonal antibody generated against the isolated polymer.

The purified carbohydrate polymer was then further analyzed for its composition, linkage, and structure at the University of George Center for Complex Carbohydrate Research. Therefore, the polymer was dialyzed in dialysis bag with a molecular cutoff of 20 kDa to remove low weight molecular contaminations. After dialysis the retentate was hydrolyzed with TFA, and size exclusion chromatography was used to isolate a homogenous sample for further analysis.

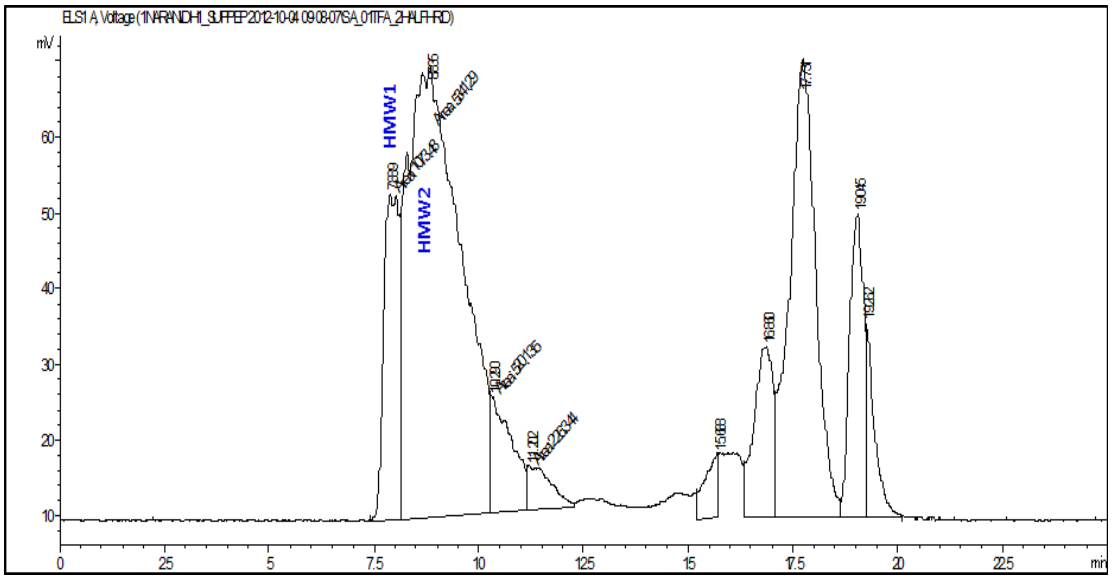

FIGURE II.3.6: Size exclusion chromatography of the isolated and dialyzed polysaccharide.

Two peaks of high molecular weight were recovered through size exclusion chromatography: HMW1 and HMW2. The main peak HMW2 was isolated and used for further analysis.

Glucosyl composition of the polysaccharide

Gas chromatography mass spectrometry was used to analyze the glucosyl composition of the sample.

Sample	Glucosyl residue	Mass (mg)	Mol %[1]
Carbohydrate polymer	Arabinose (Ara)	n.d.	-
	Ribose (Rib)	n.d.	-
	Rhamnose (Rha)	54.1	8.6
	Fucose (Fuc)	n.d.	-
	Xylose (Xyl)	n.d.	-
	Glucuronic Acid (GlcA)	n.d.	-
	Galacturonic acid (GalA)	n.d.	-
	Mannose (Man)	127.1	18.3
	Galactose (Gal)	n.d.	-
	Glucose (Glc)	262.4	37.8
	N-Acetyl Galactosamine (GalNAc)	n.d.	-
	N-Acetyl Glucosamine (GlcNAc)	301.1	35.3
	N-Acetyl Mannosamine (ManNAc)	n.d.	-
	S=	744.8	100.0

TABLE II.3.1 Monosaccharide composition of isolated polysaccharide.

According to the GC-MS analysis of the fraction of the sample, the polymer is composed of equal parts glucose and glucosamine, as well as smaller amounts of mannose and rhamnose, in a ratio of ~4:4:2:1.

Glycosyl linkage results for the polysaccharide

Glycosyl residue	Peak area %
3,4 linked Glucopyranosyl residue (3,4-Glc)	1.0
2 linked Rhamnopyranosyl residue (2-Rha)	1.3
2,3,4,6 linked Glucopyranosyl residue (2,3,4,6-Glc)	1.4
3 linked Mannopyranosyl residue (3-Man)	1.6
2,3,4 linked Mannopyranosyl residue (2,3,4,6-Man)	1.7
3 linked Rhamnopyranosyl residue (3-Rha)	1.7
2,3 linked Glucopyranosyl residue (2,3-Glc)	1.9
4,6 linked Glucopyranosyl residue (4,6-Glc)	2.1
4 linked Glucopyranosyl residue (4-Glc)	2.3
2 linked Glucopyranosyl residue (2-Glc)	2.7
Terminal Rhamnopyranosyl residue (t-Rha)	3.0
3 linked N-Acetylglucosamine (3-GlcNAc)	6.6
3 linked Glucopyranosyl residue (3-Glc)	6.8
2,3 linked Mannopyranosyl residue (2,3-Man)	9.6
2,3,4 linked Glucopyranosyl residue (2,3,4-Glc)	14.2
Terminal N-Acetylglucosamine (t-GlcNAc)	15.3
Terminal Glucopyranosyl residue (t-Glc)	19.7

TABLE II.3.2 The linkage analysis revealed that the carbohydrate polymer is a highly branched poly-Glucose (2,3,4-branched Glc 14%), Mannose (2,3,4-Man 9.6%) and poly-GlcNAc (3-linked GlcNAc ~7%) polysaccharide with a high amount of terminally linked Glc (>19%) and terminally linked GlcNAc (15%). Minor amount of 2,3-Rha (0.6%), 3-Rha (1.7%), 2-Rha (1.3%), and terminally-linked Rha (3%) were present. The composition and linkage analysis collectively suggested that the repeat unit of the polysaccharide consists of the following monosaccharides: 3-Rha, branched Man, branched Glc, t-Glc, 3-GlcNAc and t-GlcNAc in the ratio of 1:2:2:<3:1:2.

Finally, a structure of the repeat unit of the polymer could be proposed based on the glycosyl composition, linkage analysis data as well as NMR chemical shift measurements (FIGURE II.3.7).

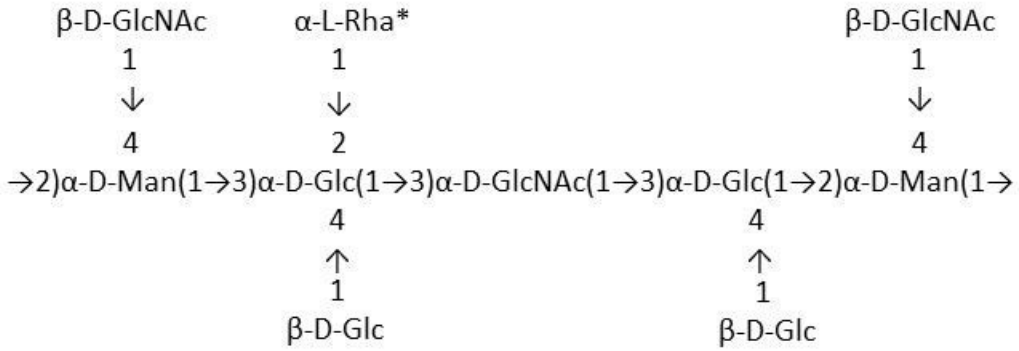

FIGURE II.3.7 Proposed structure of the repeat unit of the *M. xanthus* periplasmic carbohydrate polymer.

The properties of the carbohydrate change under osmotic pressure

As all known periplasmic glucans such as the membrane-derived oligosaccharides of *E.coli* are involved in osmoregulation, it was hypothesized that the same was true for this novel high weight molecular carbohydrate. To test this hypothesis, the cells were grown under low and high osmolarity condition in order to see whether the carbohydrate would change under these different conditions. To generate high osmolarity we added 10.6% PEG8K to the medium, a treatment which resulted in a pressure of about

1 megapascal. However, since agar under these conditions is no longer hardened, 1% phytagel was added to the CTT/PEG medium. As a control, cells were grown on CTT medium hardened with 1% phytagel only. The polymer was isolated from both of these cells grown under the different osmotic conditions using the established protocol.

Both recovered polymer samples were re-suspended in 1 ml of water and dialyzed for 72 hours to remove the ammonium sulfate that was used for the precipitation step. Upon dialysis, the final volume of water in the control sample was 1.5 ml, while the final volume of water in the dialysis bag with the polymer from cells grown under osmotic pressure was 4 ml. Moreover, the dialysis bag with the osmotically induced sample also swelled up more due to the high amount of accumulated water when compared to the control material (FIGURE II.3.9). Multiple repeats of this experiment reproducibly showed these results (TABLE II.3.3).

Experiment	Cells used to isolate (g)	Polysaccharide isolated (g)	Volume before dialysis (ml)	Volume after dialysis (ml)
1	6	0.1	1	4
2	10	0.9	3	17
3	15	2.4	4	21

TABLE II.3.3: Change in amount of water in dialysis bags before and after dialysis of material isolated under high osmotic pressure in three separate experiments.

The material isolated from cells grown under osmotic pressure also behaved differently during the isolation procedure. In contrast to the normal material, which pelleted at 20,500 rpm in the SS34 Sorvall rotor, this material did not pellet. Instead, it formed a thin film on top of the supernatant (FIGURE II.3.8). Finally, in line with its

water adsorptive properties the osmotic induced polymer was also more soluble in water than the regular polymer indicating that this material under osmotic pressure had changed its composition in such a way as to attract and retain more water.

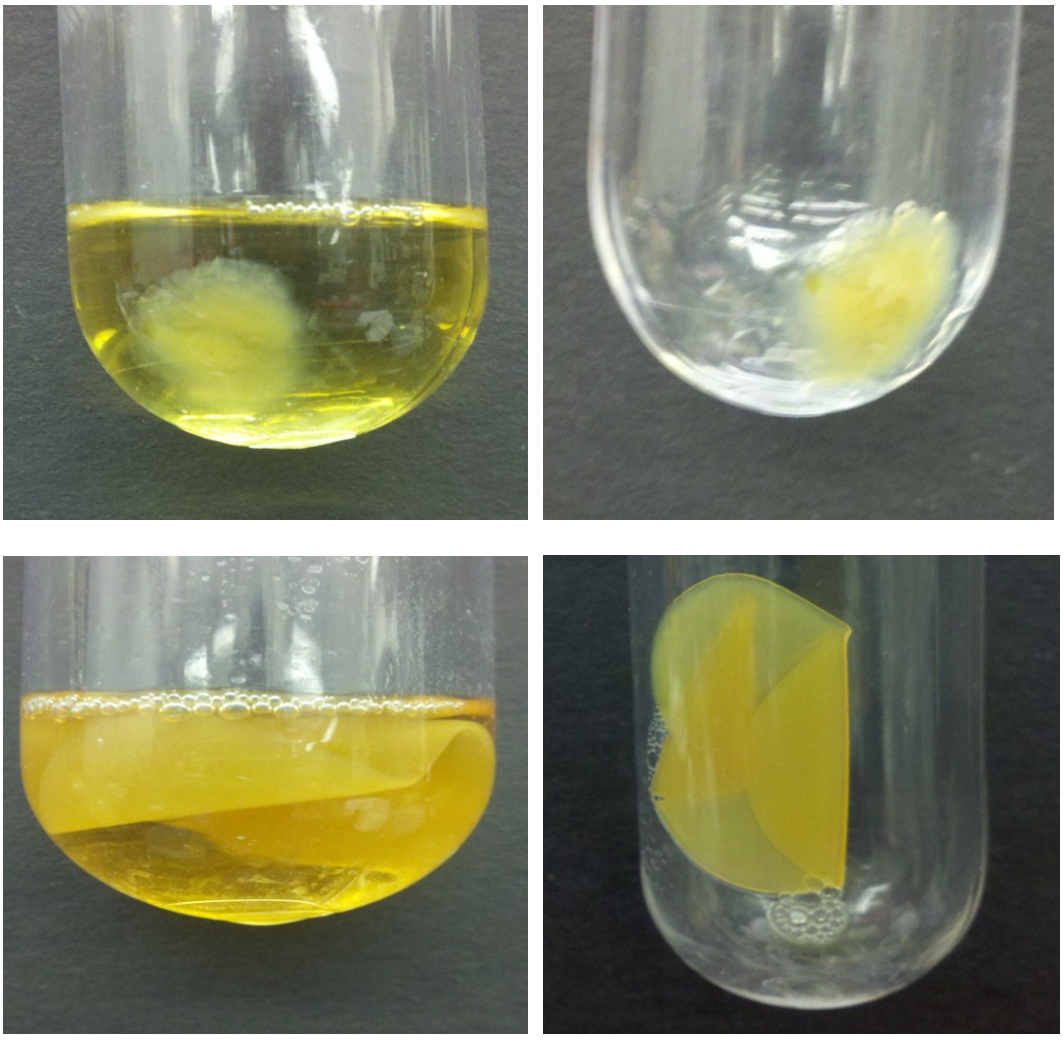

FIGURE II.3.8 Differences between the polysaccharides isolated under normal and under osmotic conditions. Top: Left: The polymer isolated from cells grown under normal conditions forms a pellet at the bottom of the tube that after decanting of the supernatant stays in place (right side). In contrast, the polymer from cells grown under osmotic pressure forms a layer that floats on top of the supernatant after centrifugation (lower left). After careful removal of the liquid, the surface film can be recovered (lower right).

The material obtained from cells grown with PEG8K is very soft, readily soluble in water (more than material obtained from regularly grown cells), insoluble in methanol, and detergent-resistant. During dialysis, the material attracted water and caused the dialysis membrane to swell up (FIGURE II.39). Final pellets from both extractions, from cells grown with PEG8K and without were re-suspended in 1 ml of water and dialyzed. After dialysis, the amount of water in each dialysis bag was measured to estimate the ability of the polymer to bind water (TABLE II.3.3). The material formed by the cells under osmotic challenge attracted anywhere from 4 to 6 times more water indicating that this material had become highly hygroscopic.

FIGURE II.3.9: Appearance of the dialysis bags containing the two polymers after dialysis. Left: Dialysis bag with carbohydrate polymer extracted from cells grown without PEG8K. Right: Dialysis bag with carbohydrate polymer extracted from cells grown with PEG8K. Note, that the bag is more swollen on the right.

II. 4 Discussion

During the thesis I isolated a novel osmoregulated polysaccharide from *M. xanthus* that appears to get modified upon high osmolarity conditions. This polysaccharide appears to represent a novel class of osmoregulated polysaccharide that differs substantially from periplasmic glucans of other bacterial species. One important difference is that this polysaccharide is a complex high, molecular weight polymer, composed not only of glucose, as in the case of OPGs, but of four different monosaccharaides: glucose, glucosamine, mannose and rhamnose. Moreover, the polymer is also highly branched, as determined by the linkage analysis. Although, we have not been able to precisely determine the specific molecular weight of the polymer, it is clear that it is at least larger than 20 kDa as it is retained in a dialysis bag with this molecular cut off. To put this value in perspective: *E. coli* periplasmic glucans are usually 5-12 glucose units long. Given the weight of one glucose unit being 180 Da, the molecular weight of the periplasmic glucan of *E.coli* is about 2 kDa. This would mean that the *M. xanthus* polymer is at least 10 times as large. However, based on the size of the partially hydrolyzed molecule in size exclusion chromatography it is more likely at least 100 times larger than the *E. coli* periplasmic glucans making it the largest known periplasmic glucan.

Although we have not been able to conclusively demonstrate that the polymer is a periplasmic glucan, a number of observations strongly support this interpretation:

1. The polysaccharide can be isolated from Δ*difE* cells which are unable to produce EPS.
2. The cells need to be shaken vigorously in a blender in order to release the polysaccharide.
3. The immuno-gold labeling of the polysaccharide in thin-sections shows that the majority of labeling is associated with the envelope of the cells.
4. The cells need only to be blended to release the polysaccharide. No SDS or other cell-lysing agents has to be used to isolate the polysaccharide, thus, it is unlikely that the material is inside the cytoplasm.

The polysaccharide is consistently purified from various *M. xanthus* strains using the protocol developed by our group. However, it becomes extremely hygroscopic only when purified from cells under osmotic stress. Polyethylene glycol is a known inducer of osmotic stress, used routinely in biochemical experiments to create conditions of low water availability (125). Thus, we predict that the polysaccharide remains chemically the same but may be modified to bind more water. Isolated samples of the modified polymer are currently being analyzed at the UGA Center for Carbohydrate Research to identify the chemical nature of the underlying change.

The periplasmic glucan is also different from other polysaccharides that have been described in *M. xanthus*. The EPS composition, for example, in earlier reports was described as being composed of glucose, galactose and mannose, with trace amounts of glucosamine (127). In later reports it was described to also contain small amounts of rhamnose and xylose (128), while other isolations indicated the presence of mannosamine

and arabinose (129). Since in none of these experiments the EPS was chemically or structurally fractionated it is impossible to say whether these chemical differences were due to the techniques used for isolation or truly compositional differences. Even more problematic is the fact that the procedures used in these experiments included boiling the cells with 0.1% SDS, which releases the periplasmic polymer that could easily contaminate "EPS" isolations. In addition, LPS of *M. xanthus* would also be expected to be isolated using these procedures and many of the monosaccharides present in these former EPS isolations are also found in LPS (130). Therefore, it is currently impossible to say what the true composition of EPS actually is and how many or how much of the sugars found in "EPS" are actually from other polysaccharides like the periplasmic glucan.

SUMMARY

In this thesis I have identified and characterized two new factors important for *M. xanthus* motility and physiology. The first factor were three PilY1 homologs, which play important roles in social motility, aggregation, EPS localization, type IV pilus biogenesis and fruiting body formation. To our knowledge, these proteins had never before been described nor had their functions been analyzed. Their discovery therefore contributes a major step forward in our understanding of these complex processes in the social soil bacterium *M. xanthus*.

The second factor was the identification of a novel osmoregulated periplasmic polysaccharide in *M. xanthus*. Analyses indicated that this polymer is of high molecular weight, highly branched, and has a complex composition of four different monosaccharides. During the work, the molecular structure of the polymer was established, which is only the second complex carbohydrate structure ever solved in myxobacteria. The fact that this polymer becomes more hygroscopic upon osmotic pressure together with its location within the periplasm indicates that it is an OPG. However, it differs in so many ways from all known OPGs that it can be classified as a novel type of this important group of bacterial polysaccharides.

BIBLIOGRAPHY

1.Henrichsen J (1972) Bacterial surface translocation: a survey and a classification *Bacteriology Reviews* 36(4): 478-503.

2.Hershey R (2003) Bacterial motility on a surface: many ways to a common goal. *Annual Reviews Microbiology* 57: 249-273.

3.Shunk (1920) A modification of Leoffler's flagella stain. *Journal of Bacteriology.* 5(2): 181-187.

4.Gerven NV., Waksman G., Remaut H (2011) Pili and flagella biology, structure, and biotechnological applications. *Progress in Molecular Biology and Translational Science*. 103: 21-72.

5.Aslam Z., Lim JH., ImWT., Yasir M., Chung YR., and Lee St (2007) *Salinicoccus jeotgali* sp. nov., isolated from jeotgal, a traditional Korean fermented seafood. *International journal of systematic and evolutionary microbiology*. 57(pt3): 633-638.

6.Harshey, R. M. (1994) Bees aren't the only ones: swarming in gram-negative bacteria. *Journal of Molecular Microbiology*. 13:389-394.

7. Duan Q, Zhou M, Zhu L and Zhu G (2012) Flagella and bacteria pathogenicity. *Journal of Basic Microbiology*. 53(1): 1-8.

8.McBride MJ (2004) *Cytophaga- flavobacterium* gliding motility. *Journal of molecular microbiology and biotechnology* 7(1-2): 63-71.

9.Hoiczyk E and Baumeister W (1998). The junctional pore complex, a prokaryotic secretion organelle, is a molecular motor underlying gliding motility in *cyanobacteria*. *Current Biology* 8: 116`1-1168.

10.C.W. Wolgemuth and G. Oster (2004). The Junctional Pore Complex and the Propulsion of Bacterial Cells. *Journal of Molecular Microbiology and Biotechnology*. 7: 72-77.

11.Houwink AL and Iterson WV (1950) Electron microscopic observations on bacterial cytology II. A study on flagellation. *Biochemica et Biophysica Acta* (5):10-44.

12.Duguid S., Dempster and Edmund. (1955) Non-flagellar filamentous appendages ("fimbriae") and hemagglutinating activity in bacterium *coli*. *Journal of pathological* bacteria 70:335-348.

13.Fronzes R., Remaut H, and Wasksman G. (2008) Architectures and biogenesis of non-flagellar protein appendages in Gram negative bacteria. *The EMBO journal.* 27(17): 2271-2280.

14.Soto, G.E., and Hultgren, S.J. (1999) Bacterial adhesins: common themes and variations in architecture and assembly. *Journal of Bacteriology* 181: 1059–1071.

15.Fernandez LA and Berenguer J. (2000) Secretion and assembly of regular surface structures in Gram-negative bacteria. *FEMS Microbiology Reviews* 24: 21-44.

16.Thanassi DG, Bliska JB, Christie PJ.(2012) Surface organelles assembled by secretion systems of Gram-negative bacteria: diversity in structure and function. *FEMS Microbiology Letters.* 36(6): 1046-82.

17. Hahn E, Wild P, Hermanns U, Sebbel P, Glockshuber R, Häner M, Taschner N, Burkhard P, Aebi U, Müller SA. (2002) Exploring the 3D molecular architecture of *Escherichia coli* type I pili. *Journal of Molecular Biology.* 323(5): 845-857.

18.Barnhart MM., Lynem J and Chapman MR (2006) GlcNAc-6P levels modulate the expression of Curli fibers by *Escherichia coli. Journal of Bacteriology.* 188(14): 5212-5219.

19.Galan JE. and Collmer A. (1999)Type III secretion machines: bacterial devices for protein delivery into host cells. *Science*. 284(5418): 1322-1328.

20.Aguilar J. Zupan J, Cameron TA, and Zambryski PC (2010) *Agrobacterium* type IV secretion system and its substrates form helical arrays around the circumference of virulence-induced cells. *PNAS*. USA. 107(8): 3758-3763

21.Pugsley AP (1993) The complete general secretory pathway in Gram-negative bacteria. *Microbiological Reviews* 57(1): 50-108.

22.Pelicic V (2008) Type IV pili*: e pluribus unum*? *Molecular Microbiology* 68(4): 827-837.

23.Mattick JS. (2002) Type IV pili and twitching motility. *Annual Review of Microbiology* 56: 289-314.

24.Nudelman E and Kaiser D. (2004) Pulling together with Type IV pili. *Journal of molecular biology and biotechnology*. 7(1-2): 52-62.

25.Craig L. Pique ME, and Tainer JA (2004). Type IV pilus structure and bacterial pathogenesis. *Nature Reviews*. 2:363-378.

26.Jarrel KF (2009) Pili and Flagella, *Current Research and Future Trends*. Caister Academic Press.

27.Burrows LL (2012) *Pseudomonas aeruginosa* twitching motility. *Annual Review of Microbiology* 66:493-520.

28.Craig L, Volkmann N, Arvai AS, Pique ME, Yeager M, Egelman EH, and Tainer JA (2006) Type IV pilus structure by cryo-electron microscopy and crystallography: implications for pilus assembly and functions. *Molecular Cell.* 23(5): 651-662.

29.Yang Z, Hu W, Chen K, Wang J, Lux R, Zhou ZH, Shi W (2011) Alanine 32 in PilA is important for PilA stability and type IV pili function in *Myxococcus xanthus*. *Microbiology* 157(pt7): 1920-1928.

30.Nunn, D. N., and S. Lory. (1991) Product of the *Pseudomonas aeruginosa* gene pilD is a prepilin leader peptidase. *PNAS.* 88:3281-3285.

31.Lory S and Storm MS (1997) Structure-function relationship of type IV prepilin peptidase of *Pseudomonas aeruginosa. Gene*. 192(1): 117-121.

32.Giltner C, Nguyen Y and Burrows L (2012) Type IV pilin proteins: Versatile molecular modules. *Microbiology and Molecular Biology Reviews* 76(4): 740-772.

33.Jakovlijevic V., Leonardy S., Hoppert M and Sogaard-Anderson L (2008) PilB and PilT are ATPases acting antagonistically in type IV pilus function in *Myxococcus xanthus. Journal of Bacteriology* 190(7): 2411-2421.

34.Maier B, Potter L, So M, Long CD, Seifert HS, Sheetz MP (2002). Single pilus motor forces exceed 100 pN. *PNAS*. 99(25): 16012-16017.

35.Collins RF, Saleem M and Derrick JP (2007) Purification and three-dimensional electron microscopy structure of the *Neisseria meningitidis* type IV pilus biogenesis protein PilG. *Journal of Bacteriology* 189(17):6389-6396

36.Craig L and Li J (2008) Type IV pili: paradoxes in form and function. *Current opinion in structural biology*. 18(2): 267-277.

37.Karuppiah V, Hassan D, Saleem M, Derrick JP.(2010) Structure and oligomerization of the PilC type IV pilus biogenesis protein from *Thermus thermophilus. Proteins*. 78(9): 2049-2057

38.Ayers M, Sampaleanu LM, Tammam S, Koo J, Harvey H, Howell PL, Burrows LL. (2009) PilM/N/O/P proteins form an inner membrane complex that affects the stability of the *Pseudomonas aeruginosa* type IV pilus secretin. *Journal of molecular biology*. 394(1): 128-142

39.Martin P, Hobbs M, Free P, Jeske Y and Mattick J (1993) Characterization of pilQ, a new gene required for the biogenesis of type 4 fimbriae in *Pseudomonas aeruginosa. Journal of Molecular Microbiology*. 9(4): 857-868.

40.Drake SL, Koomey M. (1995) The product of the pilQ gene is essential for the biogenesis of type IV pili in *Neisseria gonorrhea*. *Molecular Microbiology.* 18(5): 975-986.

41.Collins RF, Ford RC, Kitmitto A, Olsen RO, Tønjum T, Derrick JP. (2003) Three dimensional structure of the *Neisseria meningitidis* secretin PilQ determined from negative stain transmission electron microscopy. *Journal of Bacteriology.* 185(8): 2611-2617.

42.Collins RF, Frye SA, Balasingham S, Ford RC, Tønjum T, Derrick JP. (2005) Interaction with type IV pili induces structural changes in the bacterial outer membrane secretin PilQ. *Journal of Biological Chemistry*. 280(19): 18923-18930.

43.Whitchurch C. (2006) Biogenesis and function of type IV pili in *Pseudomonas species. Pseudomonas* 139-188.

44.Allen WJ, Phan G, Waksman G. (2012) Pilus biogenesis at the outer membrane of Gram-negative bacterial pathogens. *Current opinion in structural biology*. 22(4): 500-506.

45.Giltner CL, Habash M, Burrows LL. (2010) *Pseudomonas aeruginosa* minor pilins are incorporated into type IV pili. *Journal of Molecular Biology*. 398(3): 444-461.

46.Rudel T, Scheurerpflug I, Meyer TF. (1995) *Neisseria* PilC protein identified as type-4 pilus tip-located adhesin. *Nature* 373(6512): 357-359

47.Rudel T, Facius D, Barten R, Scheuerpflug I, Nonnenmacher E, Meyer TF.(1995) Role of pili and the phase-variable PilC protein in natural competence for transformation *of Neisseria gonorrhoeae. PNAS*. USA. 92(17): 7986-7990.

48.Rudel T, Boxberger HJ, Meyer TF. (1995) Pilus biogenesis and epithelial cell adherence of *Neisseria gonorrhea* pilC double knockout mutants. *Journal of Molecular Microbiology.* 17(6): 1057-1071.

49.Jonsson AB, Nyberg G and Normark S (1991) Phase variation of gonoccocal pili by frameshift mutation in pilC, a novel gene for pilus assembly. *EMBO.* 10(2): 477-488.

50.Rytkönen A, Albiger B, Hansson-Palo P, Källström H, Olcén P, Fredlund H, Jonsson AB. (2004) *Neisseria meningitidis* undergoes PilC phase variation and PilE sequence variation during invasive disease. *Journal of Infectious Diseases.* 189(3): 402-409.

51.Rudel T, van Putten JP, Gibbs CP, Haas R, Meyer TF. (1992) Interaction of two variable proteins (PilE and PilC) required for pilus-mediated adherence of *Neisseria gonorrhoeae* to human epithelial cells. *Journal of Molecular Microbiology*. 6(22): 3439-3450.

52.Scheuerpflug I, Rudel T, Ryll R, Pandit J, Meyer TF. (1999) Roles of PilC and PilE proteins in pilus mediated adherence of *Neisseria gonorrhea* and *Neisseria meningitidis* to human erythrocytes and endothelial and epithelial cells. *Infection and Immunity*. 67(2):834-843.

53.Rahman M, Källström H, Normark S, Jonsson AB.(1997) PilC of pathogenic *Neisseria* is associated with the bacterial cell surface. *Journal of Molecular Microbiology*. 25(1): 11-25.

54.Alm RA, Hallinan JP, Watson AA, Mattick JS. (1996) Fimbrial biogenesis genes of *Pseudomonas aeruginosa*: pilW and pilX increase the similarity of type 4 fimbriae to the GSP protein-secretion systems and pilY1 encodes a gonococcal PilC homologue. *Journal of Molecular Microbiology*. 22(1): 161-173.

55.Bohn YS, Brandes G, Rakhimova E, Horatzek S, Salunkhe P, Munder A, van Barneveld A, Jordan D, Bredenbruch F, Häussler S, Riedel K, Eberl L, Jensen PØ,Bjarnsholt T, Moser C, Hoiby N, Tümmler B, Wiehlmann L. (2009) Multiple roles of *Pseudomonas aeruginosa* TBCF10839 PilY1 in motility, transport and infection. *Journal of Molecular Microbiology*. 71(3): 730-747.

56.Heiniger RW, Winther-Larsen HC, Pickles RJ, Koomey M, Wolfgang MC. (2010) Infection of human mucosal tissue by *Pseudomonas aeruginosa* requires sequential and mutually dependent virulence factors and a novel pilus-associated adhesin. *Cellular Microbiology* 12(8): 1158-1173

57.Orans J, Johnson MD, Coggan KA, Sperlazza JR, Heiniger RW, Wolfgang MC, Redinbo MR. (2010) Crystal structure analysis reveals *Pseudomonas* PilY1 as an essential calcium-dependent regulator of bacterial surface motility. *PNAS* 107(3)1065-1070

58.Johnson MD, Garrett CK, Bond JE, Coggan KA, Wolfgang MC, Redinbo MR. (2011) *Pseudomonas aeruginosa* PilY1 binds integrin in an RGD- and calcium-dependent manner. *Plos One*. 6(12): e29629

59.Leroy-Dudal J, Gagnière H, Cossard E, Carreiras F, Di Martino P. (2004) Role of alphavbeta5 integrins and vitronectin in *Pseudomonas aeruginosa* PAK interaction with A549 respiratory cells. *Microbes and Infection*. 6(10): 875-881.

60.Kuchma SL, Ballok AE, Merritt JH, Hammond JH, Lu W, Rabinowitz JD, O'Toole GA. (2010) Cyclic-di-GMP-mediated repression of swarming motility by *Pseudomonas aeruginosa*: the pilY1 gene and its impact on surface-associated behaviors. *Journal of Bacteriology*. 192(12): 2950-2964.

61.Per Klemm (1994) Fimbriae: adhesion, genetics, biogenesis and vaccines. Page 32. CRC Press.

62.Bradley DE. Shortening of *Pseudomonas aeruginosa* pili after RNA-phage adsorption. *Journal of General Microbiol.* 1972 Sep;72(2):303–319

63.Skerker JM and Berg Howard (2001) Direct observation of extension and retraction of type IV pili. *PNAS* 98(12): 6901-6904

64.Holz C, Opitz D, Greune L, Kurre R, Koomey M, Schmidt MA, Maier B. (2010) Multiple pilus motors cooperate for persistent bacterial movement in two dimensions. *Physics Review Letter* 104(17): 178104.

65.O'Toole GA, Kolter R. (1998) Initiation of biofilm formation in *Pseudomonas fluorescens* WCS365 proceeds via multiple, convergent signaling pathways: a genetic analysis. *Molecular Microbiology*. 28(3): 449-461

66.Klausen M, Heydorn A, Ragas P, Lambertsen L, Aaes-Jørgensen A, Molin S, Tolker-Nielsen T. (2003) Biofilm formation by *Pseudomonas aeruginosa* wild type, flagella and type IV pili mutants. *Molecular Microbiology*. 48(6): 1511-1524.

67. Kellogg DS Jr., Peacock WL Jr., Deacon WE, Brown L, Pirkle DI (1963) *Neisseria gonorrhoeae* I. Virulence genetically linked to clonal variation. *Journal of Bacteriology* 85: 1274-1279.

68. Kellogg DS Jr, Cohen IR, Norins LC, Schroeter AL, Reising G. (1968) *Neisseria gonorrhoeae*. II. Colonial variation and pathogenicity during 35 months in vitro. *Journal of Bacteriology*. 96(3): 596-605

69.Swanson J (1963) Studies on *gonococcus* infection. IV. Pili: their role in attachment of gonococci to tissue culture cells. *The Journal of Experimental Medicine*. 137(3): 571-589

70.Woods D, Straus D, Johanson W, Berry VK and Bass J (1980) Role of pili in adherence of *Pseudomonas aeruginosa* to mammalian buccal epithelial cells. *Infection and Immunity*. 29(3): 1146-1151.

71.Korotkov KV, Sandkvist M, Hol WG (2012) The type II secretion system: biogenesis, molecular architecture and mechanism. *Nature Reviews Microbiology.* 10(5): 336-351.

72.Ayers M, Howell PL, Burrows LL. (2010) Architecture of the type II secretion and type IV pilus machineries. *Future Microbiology*. 5(8): 1203-1218.

73.Sharon N (2006) Carbohydrates as future anti-adhesion drugs for infectious diseases. *Biochemica and Biophysica Acta.* 1760(4): 527-537

*74.*Kaiser D, Robinson M, Kroos L.(2010) *Myxobacteria* , polarity, and multicellular morphogenesis. *Cold Spring Harbor perspectives in Biology.*

75. Goldman BS, Nierman WC, Kaiser D, Slater SC, Durkin AS, Eisen JA, Ronning CM, Barbazuk WB, Blanchard M, Field C, Halling C, Hinkle G, Iartchuk O, Kim HS, Mackenzie C, Madupu R, Miller N, Shvartsbeyn A, Sullivan SA, Vaudin M, Wiegand R, Kaplan HB. (2006) Evolution of sensory complexity recorded in a *myxobacterial* genome. *PNAS*. USA. 103(41): 15200-15205

76.Zusman DR, Scott AE, Yang Z, Kirby JR. (2007) Chemosensory pathways, motility and development in *Myxococcus xanthus*. *Nature Reviews Microbiology.* 5(11): 862-872

77.Hodgkin J and Kaiser D (1979) Genetics of gliding motility in *Myxococcus xanthus* (M*yxobacterales*): Two gene systems control movement. *Molecular and General Genetics*. 171:177-191.

78.Spormann AM (1999) Gliding motility in bacteria: insights from studies of *Myxococcus xanthus*. *Microbiology and Molecular Biology Reviews*. 63(3): 621-641.

79.Youderian P, Burke N, White DJ, Hartzell PL. (2003) Identification of genes required for adventurous gliding motility in *Myxococcus xanthus* with the transposable element mariner. *Molecular Microbiology.* 49(2): 555-570

80.Wolgemuth C, Hoiczyk E, Kaiser D, Oster G. (2002) How *myxobacteria* glide. Current Biology. 12(5): 369-377.

81.Mignot T, Shaevitz JW, Hartzell PL, Zusman DR. (2007) Evidence that focal adhesion complexes power bacterial gliding motility. *Science.* 315(5813): 853-856

82.MacRae TH, McCurdy D. (1977) Evidence for motility related fimbriae in the gliding microorganisms *Myxococcus xanthus*. *Canadian Journal of Microbiology.* 22(10): 1589-1593.

83.Kaiser D. (1979) Social gliding is correlated with the presence of pili in *Myxococcus xanthus. PNAS.* 76(11): 5952-5956.

84.Bowden MG, Kaplan HB. (1998). The *Myxococcus xanthus* lipopolysaccharide O-antigen is required for social motility and multicellular development. *Molecular Microbiology*. 30(2): 275-284.

85.Kaiser D and Crosby C (1983) Cell movement and its coordination in swarms of *Myxococcus xanthus. Cytoskeleton*. 3(2): 227-245.

86.Rodriguez AM, Spormann AM. (1999) Genetic and molecular analysis of cglB, a gene essential for single-cell gliding in *Myxococcus xanthus. Journal of Bacteriology.* 181(14): 4381-4390.

87.Pathak DT, Wei X, Wall D. (2012) *Myxobacterial* tools for social interactions. *Research in Microbiology*. 163(9-10): 579-591.

88.Li Y, Sun H, Ma X, Lu A, Lux R, Zusman D, Shi W. (2003) Extracellular polysaccharides mediate pilus retraction during social motility of *Myxococcus xanthus. PNAS* 100(9): 5443-5448

89.Hu W, Yang Z, Lux R, Zhao M, Wang J, He X, Shi W. (2012) Direct visualization of the interaction between pilin and exopolysaccharides of *Myxococcus xanthus* with eGFP- fused PilA protein. *FEMS Microbiology Letters*. 326(1): 23-30.

90.Lu A, Cho K, Black WP, Duan XY, Lux R, Yang Z, Kaplan HB, Zusman DR, Shi W. (2005) Exopolysaccharide biosynthesis genes required for social motility in *Myxococcus xanthus. Molecular Microbiology*. 55(1): 206-220.

91.Wall D and Kaiser D. (1999) Type IV pili and cell motility. *Molecular Microbiology*. 32(1):1-10

92.Burnham JC, Collart SA and Highison BW (1981) Entrapment and lysis of the *cyanobacterium Phormidium luridum* by aqueous colonies of *Myxococcus xanthus*. PCO2. *Archives of Microbiology*. 129:285-294.

93.J W Arnold and L J Shimkets (1988) Cell surface properties correlated with cohesion in *Myxococcus xanthus. Journal of Bacteriology*. 170(12): 5771-5777.

94.R M Behmlander and M Dworkin (1994) Biochemical and structural analyses of the extracellular matrix fibril of *Myxococcus xanthus*. *Journal of Bacteriology*. 176(20): 6295-6303.

95.Lancero H, Brofft JE, Downard J, Birren BW, Nusbaum C, Naylor J, Shi W, Shimkets LJ. (2002) Mapping of *Myxococcus xanthus* social motility dsp mutations to the dif genes. *Journal of Bacteriology*. 184(5): 1462-1465.

96.Burnham JC, Collart SA and Highison BW (1981) Entrapment and lysis of the *cyanobacterium Phormidium luridum* by aqueous colonies of *Myxococcus xanthus.* PCO2. Archives of Microbiology. 129:285-294.

97.Black WP, Xu Q, Yang Z. (2006) Type IV pili function upstream of the Dif chemotaxis pathway in *Myxococcus xanthus* EPS regulation. *Molecular Microbiology*. 61(2): 447-456.

98.Yang Z, Lux R, Hu W, Hu C, Shi W. (2010) PilA localization affects extracellular polysaccharide production and fruiting body formation in *Myxococcus xanthus*. *Molecular Microbiology*. 76(6): 1500-1513.

99.Gille C and Frommel C. (2000) STRAP: editor for STRuctural Alignments of Proteins. *Bioinformatics* 17(4): 377-378.

100.Söding J, Biegert A, and Lupas AN. (2005) The HHpred interactive server for protein homology detection and structure prediction. *Nucleic Acids Research* 33, W244--W248

101.Terashima H, Kojima S and Homma Michio (2008) Flagellar motility in Bacteria: structure and function of flagellar motor. *International review of cell and molecular biology*. 270:39-74.

102. Thomas Nordahl Petersen, Søren Brunak, Gunnar von Heijne & Henrik Nielsen (2011) SignalP 4.0: discriminating signal peptides from transmembrane regions *Nature Methods*, 8:785-786.

103.Sarah Fremgen, Amanda Williams, Gou Furusawa, Katarzyna Dziewanowska, Matthew Settles, and Patricia Hartzell (2013) MasABK proteins interact with proteins of the type IV pilin system to affect social motility of *Myxococcus xanthus. Plos One.* 8(1): e54557.

104.Harper JM, Hoff EF and Carruthers VB (2003) Multimerization of the *Toxoplasma gondii* MIC2 integrin like A domain is required for binding to heparin and human cells. *Molecular and Biochemical Parasitology*. 134:201-212.

105. Malik A, Kakii K.(2003) Pair dependent co-aggregation behavior of non-flocculating bacteria. *Biotechnology Letters*. 25(12): 981-986.

106.Campos JM and D. R. Zusman (1975) Regulation of development in *Myxococcus xanthus*: effect of 3'-5'-cyclic AMP, AMP, ADP and nutrition. *PNAS*. USA. 72:518-522.

107.Heckman KL and Pease LR (2007) Gene splicing and mutagenesis by PCR-driven overlap extension. *Nature Protocols*. 2(4): 924-933.

108.Julien, B., Kaiser, A. D. & Garza, A. (2000). Spatial control of cell differentiation in *Myxococcus xanthus*. *PNAS* 97: 9098–9103

109.Wu SS and Kaiser D (1997) Regulation of expression of the pilA gene in *Myxococcus xanthus*. *Journal of Bacteriology.* 179(24): 7748-7758.

110.Ueki T, Inouye S and Inouye M (1996) Positive-negative KG cassettes for construction of multi-gene deletions using a single drug marker. *Gene.* 183(1-2): 153-157.

111.Ramaswamy S, Dworkin M, and Downard J (1997) Identification and characterization of *Myxococcus xanthus* mutants deficient in calcoflour white binding. *Journal of Bacteriology*. 179(9): 2863-2871.

112. Shi W and Zusman D (1993) The two motility systems of *Myxococcus xanthus* show different selective advantages on various surfaces. *PNAS.* USA. 90(8): 3378-82.

113.Shimkets LJ (1986) Role of cell cohesion in *Myxococcus xanthus* fruiting body formation. *Journal of Bacteriology*. 166(3): 842-848.

114.Dobson WJ, McCurdy HD and MacRae TH (1979) The function of fimbriae in *Myxococcus xanthus* II. The role of fimbriae in cell-cell interaction. *Canadian Journal of Microbiology*. 25(12): 1359-1372.

115.Black, W. P., and Z. Yang (2004) *Myxococcus xanthus* chemotaxis homologs DifD and DifG negatively regulate fibril polysaccharide production. *Journal of Bacteriology*. 186:1001-1008.

116.Rehm BA (2010) Bacterial polymers: biosynthesis, modifications and application. *Nature Reviews*. 8: 578-592.

117.Lee S, Cho E and Jung S (2009) Periplasmic glucans isolated from Proteobacteria. *BMB Reports* 769-775.

118.Bazaka K, Crawford RJ, Nazarenko EL, and Ivanova EP (2011) Bacterial extracellular polysaccharides. In Bacterial Adhesion. *Advances in Experimental Medicine and Biology*. 715:213-226

119.Kumar AS, Mody K and Jha Bhavanath. (2007) Bacterial exopolysaccharides- a perception. *Journal of Basic Microbiology*. 47:103-117.

120.Bohin JP (2000) Osmoregulated periplasmic glucans in Proteobacteria. *FEMS Microbiology Letters*. 186: 11-19.

121.Vu B, Chen M, Crawford RJ and Ivanova EP (2009) Bacterial extracellular polysaccharides involved in biofilm formation. *Molecules.* 14: 2535-2554.

122.Markovitz,A. and Dorfman,A. (1962) Synthesis of capsular polysaccharide Hyaluronic acid by protoplast membrane preparations of group A *Streptococci. Journal of Biological Chemistry*. 237, 273–279.

123.Ruiz, Natividad; Kahne, Daniel; Silhavy, Thomas J (2009). "Transport of lipopolysaccharide across the cell envelope: the long road of discovery". *Nature Reviews Microbiology* 7 (9): 677–683

124.Varki A, Cummings R, Esko J, Freeze H, Hart G and Marth J (1999) Essentials of glycobiology Chapter 21. *Cold Spring Harbour NY*.

125. Turkan, I., Bor, M., Ozdemir, F. and Koca, H. (2005) Differential responses of lipid peroxidation and antioxidants in the leaves of drought tolerant *P. acutifolius* Gray and drought sensitive *P. vulgaris* subjected to polyethylene glycol mediated water stress. *Plant Science* 168: 223-231.

126. Durand E, Bernadac A, Ball G, Lazdunski A, Sturgis JN, Filloux A. (2003). Type II protein secretion in *Pseudomonas aeruginosa* : the pseudopilus is a multifibrilar and adhesive structure. *Journal of Bacteriology*. 185(9): 2749-2758.

127. Sutherland IW, Thomson S. (1975) Comparison of polysaccharides produced by *Myxococcus strains*. *Journal of General Microbiology*. 89(1):124–132

128. R M Behmlander and M Dworkin (1994) Biochemical and structural analyses of the extracellular matrix fiblrils in *Myxococcus xanthus. Journal of Bacteriology.* 176(20): 6295-6303.

129. Wen Shi (2005) Personal Communication. Myxococcus Conference

130.Maclean L, Perry MB, Nossova L, Kaplan H, Vinogradov E. (2007). The structure of the carbohydrate backbone of the LPS from *Myxococcus xanthus* strain DK1622. *Carbohydrate Research*. 342(16):2474-2480.

CURRICULUM VITAE

Sapeckshita Agrawal (Sapeck)
Maiden Name: Srivastava
800, 4th St. SW Apt. S319
Washington DC 20024
(413) 687-2426(cell)
sapeck.srivastava@gmail.com

EDUCATION AND TRAINING

Ph.D 2013 **Johns Hopkins University, Baltimore, Molecular Microbiology and Immunology**

Research with Egbert Hoiczyk: I have studied the role of three minor proteins in surface motility and pili function in Gram negative bacteria, *Myxococcus xanthus,* using biochemical, genetic and microscopic techniques. I have also discovered a novel high molecular weight carbohydrate polymer which plays important roles in bacterial physiology.

MS 2008 **George Washington University, Washington DC, Public Health Microbiology and Immunology Summa cum laude**

Research with David Leitenberg: Newborn cord blood samples were used for isolating lymphocytes to study their T cell composition to understand differences in immune status of babies born vaginally or by C-section. I isolated lymphocytes from whole blood samples and used flow cytometry to quantify various subsets of lymphocytes in each patient sample. Using these techniques, I analyzed blood samples of over 40 newborn babies, and also used statistics to understand the role of factors such as breast feeding versus formula feeding, birth age etc on the differences in lymphocytes.

BS 2006 **University of Massachusetts, Amherst, Biology**

Research with Lawrence Schwartz: Various strains of Drosophila melanogaster expressing amyloid proteins in their muscle tissue were subjected to climbing assays to study muscle function.

ADDITIONAL RESEARCH EXPERIENCE

2008-2009 Research with Marcelo Jacobs Lorena: siRNA was used to assess the role of proteins involved in immune pathway of malaria vector, *Anopheles gambiae*.

2008 Research with Jelena Levitskaya: liver stage of malaria parasite, *Plasmodium berghei* was studied using HC-04 primary hepatocyte cell line, to understand MHC presentation n by infected hepatocytes.

STUDENT MENTORING/ LEADERSHIP EXPERIENCE

2009-current	**Sommer scholar fellow** at Johns Hopkins School of Public Health
2004-2006	**Resident leader**; organized community events, advised residents on academics and social issues at UMASS, Amherst
2006	**Summerfuel camp counselor**; advised pre-college students on curricular/extracurricular events and issues.
2004	**Academic advisor** to incoming undergraduates at UMASS, Amherst; helping students select classes and majors; registration.
2004	**New Students Orientation Leader** for incoming students at UMASS, Amherst
2003	**Community leader** at resident hall; responsible for working with students to organize community-building events

TEACHING AND EDITORIAL EXPERIENCE

Trained Masters and bachelors students in scientific project development, setting up controlled experiments, molecular biology techniques such as gene deletions, protein over-expression, spectrophotometry, bacterial growth and maintenance techniques, etc

Reviewed and edited multiple papers and *Myxococccus* book chapter (3rd Ed) with thesis advisor Egbert Hoiczyk

LAB TECHNICAL SKILLS

DNA	Genomic and plasmid DNA extraction and purification, MolecularCloning, plasmid construction, gene deletions, gene expression, DNA Electrophoresis, site directed mutagenesis, epitope tagging.
RNA	RNA extraction and preparation, RTPCR, qRTPCR, siRNA
PROTEIN	Expression with various tags, His, FLAG, myc, HA, purification, native protein isolation using biochemical techniques such as salting out, protein refolding techniques using columns and urea, western blotting, pull-down assays
MICROSCOPY	Light, Transmission electron and fluorescence microscopy
OTHER	Flow Cytometry, Thin Layer Chromatography and purification of small molecules using TLC, carbohydrate analysis tests.
SOFTWARE	VELOCITY, STRATA, DNAMAN, CLUSTALW, SAP, SAS, R, BLAST,
CELLS & ORGANISMS	*E.coli, Pseudomonas aeruginosa, Myxococcus xanthus*, Hepatic Cell line, Red Blood cells, *Drosophila melanogaster, Anopheles gambiae,*

HONORS AND AWARDS

2008-present	Sommer Scholar Fellowship, Johns Hopkins School of Public Health
2006	Summa Cum Laude, George Washington University.
2005	Commonwealth College Honors Research Grant Recipient, University of Massachusetts, Amherst.
2004	University of Massachusetts, Amherst ALANAI Honor Society Scholar Award
2002-2006	Dean's List, University of Massachusetts, Amherst
2002	Coca-Cola Scholarship for Community Service, Côte d'Ivoire

PUBLICATIONS

Kim, C., **Srivastava, S**., Rice, M., Godenschwege T.A., Bentely, B., Ravi, S., Shao, S., Woodward, C.T., Schwartz, L.M. Expression of Human Amyloid Precursor Protein in the skeletal muscles of *Drosophila* results in age- and activity-dependent muscle weakness. **BMC Physiology** 2011; 11:7.

Agrawal, S., and Hoiczyk,E. The functions of different type IV pilus tip proteins in swarming, piliation, cell aggregation and fruiting body formation of *Myxococcus xanthus*. 2013 (In preparation to Mol Micro)

Agrawal, S., and Hoiczyk, E. Characterization of a novel high molecular weight periplasmic carbohydrate of *Myxococcus xanthus*. 2013 (In submission to PNAS).

Agrawal, S., Stoneburner E., and Hoiczyk E. Characterization and purification of *Myxococcus* EPS and associated genes. 2013 (In preparation)

Mohamed MA., **Srivastava, S**., Aly, H., Leitenberg, D. Development of T-cell Activation molecules in Preterm Infants 2013 (In preparation)

CONFERENCES AND POSTERS

2011	*Myxococcus xanthus* Annual Conference- Presentation
2010	Gordon Research Conference on Bacterial cell Surface Structures
2010	Delta Omega Poster Competition, Poster
2009	*Myxococcus xanthus* Annual Conference
2008	Pediatric Academic Society meeting- Poster
2006	12th Annual Massachusetts Statewide Conference for Undergraduates- Presentation

CERTIFICATES

2013	Vaccine Science and Policy, Johns Hopkins University
2013	Writing in the Sciences, Stanford University
2012	Clinical Vaccine Trials and Good Clinical Practice, Johns Hopkins University

REFERENCES

Dr. Egbert Hoiczyk (Assistant Professor, Ph.D. Thesis Advisor)
Department of Molecular Microbiology and Immunology
The Johns Hopkins University
615 N. Wolfe St. Baltimore MD, 21205
(443) 287 – 2898
ehoiczyk@jhsph.edu

Dr. Nicole Parrish (Associate Direction of Mycobacteriology, Ph.D Thesis Committee member)
Department of Pathology
The Johns Hopkins University
600 N. Wolfe St. Baltimore MD, 21287
(410) 550 – 3525
nparrish@jhmi.edu